Universidad Autónoma de Madrid

Facultad de Ciencias

Departamento de Biología Molecular

Live analysis and function of Myc-mediated cell competition in mouse pluripotent stem cells

Doctoral thesis

Covadonga Díaz Díaz

Madrid, April 2017

Director: Dr. Miguel Torres Sánchez

À la plus folle. JTA.

La duda es uno de los
nombres de la inteligencia

Jorge Luis Borges

This work was performed in Miguel Torres' laboratory in the Cell and Developmental Biology Area at the Centro Nacional de Investigaciones Cardiovasculares (CNIC) in Madrid.

The CNIC is supported by the Ministry of Economy, Industry and Competitiveness (MEIC) and the Pro CNIC Foundation, and is a Severo Ochoa Center of Excellence (SEV-2015-0505).

This study was funded by grants RD12/0019/0005 and RD16/0011/0019 (TerCel, RETICS); S2010-BMD-2315 (Comunidad de Madrid); BFU2012-31086 (MINECO) and BFU2015-71519-P (MEIC).

Covadonga Díaz Díaz was recipient of a FPU fellowship from the MECD (FPU12/02114).

Index of contents

SUMMARY

In the early mouse embryo and in embryonic stem cell (ESC) cultures the transcription factor Myc exhibits a cell-to-cell heterogeneous pattern. Cells expressing low levels of Myc are eliminated from the population by cell competition. Myc has been reported to promote cell reprograming to pluripotency and to regulate cell anabolism and proliferation in ESCs; however, the biological role of Myc-dependent endogenous cell competition and the dynamics and regulation of Myc during this process remain unknown.

Here we develop a new image analysis tool that allows us to track the temporal evolution of endogenous Myc levels, perform neighbourhood analysis in ESC cultures and generate 3D+t computerized data. We show that despite Myc degradation and resynthesis during mitosis, Myc levels are mostly heritable in ESC lineages. Cell competition results from random interactions between cells with high discrepancies in Myc levels. Myc-low cells ("losers") temporally integrate contacts with Myc-high cells ("winners"), which leads to a progressive decrease in their own Myc levels until dying. Interestingly, endogenous Myc levels correlate with the pluripotency status; differentiation-primed cells express low Myc levels and are outcompeted by Myc-high naive ESCs. Indeed, cell competition inhibition results in an accumulation of primed cells. These observations in ESCs correlate with findings in the mouse epiblast. Moreover, we show that Myc levels directly determine the competitive ability of ESCs irrespective of the pluripotency status.

Our results identify Myc as a mediator between differentiation status and competitive ability of pluripotent cells. Myc-driven endogenous cell competition thus acts as a mechanism to protect pluripotent stem cell pools from differentiation.

Tanto en el embrión temprano de ratón como en cultivos de células madre embrionarias (CMEs), el factor de transcripción Myc muestra un patrón de expresión heterogéneo. Las células que expresan menos niveles de Myc son eliminadas de la población mediante competición celular. Se ha demostrado que Myc promueve la programación celular hacia un estado de pluripotencia y regula el anabolismo y la proliferación en CMEs; sin embargo, la función biológica de la competición celular endógena dependiente de Myc, así como la regulación y dinámica de la expresión este gen durante este proceso aún se desconocen.

En esta tesis desarrollamos una novedosa herramienta de análisis de imagen, a partir de la cual realizamos análisis de células individuales y sus vecindarios y generamos un sistema de datos 3D+t computarizados. De esta manera demostramos que, a pesar de que Myc se degrada y se vuelve a sintetizar rápidamente durante la mitosis, sus niveles de expresión son en su mayor parte heredables. Además, la competición celular se desencadena por interacciones aleatorias entre células con grandes diferencias en sus niveles de Myc; de forma que las células que poseen bajos niveles de Myc ("perdedoras") integran en el tiempo contactos con células con mayor expresión ("ganadoras") lo que lleva a una reducción progresiva en sus propios niveles hasta que mueren. Cabe resaltar que los niveles endógenos de Myc correlacionan con el estado de pluripotencia; las células en un estado más avanzado de diferenciación expresan menos Myc siendo eliminadas por células más indiferenciadas y con altos niveles de expresión. De hecho, la inhibición de la competición celular produce una acumulación de células en proceso de diferenciación. Estas observaciones correlacionan con resultados obtenidos en estudios realizados en epiblasto de ratón. Además, demostramos que la eficiencia competitiva viene directamente determinada por los niveles de Myc independientemente del estado de pluripotencia.

Estos resultados señalan a Myc como un intermediario entre el estado de diferenciación y la capacidad competitiva de las células pluripotentes. Por lo tanto, la competición celular endógena promovida por Myc funciona como un mecanismo de protección de pobolaciones de células madre pluripotentes frente a la diferenciación.

Index of figures, tables and videos

Figures

Tables

Supplementary table is provided in the digital format of the thesis.

Videos

Supplementary videos are provided in the digital format.

Video 1. ESC colony showing GFP-Myc levels (green) and tdTomato reporting the cell membrane (red).

Video 2. ESC colony showing cell segmentation and tracking. Colors when segmented represent different cell identities.

Video 3. ESC colony displaying segmented nuclei, with green levels representing endogenous GFP-Myc levels. ID labeling across mitosis shows cell tracing.

Video 4. Caspase3 activity (red) reporter identifying an apoptotic cell (arrow) in an ESC colony.

Video 5. Hoechst58 (blue) identifying an apoptotic cell (arrowhead) in an ESC colony.

Video 6. ESC colony showing a dying cell. These cells are easily recognized by the changes in the membrane, which collapses during apoptosis.

Video 7. ESC colony tracing the movements of a PCD (loser) and its associated PCD-MHN (winner) in the time period preceding loser death.

Video 8. An *iMOS*$^{T1\text{-}myc}$ ES colony showing the onset of EYFP-Myc-overexpression cells following tamoxifen induction.

Video 9. An iMOS$^{T1\text{-}myc}$ ES colony showing the death of cells (arrowheads) neighboring EYFP-Myc-overexpressing cells.

Video 10. Time lapse of an *iMOS*$^{T1\text{-}myc}$ / GFP-Myc mixed colony.

Abbreviations

2i: 2 inhibitors
5mC: DNA methylation
BMP: Bone Morphogenetic Protein
Bst: Belly spot and tail
Cdk4: Cyclin-Dependent Kinase4
CHIRON: CHIR99021 (inhibitor)
Dgl: Discs Large
Dpp: Decapentaplegic
ECFP: Enhanced Cyan Fluorescent Protein
EDAC: Epithelial Defence Against Cancer
EMT: Epithelial-Mesenchymal Transformation
EPC: ectoplacental cone
EpiLCs: Epiblast-like Cells
EpiSCs: Epiblast Stem Cells
ERK: Extracellular Regulated Kinase
ESC: Embryonic Stem Cell
ExE: Extraembryonic Ectoderm
EYFP: Enhanced Yellow Fluorescent Protein
FGF: Fibroblast Growth Factor
GSC: Germline/Spermatogonial Stem Cell
GSK: Glycogen Synthase Kinase 3
ICM: Inner Cell Mass
iMOS: Inducible Mosaic
iPSC: induced Pluripotent Stem Cell
JAK: Janus Kinase
JNK: c-Jun N-terminal Kinase
Klf4: Kruppel Like Factor 4
KO: Knockout
Lgl: Lethal Giant Larvae
LIF: Leukemia Inhibitory Factor
MAPK: Mitogen-Activated Protein Kinase

MDCK: Madin-Darby Canine Kidney
MEF: Mouse Embryonic Fibroblast
MHN: Myc-Highest Neighbour
ML-NDC: Myc-Low Non-Dying Cell
Myc-H: Myc-High
Myc-L: Myc Low
Myc-M: Myc-Medium
Myc: Myelocytomatosis oncogene
Mycl: v-myc avian myelocytomatosis viral oncogene lung carcinoma derived
Mycn: v-myc avian myelocytomatosis viral related oncogene, neuroblastoma derived
NDC: Non-Dying Cell
PD03: PD0325901 (inhibitor)
PDC: Prospective-Dying Cell
PE: Primitive Endoderm
PGC: Primordial Germ Cell
PI3K: Phosphatidylinositol 3-Kinase
RpL24: Ribosomal Protein L24
Sox2: SRY (sex determining region Y)-box 2
SPARC: Secreted Protein Acidic Cysteine-Rich
SSL: Spline Smooth Line
STAT: Signal Transducer and Activator of Transcription
SWH: Salvador/Warts/Hippo
TE: Trophectoderm
TET: Ten-eleven translocation
TFCP2l1: Transciption Factor CP2 like1
TGC: Trophoblast Giant Cell
TGFb: Transforming Growth Factor beta
TS: TE stem
VprBP: Vpr (HIV-1) binding protein
Vps25: Vacuolar Protein-Sorting-Associated protein 25
WT: Wild Type

INTRODUCTION

Cell competition consists in the fitness comparison between viable neighbouring cells resulting in the elimination of the less fit cells (Figure 1). This phenomenon was firstly described in *Drosophila* and currently has been characterized in many biological scenarios and is envisioned as an important tissue homeostatic mechanism in metazoans.

In mammals, pluripotent cells of the early mammalian embryo show a natural cell-to-cell heterogeneity in Myc levels, which leads to the competitive elimination of Myc-low cells from the embryonic lineage. The mechanism and the biological relevance of this phenomenon, however remain unknown. In this thesis, we aim to elucidate the mechanisms and biological basis of endogenous cell competition regulated by Myc in the context of Embryonic Stem Cells (ESCs) and the early mammalian embryo.

1. Cell competition

1.1. The discovery of Cell Competition: early studies in flies

Forty years ago, Ginés Morata and Pedro Ripoll reported the phenomenon while studying the proliferation of *Drosophila* cells mutant for *Minute* genes, in which ribosomal proteins are affected. *Minute* mutations affect protein synthesis ability and produce cellular lethality in homozygosis, while heterozygous flies are viable and nearly normal but show slower development due to a reduced proliferative rate. When a mosaic of heterozygous (*M*/+) and wild-type (WT) cells were induced in wing imaginal discs, *M*/+ cells, which otherwise would be viable, were eliminated due to confrontation with WT cells (Morata and Ripoll, 1975) (Figure 1). Simpson confirmed the previous observations and observed that elimination of *M*/+ clones in a WT background did not take place when larvae were starved. Since starvation induces generally reduced growth rates, these experiments strongly suggested that a limitation of growth/proliferation of *M*/+ determines the competitive elimination of *M*/+ cells and that the mechanism underlying *M*/+ cell depletion was related to the metabolic control of cell growth (Simpson, 1979). The requirement of a differential growth rate for the elimination of *M*/+ cells was later confirmed by the confrontation

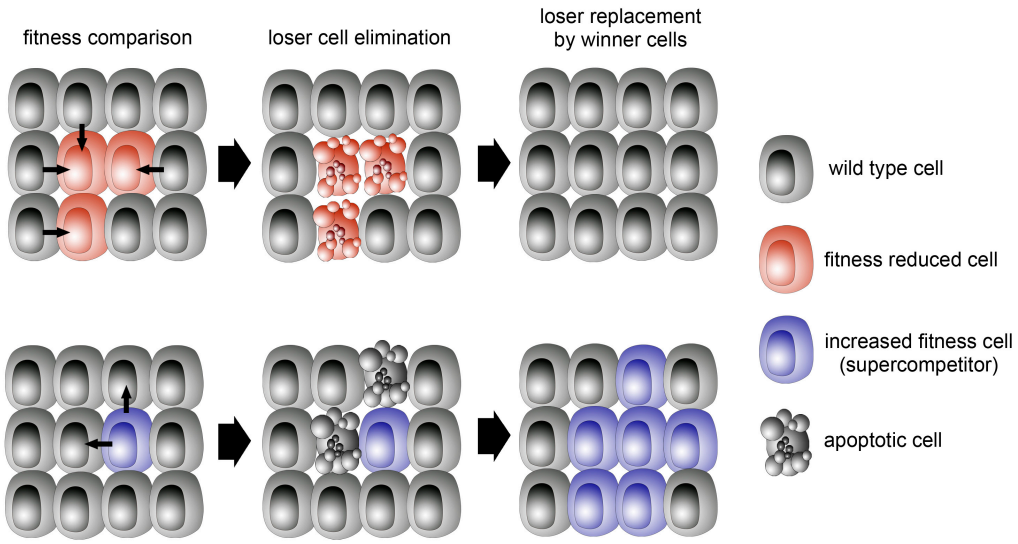

Figure 1. Cell competition and supercompetition.

Schematic representation of the cell competition process. In cell competition, information about fitness status is locally exchanged between cells. Less fit, but otherwise viable, cells are outcompeted by higher-fitness cells undergoing apoptosis. Loser cells are replaced by fitter winner cells, which overproliferate.
High-fitness cells generated in a WT background also lead to the elimination of the WT loser cells and to the expansion of winner cells in a process known as supercompetition.

of *Minute* mutations with variable severity (Simpson and Morata, 1981). In these models, competition did not affect the final size of the wings or compartments, suggesting the compensatory proliferation of WT cells. Moreover, cell competition was shown by these studies to result from local interactions between slow- and faster-growing cells (Simpson and Morata, 1981). However, cell competition was ineffective across compartment borders and WT clone expansion was restricted to well-defined and reproducible frontiers, which suggests that wing disc are divided in non miscible cell populations (compartment boundary) (Simpson and Morata, 1981).

It was not until many years later that cell competition became again a subject of interest when the phenomenon was reported to require short-range interactions and to be executed by apoptosis of loser cells in *Drosophila* imaginal discs (Abrams, 2002; Milan *et al.*, 2002; Moreno *et al.*, 2002).

1.2. Supercompetition and the transcription factor Myc

Supercompetition is as a type of cell competition in which cells with experimentally increased fitness eliminate neighbouring WT cells, thereby overcolonising tissues (Abrams, 2002) (Figure 1). The first gene to be linked to this definition was the proto-oncogene *dMyc*. *dMyc* is the fly homologue of the mammalian family of *Myc* transcription factors and regulates many downstream targets involved in cell growth and cell anabolism (Johnston *et al.*, 1999; de la Cova and Johnston, 2006). In 2004 two pioneer papers presented the role of this proto-oncogene in cell competition by inducing dMyc overexpressing clones in the wing disc (de la Cova *et al.*, 2004; Moreno and Basler, 2004). These clones were able to expand at the expense of WT cells until they filled the compartment (Figure 1). Apoptosis via JNK (Moreno and Basler, 2004) and *hid* activation in the loser cells (de la Cova *et al.*, 2004) was required in this process. In this context, dMyc-overexpressing cells acted as "supercompetitors" and the WT cells behaved as "losers" (Figure 1). The discovery of supercompetition induced by Myc led to propose that early steps of tumour formation could be driven by this phenomenon (Rhiner and Moreno, 2009), which generated a new wave of interest in cell competition.

On the contrary, downregulation of dMyc in cells led to their elimination, in similarity to observations with *M/+* clones (Johnston *et al.*, 1999; de la Cova *et al.*, 2004; Moreno and Basler, 2004). This suggested that dMyc was a general driver of cell competition by controlling cell's anabolic machinery. Interestingly, cells with two extra *dMyc* copies, which behave as supercompetitors in front of WT cells, instead behaved as "losers" when confronted with cells with four extra copies of dMyc (Moreno and Basler, 2004) supporting the idea that competition is based on intercellular comparison of relative Myc levels and not on cell-autonomous sensing of absolute Myc level.

In addition, these studies ruled out a strict relationship between cell growth or proliferative activity and competitive ability, since overexpression of factors inducing cell growth (PI3K Dp110) or cell cycle regulators (CyclinD and Cdk4) generated large clones but were unable to eliminate surrounding WT cells, therefore Myc and *Minute*

and no other proliferation/growth regulators affect specific competitive pathways (de la Cova *et al.*, 2004; Moreno and Basler, 2004).

1.3. Pathways involved in cell competition in *Drosophila*

After the discovery of *Minute* and Myc-driven competition, many studies have tried to shed light on this field by finding out new pathways and molecules involved in this process. These factors can be classified into two groups depending of the kind of cell competition they induce (Figure 2).

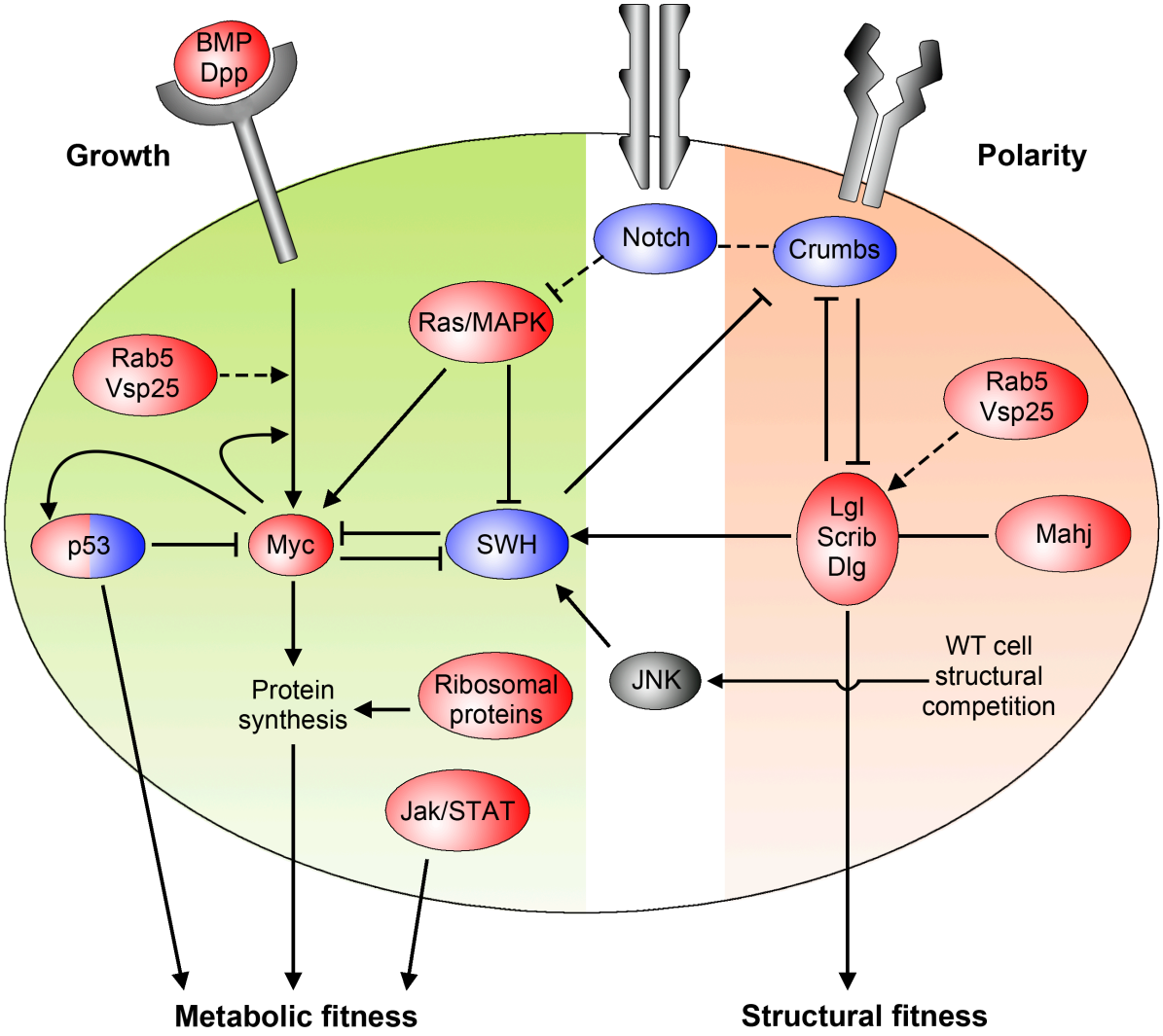

Figure 2. Pathways involved in metabolic and structural competitive fitness.

Schematic of the main pathways involved in structural and metabolic cell competition. Cell selection is initiated by mutations or pathways that generate differential fitness activity between neighbouring cells triggering cell competition. On one hand, metabolic fitness is determined by the anabolic activity of the cell, specifically by protein synthesis machinery. This machinery is activated by Myc, on which cellular growth and proliferative pathways converge. Even though the JAK/STAT pathway does not depend on Myc signalling, it also affects cell metabolic fitness.
On the other hand, structural fitness is determined by the apico-basal polarity machinery. When polarity pathways are mutated the structural fitness is decreased and the SWH pathway is repressed leading to an increase in growth/proliferation. Since competitive behaviours between isolated mutant and surrounding WT cells counteract SWH pathway repression by JNK, polarity-deficient cells are thus outcompeted. However, when polarity-deficient cells elude competition, SWH pathway is effective and trigger overgrowth of mutant cells. The Notch pathway and the endocytic pathway (Rab5, Vsp25) may interact with both metabolic and structural fitness pathways, but their specific involvement has not been reported yet.
Ellipses in red represent factors whose gain of function increases fitness and blue ellipses represent those factors whose gain of function reduce fitness.
Filled arrows indicate activation, whereas bars mean inhibition or blockade of target activity. Dashed lines show a deduced effect and a solid line indicates a known downstream target. (Based on (Claveria and Torres, 2016)).

The first group includes factors that affect metabolic pathways and are likely to induce cell competition by producing contrasting anabolic ability in neighbouring cells (Figure 2). This group includes the classical factors inducing cell competition, like *Minute* mutations, the BMP/Dpp pathway and Myc. This group also includes other pathways involved in growth/survival signal reception or transduction to the cell's anabolic machinery, such as the Rab5 and Vps25 endocytic pathways (Moreno and Basler, 2004; Herz *et al.*, 2006), the Ras/MAPK pathway (Prober and Edgar, 2000) and the JAK/STAT pathway (Rodrigues *et al.*, 2012). In addition, cell competition can also be induced by mutations in the Salvador/Warts/Hippo pathway, which is a central regulator of growth, cell death and tissue homeostasis (Tyler *et al.*, 2007; Neto-Silva *et al.*, 2010; Ziosi *et al.*, 2010; Chen *et al.*, 2012). The nature of competitiveness regulation by these pathways is likely similar, since hierarchical regulatory interactions have been established between the various pathways involved in metabolic cell competition. Myc acts downstream of various cell competition-inducing pathways like the BMP/Dpp (Doumpas *et al.*, 2013), Ras/MAPK (Prober

and Edgar, 2000; Moreno and Basler, 2004) and SWH (Neto-Silva *et al.*, 2010; Ziosi *et al.*, 2010). Moreover, BMP/Dpp signal transduction is enhanced by a positive feedback that involves Myc and enhanced protein synthesis is required downstream of Myc to induce cell competition (Moreno and Basler, 2004). Although the STAT pathway does not show any apparent epistatic relationship during cell competition with the Myc, SWH, or *Minute* pathways (Rodrigues *et al.*, 2012), it seems to affect the same cellular parameters, because Myc-low cells are rescued by STAT hyperactivation and STAT-deficient cells are rescued when confronted with *Minute* mutant cells (Rodrigues *et al.*, 2012).

The second group of cell competition inducers includes factors affecting polarity and epithelial integrity and therefore define a different class of competitive interactions known as structural cell competition (Figure 2). Extrusion from the epithelium is the typical way of eliminating cells in this type of competition and cell death is not always involved in this process. Structural cell competition is induced by alterations affecting components of the canonical pathway regulating apico-basal polarity, such as Lgl (Menendez *et al.*, 2010; Tamori *et al.*, 2010), Scribble (Brumby and Richardson, 2003), Dlg (Woods and Bryant, 1991), Mahjong/VprBP (Tamori *et al.*, 2010) and Crumbs (Hafezi *et al.*, 2012). In addition, the role of Rab5 and Vps25 in cell competition may also be related to the structural organization of the cell, since the endocytic pathway also affects apico-basal polarity (Lu and Bilder, 2005). Yet, although there is also cross talk between structural and metabolic cell competition, these pathways have very different natures. In fact, in various cases, the mutations that induce the loser phenotype in structural competition, however promote metabolic changes typical of winner cells in metabolic competition, indicating that structural alterations in epithelial tissues overrule metabolic activity in competitive interactions. An additional difference is that both winner and loser cells in metabolic competition usually respect normal tissue architecture, while winners or losers in structural cell competition can produce tumorous growth.

Finally, there are some other pathways that induce cell competition but whose mechanisms and relationships to the canonical pathways have not been completely resolved, such as the Wnt pathway (Vincent *et al.*, 2011; Rodrigues *et al.*, 2012) or patterning mismatches (Adachi-Yamada *et al.*, 1999; Milan *et al.*, 2002).

1.4. Cell competition in mammals

The first study suggesting that cell competition could also take place in other metazoans than insects was the analysis of a mouse mutation equivalent to the fly *Minute* mutants. The *Bst* mice mutants are defective in ribosomal protein L24. While *Bst* homozygous mutant mice are not viable, heterozygous mice showed a kinked tail, decreased pigmentation and retinal defect but are viable and normal-sized (Oliver *et al.*, 2004). As in the *Drosophila* system, cells heterozygous for *RpL24* were disproportionately disadvantaged with respect to WT cells in mouse chimeras (Oliver *et al.*, 2004). However, whether this observation was due to cell autonomous features of the *Bst* mutants or indeed reflects competitive interactions has not been addressed.

A second study pointed out to the occurrence of cell competition in liver regeneration. In aged rat livers, host hepatocytes were outcompeted by transplanted fetal hepatocytes, apparently by local interactions that promoted resident hepatocyte death, which facilitated long-term repopulation post-transplantation (Oertel *et al.*, 2006).

Following these pioneering studies, cell competition based on stress and mediated by p53 was described (Figure 2). Stress signals induce p53-mediated cell death in *Drosophila* and either cell death or cell cycle arrest and repair in mammals. In bone marrow transplants, cells sublethally irradiated behaved as losers in a p53-dependent manner when confronted with non-irradiated cells (Bondar and Medzhitov, 2010). In addition, when a mosaic p53 mutant bone marrow is irradiated only p53-deficient clones were recovered (Marusyk *et al.*, 2010). In these two studies, a senescence-like phenotype, rather than apoptotic elimination, was induced in the outcompeted cells (Bondar and Medzhitov, 2010; Marusyk *et al.*, 2010). In this context, cell competition would be the result of cells comparing their p53 activity levels, resulting in the outcompetition of the p53-high population. Given the role of p53 in transducing stress situations, this mechanism would ensure the elimination of stressed cells whenever unstressed cells are available in the surroundings.

Epithelial monolayers in culture derived from the Madin-Darby canine kidney (MDCK) have also emerged as an important *in vitro* system for studying cell

competition in mammalian cells. Studies with structural cell competition pathways have shown that mutations in *Lgl*, its partner *Mahjong* (Tamori *et al.*, 2010) or *Scribble* (Norman *et al.*, 2012) induce cell competition in the MDCK culture system.

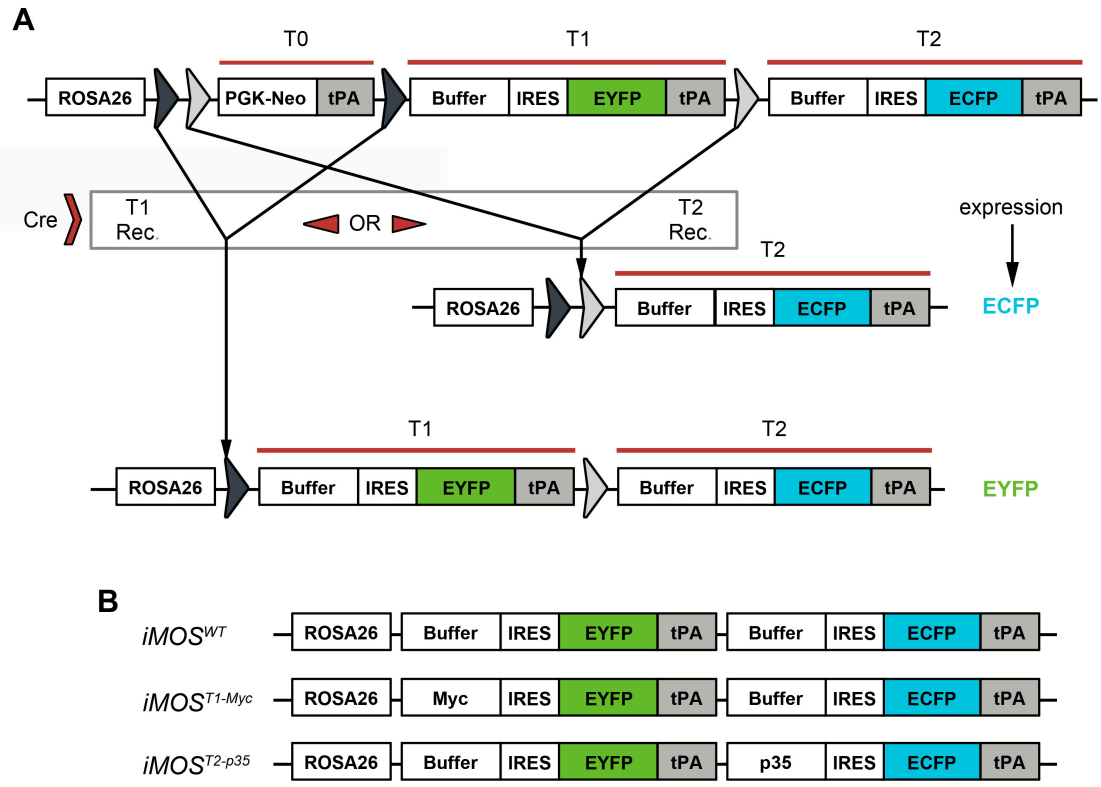

Figure 3. Schematic representation of the *iMOS* system construction.

A. A recombinase-based system for genetic mosaic induction was obtained by using two different *loxP* sequence variants that recombine with homotypic but not heterotypic sequences. The three cassettes flanked by the *loxP* sites end in a triple polyadenylation signal blocking the expression of the following transcriptional units. Upon *Cre* expression, either the transcriptional unit T0 is excised, leading to the expression of T1 or both T0 and T1 are eliminated leading to the expression T2. This system allows to randomly generate a mosaic with two labelled cell populations. The construct is targeted to the ubiquitous *Rosa26* locus, whose expression gives rise to a policistronic mRNA expressing a buffer sequence or a protein of interest and a fluorescent reporter protein, either the yellow fluorescence protein (EYFP) or the cyan fluorescent protein (ECFP). The recombination frequency of EYFP cells is 75% and that of the ECFP cells 25%. This difference is due to the different distances between the *loxP* sites. **B**. Schematic representation of the *iMOS* lines used in this thesis. In $iMOS^{WT}$, both labelled population are WT. $iMOS^{T1\text{-}Myc}$ generates an EYFP Myc-overexpressing cell population and an ECFP WT population. In $iMOS^{T2\text{-}p35}$, EYFP cells are WT while ECFP cells express the baculoviral apoptosis inhibitor p35. (Based on (Claveria *et al.*, 2013)).

This model also showed the so-called Epithelial Defence Against Cancer (EDAC) which consists in the competitive elimination of cell carrying oncogenic mutations, like *Rasv12* or *Src*, by apical extrusion from the epithelial sheet (Hogan *et al.*, 2009; Kajita *et al.*, 2010). In this model maintenance of epithelial homeostasis only occurs when WT cells win, whereas when the defective cells escape from cell competition, they give rise to tumour formation (Hogan *et al.*, 2009; Kajita *et al.*, 2010).

Additional cases of cell competition have been recently described when cells lacking the Notch pathway are confronted with WT cells in the adult mouse esophageal epithelium (Alcolea *et al.*, 2014) (Figure 2). WT cells were progressively eliminated from the tissue by their Notch-deficient neighbour clones, which underwent overgrowth (Alcolea *et al.*, 2014).

Furthermore, recent studies have shown that Myc-dependent cell competition also takes place in the early mouse embryo. Myc-induced supercompetition was characterised in mouse embryos by using a system of inducible mosaics based on *Cre* recombination, which generated two different populations (Claveria *et al.*, 2013) (Figure 3). One cell population overexpressed Myc under the expression of the ubiquitous *Rosa26* promoter and the other population remained WT and was selectively eliminated from the epiblast (Claveria *et al.*, 2013). This demonstrated that supercompetition could also be induced in the embryo and that it provoked the phenotypically silent replacement of WT cells. In addition, it was shown that apoptosis of WT loser cells was needed for this replacement and that competition was contact-dependent, was apoptotic rate was increased in WT cells in direct contact with Myc overexpressing cells (Claveria *et al.*, 2013). In this study cell competition was also explored *in vitro* in mouse ESCs, where Myc induced cell competition could also be shown (Claveria *et al.*, 2013). In a similar study, it was reported that Bmpr1a (BMP receptor 1a) knock out ESCs decreased their Myc levels when compared with their WT counterparts and were subsequently outcompeted (Sancho *et al.*, 2013). Interestingly, it was also reported that Myc activation led to induced cell competition in several tissues and organs of the developing and adult mouse (Claveria *et al.*, 2013; Villa del Campo *et al.*, 2014).

All these assays performed in mammalian models demonstrated that cell competition is widespread in metazoans and not restricted to just *Drosophila* wing discs or Minute mutations. In addition, they identify the Myc pathway as a conserved central regulator of cell competition.

1.5. Endogenous cell competition

All of the mentioned findings so far rely on experimental introduction of stress or mutations and did not address the potential roles of spontaneous cell competition in normal development or tissue homeostasis. Endogenous cell competition however has been detected in the mouse epiblast, where cells express naturally heterogeneous levels of Myc (Claveria *et al.*, 2013; Sancho *et al.*, 2013) (Figure 4). During the different phases of epiblast development, abundant cell death is observed, showing a peak at 6 days of development, just before the onset of differentiation and gastrulation (Poelmann, 1980; Heyer *et al.*, 2000; Plusa *et al.*, 2008). This maximal incidence of death is partially due to sensitivity to DNA damage and mediated by a p53-dependent quality check (Heyer *et al.*, 2000) and in part regulated by Myc levels (Claveria *et al.*, 2013). Epiblast cells with lower Myc levels preferentially undergo apoptosis due to their confrontation with neighbours with higher Myc levels. This elimination thus results in the recruitment of the pool of cells with higher Myc levels to the developing embryo (Figure 4). When cell death is inhibited by p35 overexpression, rescued cells express relatively lower Myc levels than the rest, indicating that in normal conditions the Myc-low cell population is eliminated (Claveria *et al.*, 2013). Spontaneous cell competition between cells expressing contrasting Myc levels was also detected in mESC cultures (Claveria *et al.*, 2013). However, the biological basis, dynamics and mechanisms of Myc-mediated cell competition remain unknown.

An additional example of endogenous competition has recently been reported for T-cell progenitors in the mouse thymus (Martins *et al.*, 2014). Bone marrow derived colonizing cells outcompeted resident progenitor cells upon competition for the survival factor Interleukin7. Cell competition was needed to continuously renovate the pool of thymic T cell precursors with fresh cells from the bone marrow

(Martins *et al.*, 2014). Since abolishment of this replacement led to cancerous formation of thymic cells, cell competition would be playing a tumour suppressor role in this phenomenon.

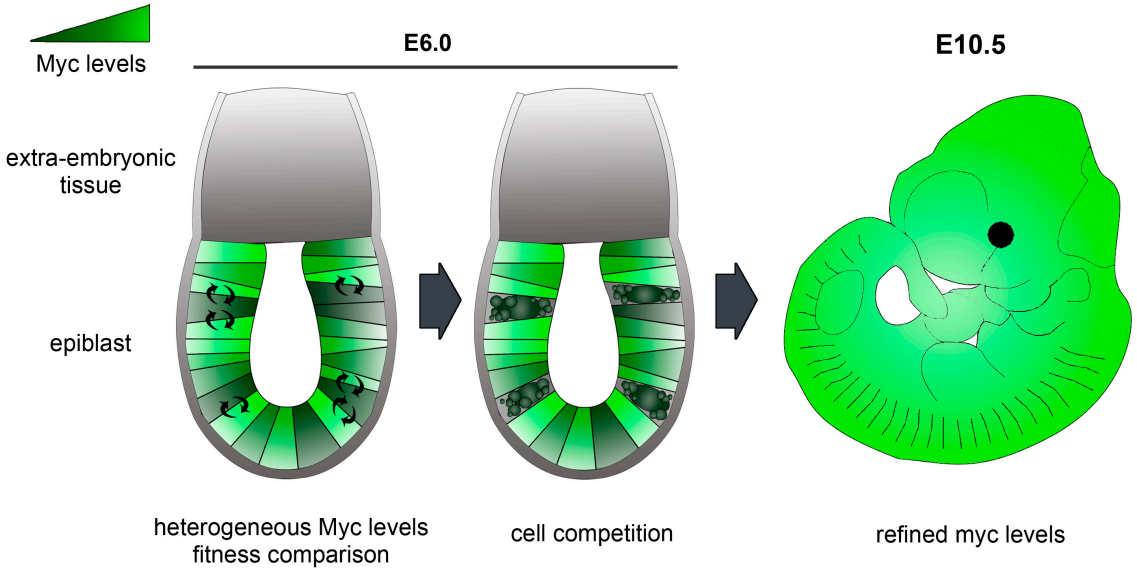

Figure 4. Endogenous cell competition.

During normal mouse development, Myc levels in the epiblast are intrinsically expressed in a heterogeneous pattern. This produces contacts between cells with high and low-Myc levels, which are fitter and less fit cells, respectively. Myc discrepancies between neighbouring cells leads to outcompetition of the less fit population and a selection of the epiblast cell pool. This process refines the epiblast cell population, giving rise to a final embryo composed by the Myc-high fitter cells from the initial pool. (Based on (Claveria *et al.*, 2013)).

Finally, cell competition has been shown to counter-select naturally viable, but suboptimal cell clones in mammalian fibroblasts (Penzo-Mendez *et al.*, 2015).

1.6. Mechanisms of cell competition

The mechanisms by which cells are able to compare their fitness have been intensively investigated. Although several hypotheses have been proposed trying to clarify how competitive interactions occur, complete understanding of the

phenomena observed is far from complete. The different mechanisms and interactions proposed to take place between competing cells are explained here.

1.6.1. Ligand capture model

This was the first model discussed (Morata and Ripoll, 1975), and received support from studies indicating that cells compete for growth/survival factor signals (Moreno *et al.*, 2002). This model was supported by the observation that loser cells presented lower level of Dpp signalling (a secreted protein member of the TGFb family and the fly orthologue of mammalian BMPs) and an excess of Brinker activated by the JNK pathway and triggering apoptosis (Moreno *et al.*, 2002). However, in several studies the Dpp distribution does not correlate with the intensity of cell competition (Burke and Basler, 1996; de la Cova *et al.*, 2004; Martin *et al.*, 2009). Moreover, in various scenarios where Dpp growth factors are present in excess still competitive behaviours take place (Senoo-Matsuda and Johnston, 2007; Hogan *et al.*, 2009; Tamori *et al.*, 2010; Norman *et al.*, 2012; Claveria *et al.*, 2013; Sancho *et al.*, 2013; Mamada *et al.*, 2015). All these observations suggest that Dpp signalling might result from the execution of competitive program more than being its driving force.

Even though this model gave gratifying explanations, the trophic theory did not address many aspects related to the phenomena, such as the related compensatory proliferation or the mechanism of fitness comparison (Adachi-Yamada and O'Connor, 2002; Gibson and Perrimon, 2005; Shen and Dahmann, 2005).

1.6.2. Models based on fitness reporting

This type of models propose that cells directly report their fitness status to neighbouring cells resulting in the dismissal of cells with comparative lower fitness. The Flower pathway has been the first model proposed for this kind of interaction (Rhiner *et al.*, 2010). Flower is a transmembrane protein ubiquitously expressed in *Drosophila*. This protein has three isoforms differing in their C-terminal regions that are exposed to the extracellular space. Less fit cells specifically express one of the isoforms (Flower-lose isoforms), which promotes context-dependent apoptosis only

when surrounding cells express the ubiquitous form (Rhiner *et al.*, 2010). The Flower code has been observed to function in a variety of scenarios, such as cell competition driven by *Minute*, Myc, Dpp and Scribble, however it is not detected when apoptosis is induced by direct cell death inducers (Rhiner *et al.*, 2010). Since loss of Flower neither affects growth nor homeostasis of tissues, Flower has been proposed to function as a label of loser cells, being considered a dedicated effector of cell competition.

Finally, Crumbs has also been shown to report fitness between prospective winner and loser cells (Hafezi *et al.*, 2012) (Figure 2). As mentioned previously, Crumbs is a transmembrane protein component of the apico-basal polarity system. This protein differentially expressed in neighbouring cells determining the winner and loser fate in a context-dependent manner and mutations that alter fitness also alter Crumbs levels (Hafezi *et al.*, 2012).

However, the molecular mechanisms involved in the ability of the Flower and Crumbs systems to mediate quantitative fitness comparison between cells is still unresolved.

On the other hand, other authors have proposed the release of diffusible signals as a mechanism to report fitness. This concept emerged from experiments where *Drosophila* S2 WT cells were out-competed when co-cultured with Myc-overexpresing cells separated by a permeable membrane (Senoo-Matsuda and Johnston, 2007). Additional experiments showed that conditioned medium from cultures undergoing Myc-induced competition, but not from cultures expressing Myc in a homogenous manner, was able to induce WT cell death (Senoo-Matsuda and Johnston, 2007). These studies suggested a model in which diffusible factors produced during competition induce loser cell elimination. In this model, prospective loser cells are not specifically targeted, and therefore winner cells should activate a mechanism that protects them or sensitizes loser cells to the killer signal. The combination of the killing signal with winner-specific resistance to it would constitute the fitness comparison mechanism. These experiments however may only apply to certain models of cell competition, since similar experiments in *Drosophila* (Portela *et al.*, 2010) and mammalian models showed inconsistent results. In mouse ESCs and

mouse fibroblasts, conditioned medium experiments did not induce cell competition and apoptosis was only increased in cells adjacent to Myc-overexpressing cells (Claveria *et al.*, 2013; Penzo-Mendez *et al.*, 2015). In contrast, in BMP-induced mESC cell competition models, diffusible signals were reported to be responsible for competitive interactions (Sancho *et al.*, 2013). Remarkably, *in vivo* studies show that very short range or direct contact was needed for the elimination of less fit cells (Simpson and Morata, 1981; Moreno *et al.*, 2002; Moreno and Basler, 2004; Li and Baker, 2007; Claveria *et al.*, 2013) and that cell competition does not cross compartment boundaries (Simpson and Morata, 1981), therefore even in the scenarios in which diffusible factors are involved, they would mostly act locally. These results suggest that the molecular mechanism that determine competitive interactions may depend on the model being studied and further analysis needs to be done to elucidate this question and identify the putative signals involved.

Possible examples of competition based on diffusible molecules have been recently reported. An innate immunity-related recognition mechanism has been characterised in cell competition in *Drosophila* imaginal discs (Meyer *et al.*, 2014). In this study, it was shown that activation mediated by the diffusible signal Späztle of Toll-related receptor is required for low-Myc and elimination of *Minute* mutant cells (Meyer *et al.*, 2014). Another diffusible killer activity has also been identified during neuronal competition for target innervation in mammals (Deppmann *et al.*, 2008).

1.6.3. Mechanical models

Several studies have proposed mechanical stress as an independent inducer of cell competition in epithelia, where cells compete for limited available space (Shraiman, 2005; Eisenhoffer *et al.*, 2012; Marinari *et al.*, 2012; Paoli *et al.*, 2013). These models may be applied to structural cell competition, where alterations in the apico-basal polarity can alter attachment forces among cells and between cells ant the basal membrane. Mechanical stress seems not to be involved in metabolic cell competition (Senoo-Matsuda and Johnston, 2007; Claveria *et al.*, 2013; Sancho *et al.*, 2013; Mamada *et al.*, 2015; Penzo-Mendez *et al.*, 2015). In addition, entosis has been shown to be the predominant mechanism of cell competition between Ras-Rac-transformed cells and WT human cells (Sun *et al.*, 2014b). Entosis is a type of cell

death initiated when living cells are engulfed by other cells of the same kind (Overholtzer *et al.*, 2007). The ability of a cell to engulf can determine the winner and loser phenotype in some models and is determined by mechanical differences between cells. High deformability controlled by RhoA and actomyosin was reported to be sufficient to explain the winner status, whereby this higher deformability enables cell to engulf their neighbours (Sun *et al.*, 2014b). In addition, E-cadherin overexpression transformed cells induce entosis-mediated cell competition (Sun *et al.*, 2014a). Nevertheless, in some cases the inner cell escapes and does not die, suggesting that cell engulfment events do not always lead to cell death and that the strive for survival of the engulfed cell might represent a fitness status test (Overholtzer *et al.*, 2007).

1.7. Loser cell clearance and replacement

Several mechanisms have been proposed for the clearance of cell corpses after the activation of the apoptotic pathway in those cells. Extrusion from the epithelial layer and phagocytosis are the two main mechanisms for eliminating loser cells. In vertebrate models apical extrusion is predominant (Gu and Rosenblatt, 2012; Lolo *et al.*, 2013) while basal extrusion is predominant in *Drosophila* epithelia (Grzeschik *et al.*, 2010; Tamori *et al.*, 2010; Lolo *et al.*, 2013), where dead cells are engulfed and remove by haemocytes (Lolo *et al.*, 2012). The sphingosine-1-phosphate and Rho pathways have been shown to be involved in extrusion of dead cells (Gu *et al.*, 2011) and release of tyrosyl-tRNA synthetase by loser cells stimulates hemocyte recruitment and phagocytic activity (Casas-Tinto *et al.*, 2015).

In the Minute model, some studies report that engulfment seems to be the main system to eliminate *Minute* mutant cells (Li and Baker, 2007). In this context, mutations in essential components for the phagocytic process prevent competition suggesting that engulfment may be upstream of the initiation of the death machinery (Li and Baker, 2007), however these findings have not been confirmed in further experiments (Lolo *et al.*, 2012). Studies have also reported the elimination of polarity mutant cells by engulfment (Ohsawa *et al.*, 2011), contrasting with others in which this process seems not to be required for elimination of the Minute mutant cells, polarity defective cells or WT loser cells in the dMyc supercompetition model (Lolo *et*

al., 2012). Engulfing by neighbouring cells is also observed in mouse ES and epiblast cells (Claveria *et al.*, 2013). Notably, in these scenarios complete engulfment of intact cells is observed, suggesting that entosis may be involved in the competition process, although further studies would be needed to confirm this (Claveria and Torres, 2016).

After dead cell elimination, expansion of the winner cells allows the replacement of the loser population. Proliferation signals produced by loser cells stimulate this compensatory growth, and these signals may be stress-induced or apoptosis-induced (Claveria and Torres, 2016). Interestingly, a proliferative state is not required for cell competition. In a model of postmitotic competition in the *Drosophila* ovarian epithelium, winner cells undergo hypertrophy instead of overproliferation to fill the space left by the loser population (Tamori and Deng, 2013).

1.8. Physiological roles of cell competition

Cell competition is a mechanism senses and optimizes cell fitness in a wide variety of contexts. An important remark is that while cellular fitness is an intrinsic property cells, the outcome of cell competition is determined by fitness comparison with neighbours. The role of cell competition as a fitness-quality control suggests that this mechanism is important in maintaining healthy tissues and its failure might be involved in a wide range of diseases. However, most cell competition models reported are experimentally induced, which limits the identification of its physiological roles. Investigations of natural cell competition need to be explored further, however this is hampered by the pleiotropy of the majority of the pathways involved in this phenomenon (Claveria and Torres, 2016).

1.8.1. Tissue quality control

The first study describing cell competition, already suggested that it could function as a potential quality control mechanism through eliminating less fit cells (Morata and Ripoll, 1975). Later experiments also suggested a role in regulating organ size during development (de la Cova *et al.*, 2004; Moreno and Basler, 2004).

Myc-driven endogenous cell competition in the pregastrulation embryo (Claveria *et al.*, 2013) suggests the implication of competitive behaviours in a natural quality control checking in the epiblast. Interestingly, due to the pluripotency of epiblast cells, these can be eliminated and replaced without compromising embryo development (Claveria and Torres, 2016).

Recently, Azot has been characterized as a mediator of apoptosis induction specifically in several types of cell competition, but not in other stress-response pathways, in *Drosophila* (Merino *et al.*, 2015). The function of Azot in cell death induction is therefore strongly linked to cell competition-induced cell death. Loss of Azot leads to accumulation of defective cells and premature aging (Merino *et al.*, 2015), indicating an important role of tissue quality control during *Drosophila* development and adult tissue homeostasis.

An interesting example of natural cell competition controlling tissue quality is the analysis of lineage displacement in the *Drosophila* female germline, in which cell competition has been proposed to maintain the boundaries between the GSC niche and the differentiating compartment (Jin *et al.*, 2008; Rhiner *et al.*, 2009). Therefore, the proposed function of cell competition is GSC stemness maintenance, although its relevance in maintaining GSC quality during normal oogenesis has not been explored (Jin *et al.*, 2008; Rhiner *et al.*, 2009).

1.8.2. Regeneration

Several studies suggest the implication of cell competition in regeneration. When fetal hepatocytes are transplanted into a damaged adult liver, transplanted cells replace resident cells by progressively eliminating them (Oertel *et al.*, 2006). This colonization of the tissue is not only due to their increased proliferative activity, but also to the induction of cell death of the adult hepatocytes localized close to transplanted cells (Oertel *et al.*, 2006). In addition, experiments in mouse adult heart show that Myc-overexpressing cardiomyocytes can replace WT cells without modifying the function and anatomy of the heart, suggesting a potential role of cell competition also in the maintenance of the myocardium (Villa del Campo *et al.*,

2014). More recently, in a model of *Drosophila* neural regeneration, it has been shown that the comparison of neuronal fitness leads to the elimination of non-scarred injured tissue, helping the damage resolution (Moreno *et al.*, 2015).

1.8.3. Cancer

Finally, the relevance of cell competition for cancer has been extensively hypothesized and explored. Interestingly, cell competition has been characterized both as a tumour-suppressing and as tumour-promoting mechanism.

On one hand, although the expression levels that drive metabolic cell competition do not disrupt normal development or tissue homeostasis, the pathways involved in promoting the winner phenotype promote oncogenesis in humans and tumour formation in experimental models (Claveria and Torres, 2016). Supercompetition has been linked to field cancerization models in which cells carrying pre-oncogenic lesions silently expand in tissues at the expense of surrounding normal cells (Rhiner and Moreno, 2009). Examples of this are the expansion of *Kras* mutation in the intestine (Snippert *et al.*, 2014) and *Notch* mutations in the oesophagus (Alcolea *et al.*, 2014), both driving experimental field cancerization. Other studies connect flower deficiency (Petrova *et al.*, 2012) and SPARC overexpression (Petrova *et al.*, 2011; Yamada *et al.*, 2015) with tumour formation. More recently, cell competition has also been implicated in tumour expansion and invasiveness once the tumour is established (Eichenlaub *et al.*, 2016; Suijkerbuijk *et al.*, 2016).

On the other hand, the pathways involved in structural cell competition are also linked with oncogenesis and carcinoma formation in a variety of tissues. In this case, the tumour-promoting phenotype is mostly associated with the loser fate, indicating a tumour supressing role for cell competition (Kajita and Fujita, 2015; Claveria and Torres, 2016). Other experiments show a tumour-suppressing role when mutations affect individual cells or small number of cells but a tumour-promoting role of cell competition in larger growing tumours (Ballesteros-Arias *et al.*).

2. Early development of the mouse embryo, ESCs and pluripotency

2.1. From fertilization to gastrulation

Development of the zygote or fertilized egg proceeds through symmetric cleavage divisions until the morula is formed. Cells at the early morula stage are totipotent blastomeres, which are able to give rise to all embryonic and extra-embryonic lineages (Gardner, 1998). Removal of one or more cells at this stage (6 to 8-cell embryo) does not affect normal development (Nichols and Smith, 2009). Moreover, the fate of the individual cells can be manipulated by changing their position within the embryo (Hillman *et al.*, 1972) (Figure 5).

After a fixed number of cell cycles, the individual blastomeres compact and at 32-cell stage those blastomeres on the periphery differentiate and form an epithelium called trophectoderm (TE) (Selwood and Johnson, 2006) while a group of cells known as the inner cell mass (ICM) remain internal and pluripotent. Pluripotency is defined as the ability to generate all embryonic cell lineages but not the complete set of extraembryonic tissues. The appearance of the blastocoel, a cavity below the TE produced by fluid pumping, generates the blastocyst (Nichols and Smith, 2009). The ICM then segregates in epiblast, constituted by pluripotent cells precursors of the embryo proper, and the hypoblast or primitive endoderm (PE), which mostly contributes to extraembryonic or non-definitive endoderm. At E3.5, before implantation in the uterus, the three lineages of the blastocyst are well established and this process is autonomous with respect to external cues from fertilization to implantation (Figure 5).

Initial models of epiblast-primitive endoderm segregation considered the early ICM as a homogeneous population in which cells were allocated to the two lineages according to their position with respect to the blastocoel (Chazaud *et al.*, 2006). However, later studies showed that the ICM is already heterogeneous at E3.5. The random “salt and pepper” expression of two transcription factors in a mutually exclusive manner, Nanog and Gata6, determines the two lineages within a single cell population and then these lineages segregate by sorting out into the primitive

endoderm, facing the blastocoel, and the epiblast, positioned between the trophectoderm and the primitive endoderm (Chazaud *et al.*, 2006) (Figure 5).

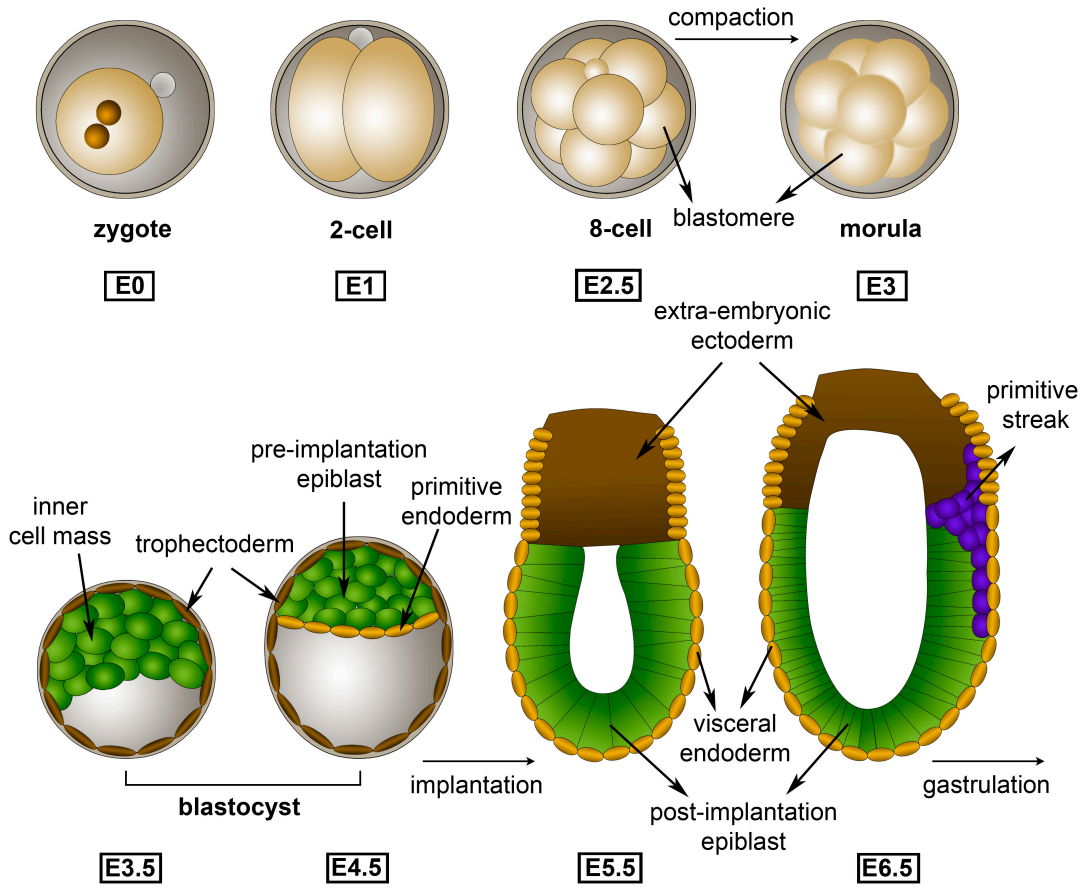

Figure 5. Overview of some stages of early mouse embryogenesis.

Frontal view of the pre- and post-implantation embryo at different stages. The zygote undergoes symmetric cleavages giving rise to the morula, which is then compacted. At E3 blastomeres start to segregate and form the trophectoderm, which is the first event of differentiation. At E3.5, the second event of differentiation takes places and some cells from the inner cell mass form the primitive endoderm. Later, the blastocyst hatches from the zona pellucida and implants in the uterine wall. The primitive endoderm migrates to become the parietal and visceral endoderm, which covers the epiblast. At E6, the epiblast is a monostratified epithelium. Gastrulation begins at E6.5 when some cells of the posterior pole undergo an epithelial-mesenchymal transformation to generate mesoderm and form the primitive streak.

Later, the blastocyst hatches from the zona pellucida and implants in the uterine wall. As a natural selection checkpoint, only embryos able to hatch continue developing, invading the maternal tissue and implanting (Bedzhov *et al.*, 2014). After implantation, the trophectoderm becomes the trophoblast and contributes to extraembryonic membranes, while the epiblast generates the embryo plus some extra-embryonic tissues. In the first two days post-implantation, the mural trophectoderm (cells that surrounds the blastocyst cavity that are not in contact with the ICM) gives rise to polyploid Trophoblast Giant Cells (TGCs), which represent the first terminally differentiated cell type (Bedzhov *et al.*, 2014). Contrary to this, the polar TE, which surrounds the outer surface of the ICM, is the source of multipotent progenitors, the TE stem (TS) cells. These cells proliferate and become the ectoplacental cone (EPC) that builds the proximal half of the egg cylinder and later contributes to the placenta, and the extraembryonic ectoderm (ExE). The primitive endoderm migrates to become the parietal endoderm, which covers the inner surface of mural TE, and the visceral endoderm, which covers the egg cylinder and epiblast. By six days after fertilization, the epiblast is a cup-shaped monostratified epithelium of ~1000 cells (Figure 5).

At 6.5 days after fertilization the first morphological sign of embryonic patterning is evident when gastrulation begins (Beddington and Robertson, 1999). Some cells of the future posterior pole of the epiblast, which is apparently a homogeneous epithelium, undergo epithelial-mesenchymal transformation (EMT) to generate mesoderm and form the primitive streak (Beddington and Robertson, 1999). Cells move through the streak and spread forward to form mesoderm. The visceral endoderm is replaced by the definitive endoderm that derives from the epiblast (Figure 5). During the next hours, the streak elongates from the rim to the distal tip of the cup and the node forms. This specialized structure is considered homologous to the organizer of other vertebrate embryos and gives rise to the axial gastrulating cells that comprise the axial mesoderm (future prechordal plate and notochord) and the definitive gut endoderm (Beddington and Robertson, 1999).

2.2. Embryonic Pluripotency: defining the Naive and Primed pluripotent states in mammalian development

The mammalian egg is totipotent as it can give rise to the entire embryo. However, this does not mean that the zygote can directly differentiate into the all cell types. In fact, the egg and the blastomeres derived from it produce directly only two types of cells: trophectoderm cells and cells from the inner cell mass (Nichols and Smith, 2009).

As mentioned before, pluripotency is the capacity of cells to produce all three embryonic germ layers, but not trophectoderm-derived extra-embryonic tissues (Hanna *et al.*, 2010). Pluripotency is not a single status, but evolves in a highly dynamic manner through different stages of pre- and post-implantation development. To develop, the ICM must be able to generate other cell types in a flexible manner (Gardner and Beddington, 1988; Nichols and Smith, 2009). The early ICM is the founder pluripotent population. Once it segregates into PE and epiblast at the late blastocyst stage, the epiblast retains the pluripotency, while the PE loses it and commits with the endodermal fate. Following segregation of PE, the epiblast of the late blastocyst (embryonic day 4.0) acquires a pluripotency state known as "naive" or "ground state" (Hackett and Surani, 2014). The naive state pluripotent epiblast is functionally and molecularly different from blastomeres and early inner cell mass (Gardner, 1998; Kurimoto *et al.*, 2006; Kaji *et al.*, 2007; Nichols and Smith, 2009). The naive state is characterized by homogenous expression of key pluripotency transcription factors and by the elimination of gametic epigenetic silencing, which results in a generalized hypomethylated "open" chromatin state, including both X-chromosomes in female embryos. The "naive state" is therefore considered as the unrestricted pluripotent state in which cells show an unbiased developmental potential.

Departure from the naive status starts in the epiblast shortly after implantation; however, pluripotency is maintained for several days before differentiation starts during gastrulation (E6.5). The transit between naive-state epiblast cells takes place in a continuum manner in which cells transit through a "formative" phase into an "primed" pluripotency state before they actually commit

with a particular fate and differentiate (Nichols and Smith, 2009; Hackett and Surani, 2014; Kalkan *et al.*, 2017).

In addition, both states are characterized by expressing the core pluripotency network. Initially this regulatory network was almost exclusively referred to a small set of transcription factors, Oct4, Sox2 and Nanog (Orkin, 2005). These three factors converge and form the primary, yet central, network that governs the robust pluripotent state. On one hand, Oct4 is essential for early mouse development and maintenance of the ES cell pluripotency (Nichols *et al.*, 1998). On the other hand, Sox2 is generally considered a transcriptional partner of Oct4 (Avilion *et al.*, 2003). And finally, the presence of Nanog in tissue culture relieves the requirement for LIF by promoting ES cell self-renewal (Chambers *et al.*, 2003; Mitsui *et al.*, 2003). In spite of the relevance of these key transcription factors and their cooperative autoregulation to maintain ESCs properties, some studies also point to the involvement of additional factors that either provide feed-forward regulations to stabilize the pluripotency network, or exert other cellular functions required for ESC identity maintenance (Ivanova *et al.*, 2006; Wang *et al.*, 2006; Zhou *et al.*, 2007).

2.3. Naive and Primed stem cell pluripotent states in culture

The different types of pluripotency observed in vivo can be captured in apparently equivalent states in cultured cells. The transient nature of naive pluripotency is captured *in vitro* in ESCs derived from the ICM or through experimental reprogramming (Evans and Kaufman, 1981; Martin, 1981; Yamanaka and Blau, 2010; Hackett and Surani, 2014) (Figure 6). ESCs represent a surrogate *in vitro* model of the naive epiblast status that, under permissive culture conditions, keeps naive pluripotent capacity while undergoing self-renewal. On the other hand, both *in vitro* models of epiblast stem cells (EpiSCs) derived from late epiblast (Brons *et al.*, 2007; Tesar *et al.*, 2007) and epiblast-like cells (EpiLCs), which are derived from ESCs showing a cellular state highly similar to pregastrulating epiblasts but distinct from EpiSCs (Hayashi *et al.*, 2011), capture the primed pluripotent state (Figure 6), which provides another system to study pluripotency and cell fate decisions.

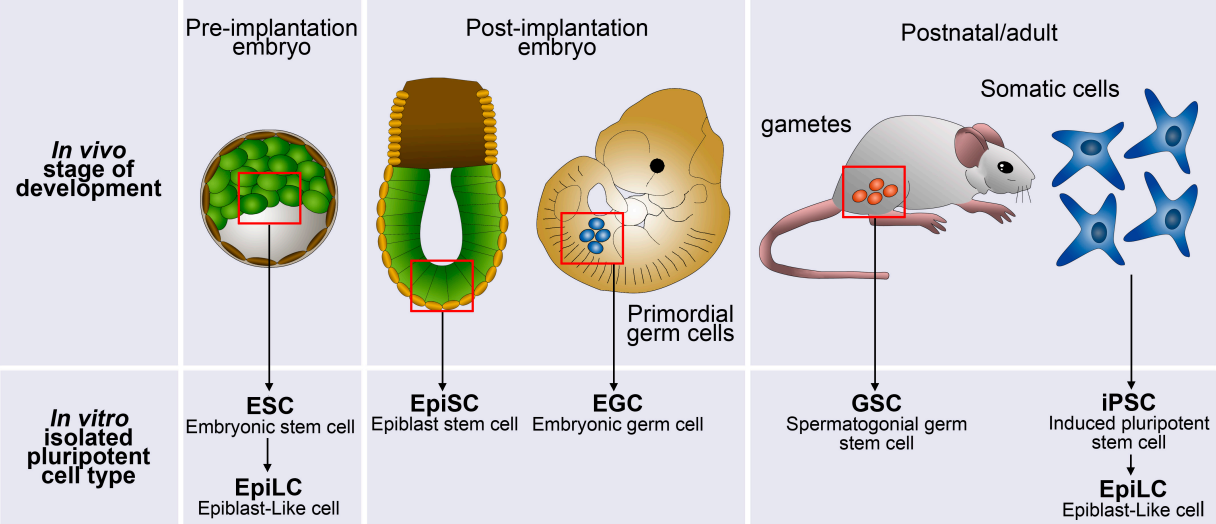

Figure 6. Scheme of different types of mouse pluripotent stem cells and their sources.

Several pluripotent cell types can be derived by explanting cells at various stages of early mouse embryonic development. ESCs are derived from cells harvested at the blastocyst stage. Pluripotent cells derived from post-implantation embryo give rise to epiblast stem cells (EpiSCs). Embryonic germ cells and spermatogonial germ cells (GSC) are derived from primordial germ cells (PGCs) from embryos and spermatogonial progenitors from adults respectively. Alternatively, somatic cells can be directly reprogrammed *in vitro* by exogenous expression of transcription factors generating induced pluripotent stem cells (iPSCs). In addition, epiblast-like cells (EpiLCs) can be generated from either ESCs or iPSCs in a progressive process.

The definition of both states implies that the naive ESCs correspond to a more immature state of pluripotency whereas the primed state is prone to differentiate, which is reflected, for example, in the state of X-chromosome inactivation. In naive female cells, both chromosomes are active; on the contrary, primed EpiSCs have already undergone X-chromosome inactivation (Hanna *et al.*, 2010).

Furthermore, the two pluripotent states exhibit distinct molecular signatures and *in vitro* growth properties (Figure 7). In addition, the two states depend on signalling pathways that often antagonize each other (Hanna *et al.*, 2010). Although the core pluripotency network is expressed in both naive and differentiating-primed states (Wang *et al.*, 2006), they differ in the signalling pathway they rely on (Figure 7). The BMP/SMAD signalling pathway (Ying *et al.*, 2003) and LIF/STAT3 (Smith *et al.*, 1988) maintain naive pluripotency of ESCs, whereas FGF/MAPK promotes

transition to the primed state and, together with Activin/Nodal promote definitive differentiation (Brons *et al.*, 2007; Tesar *et al.*, 2007) (Figure 7).

Based on this knowledge, different culture conditions can promote the different states of pluripotency found in the embryo. Fetal bovine serum, together with mouse embryonic fibroblasts (MEFs), was originally used to derive ESCs (Martin and Evans, 1975). Serum contains BMP4, which is crucial for activating Inhibitor of Differentiation (*Id*) genes via SMAD pathway (Figure 7). Serum can be thus substituted by overexpression of *Id* genes or exogenous addition of BMP4 (Hackett and Surani, 2014). However, serum contains as well FGF and activin-like activities that promote exit from the ground state and differentiation and MEFs were important in limiting this differentiation promotion. LIF, which activates the JAK-STAT3 signalling pathway (Figure 7), was later reported to be essential for enabling the proliferation of ESCs without MEFs (Smith *et al.*, 1988; Williams *et al.*, 1988).

Maintenance of naive pluripotency can be achieved by serum/LIF culture conditions. However, in these conventional conditions self-renewal is maintained by abrogation or counterbalance of differentiation stimuli downstream of their effects. Therefore, in serum/LIF ESCs exist in a battleground of competing signals and exhibit heterogeneous expression of pluripotency markers that gives rise to metastability. In fact, only a fraction of these cells correlate with the pre-implantation epiblast, as shown by transcriptional and epigenetic profiling (Ying *et al.*, 2008; Marks *et al.*, 2012; Boroviak *et al.*, 2014).

It is thus preferable to insulate, rather than counteract, differentiation stimuli in order to stabilize upstream naive state. Two inhibitor (2i) molecules have been found sufficient to protect ESCs from differentiation stimuli and select against differentiating cells. PD03 (PD0325901) inhibits FGF/ERK signalling pathway by blocking ERK1/2 phosphorylation (Ying *et al.*, 2008), which appears to drive transition from naive to primed state (Kunath *et al.*, 2007) (Figure 7). In the presence of PD03 LIF is still required to support ESC naive and self-renewing state. GSK3 inhibition enhances ESC self-renewal (Sato *et al.*, 2004; Ogawa *et al.*, 2006), and the inclusion of the GSK3 inhibitor, CHIRON (CHIR99021) (Figure 7) in addition to PD03 sustains ESC naive state propagation, even in the absence of LIF or

serum/BMP4 (Ying *et al.*, 2008). Collectively PD03 and CHIRON inhibitors are known as the "2i" culture system. In 2i/LIF cultures most of ESCs exhibit molecular and functional properties corresponding to an optimized state of naive pluripotency that is closely comparable to the developmental ground state in vivo. Therefore, ESCs in 2i cultures retain the essential features of early epiblast pluripotent cells (Boroviak *et al.*, 2014), being considered the best current approach as a model for naive epiblast cells.

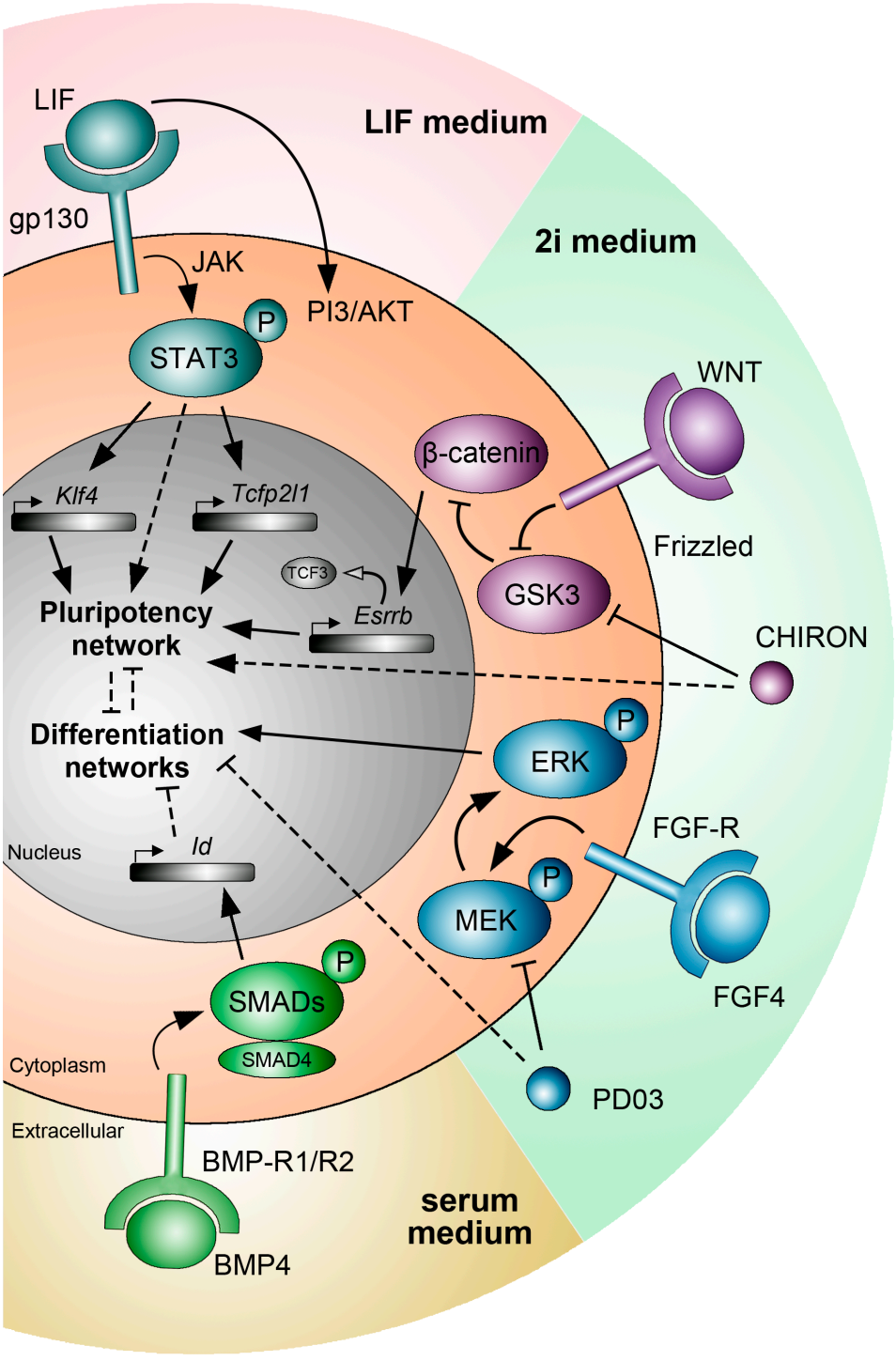

Figure 7. Schematic of the main extrinsic signalling pathways that determine the naive and primed pluripotent states.

Naive and primed mouse pluripotent stem cells can be positively or negatively regulated by different signalling pathways. LIF mainly acts phosphorylating STAT3 via JAK, which activates *Tfcp2l1* and *Klf4* reinforcing the pluripotency network. When cells are grown with serum, BMP4 is present in the medium and functions via SMADs to activate *Id* genes blocking the differentiation networks. When 2i medium is used to culture cells, CHIRON acts via GSK3 inhibition, mimicking canonical WNT signalling. GSK3 blockade leads to β-catenin stabilization, which abrogates TCF3-mediated repression of pluripotency genes, including *Esrrb*. PD03 blocks MEK activity of the FGF signalling cascade. FGF activates the MAPK pathway leading to MEK phosphorylation that phosphorylates and activates ERK. The active form of ERK promotes transition to a primed state. Filled arrows indicate activation, whereas bars mean inhibition or blockade of target activity. Dashed lines show an indirect or deduced effect and a solid line indicates a direct or known downstream target. (Based on (Hackett and Surani, 2014)).

Additionally, investigation about pluripotency has been enhanced after the discovery of cell reprogramming by forced expression of a set of transcription factors, which also provided an enormous potential for regenerative medicine. Previous studies show that somatic cells can be reprogrammed by transferring their nuclear contents into oocytes (Wilmut *et al.*, 1997) or by fusion with ESCs (Tada *et al.*, 2001; Cowan *et al.*, 2005) indicating that unfertilized eggs and ES cells contain factors that can confer totipotency or pluripotency to somatic cells. However, a later works demonstrated the flexibility of cellular identity by the full reprogramming of differentiated somatic cells to pluripotent stem cells through forced expression of a set of transcription factors. These new generated pluripotent cells are called induced pluripotent stem cells (iPSCs) (Takahashi and Yamanaka, 2006). The initial genes identified as responsible for reprograming adult cells are *Oct3/4*, *Sox2*, *Klf4* and *Myc* (Takahashi and Yamanaka, 2006).

3. The proto-oncogene Myc family in development

3.1. Functions of the transcription factors of the Myc family in mammalian development

During the last decades, the role of the proto-oncogene *Myc* gene family (comprising 3 transcription factors: Myc, Mycn and Mycl) in normal and cancer cells has been extensively studied. The fact that *Myc* genes are deregulated in most tumours has attracted attention across the cancer research field. Nevertheless, in this thesis we are interested in non-oncogenic roles of this family in normal development, pluripotency and cell competition. The three main members of the proto-oncogenic Myc family are involved in several cellular processes, such as the regulation of cellular proliferation, differentiation and apoptosis (Meyer and Penn, 2008). The role of Myc proteins in development has been intensively investigated. Even though Mycl is widely expressed in the mouse embryo, it appears not to be necessary for embryonic development, as *Mycl* knockout mice develop normally (Hatton *et al.*, 1996). Contrary to this, Myc deficient embryos die before E10.5 due to hematopoietic and placental defects (Trumpp *et al.*, 2001; Dubois *et al.*, 2008) and embryos lacking Mycn are die at E11.5 exhibiting neuroectodermal and heart defects (Charron *et al.*, 1992), indicating that endogenous Myc and Mycn are critical for completing embryogenesis. However, they have also been shown to be separately dispensable for murine embryonic stem cell function. The lack of phenotype of the single KOs suggests highly redundant functions of Myc and Mycn (Malynn *et al.*, 2000). Moreover, recently it has been shown that Myc and Mycn cooperate in maintaining the ESC proliferative program (Scognamiglio *et al.*, 2016).

3.2. Myc factors and pluripotency

Myc has been reported to regulate cell cycle regulation, cell growth and metabolism in ESC, by regulating a different subset of genes than those targeted by the core pluripotency network transcription factors (Chen *et al.*, 2008; Hu *et al.*, 2009; Kim *et al.*, 2010; Claveria *et al.*, 2013; Gu *et al.*, 2016; Scognamiglio *et al.*, 2016) and has multiple roles in several stem and progenitor cell types (Laurenti *et al.*,

2009). Myc also controls the balance between self-renewal and differentiation in adult hematopoietic stem cells (Wilson *et al.*, 2004).

Additionally, in ESCs cultured in serum plus LIF, Myc proteins have been suggested to sustain pluripotency through repression of the primitive endoderm master regulator GATA6 and contribute to the cell cycle control by regulating the mir-17-92 miRNA cluster (Smith *et al.*, 2010).

Furthermore, Myc has been described to promote cell reprogramming of somatic cells into a naive pluripotent status in cooperation with transcription factors of the core pluripotency network, such as Oct4, Sox2 and Klf4 (Cartwright *et al.*, 2005; Takahashi and Yamanaka, 2006). In addition, primed EpiSCs can also be reverted to the naive state by overexpressing Klf4 or Myc in EpiSCs under LIF-exposure conditions (Guo *et al.*, 2009; Hanna *et al.*, 2009). More recently, ESC self-renewal capacity has been reported to be maintained thanks to a Myc-dependent self-propagating epigenetic memory, which is established by a Myc-driven positive feed-back loop (Fagnocchi *et al.*, 2016).

Even though several studies have tried to shed light on the relationship between Myc and pluripotency and some roles have been reported both *in vivo* and *in vitro*, the precise role of Myc with respect to pluripotency states in embryos and cultured cells remain elusive.

OBJECTIVES

In the field of Cell Competition, many studies have tried to shed light on how fitness comparison is produced between neighbouring cells and results in the elimination of the less fit cells. Natural cell-to-cell heterogeneity in Myc levels has been reported to trigger cell competition both in early mouse development and ESCs. In this thesis, we aimed to perform further studies to understand the dynamics of Myc-related endogenous cell competition and explore the biological relevance of this phenomenon during normal mouse development and ESC maintenance.

The specific aims of this thesis were:

Generate a new time-lapse microscopy and image analysis tool to track Myc levels during cell competition in ESCs.

Determine the dynamics of Myc heterogeneity and how it is regulated in pluripotent cells.

Determine how the cell-to-cell Myc heterogeneous levels lead to cell competition and the dynamics of Myc expression during the process.

Determine the biological basis of Myc-driven endogenous cell competition *in vitro* and *in vivo*.

MATERIALS AND METHODS

1. Mouse lines and mESC derived lines

The *iMOS*^{WT}, *iMOS*$^{T1\text{-}Myc}$ and *iMOS*$^{T2\text{-}p35}$ mouse lines have been previously described (Claveria *et al.*, 2013). After recombination both labelled populations are WT in the *iMOS*^{WT} cell line. In the *iMOS*$^{T1\text{-}Myc}$ the EYFP population overexpresses Myc and ECFP cells are WT. In the *iMOS*$^{T2\text{-}p35}$ the EYFP population is WT and the ECFP population expresses the baculoviral apoptosis inhibitor p35.

Sox2Cre mice (Hayashi *et al.*, 2002) were used to activate the *iMOS*$^{T2\text{-}p35}$ line when the experiment was performed in embryos and to generate the Myc KO from the Myc$^{flox/flox}$ line.

The GFP-Myc reporter line has been previously described (Huang *et al.*, 2008). Homozygous mice are viable and show no apparent phenotypic alterations.

WT mice used are of the CD1 strain.

Mouse embryonic stem cells were derived from E3.5 embryos from the following mouse lines: *iMOS*^{WT}, *iMOS*$^{T1\text{-}Myc}$, *iMOS*$^{T2\text{-}p35}$ and GFP-Myc. The protocol for establishing ESC lines is explained below.

2. E5-6 embryo harvest

Mice embryos were extracted at different developmental stages. Vaginal plugs were checked every morning. Midday of the day when vaginal plug is detected is considered gestational day 0.5 (E0.5). To obtain the embryos, females were sacrificed by CO_2 inhalation and abdominal cavity was opened to expose the uterus, which was transferred to sterile PBS. Then working in cold PBS under the scope, muscular uterine wall was carefully ripped and then the decidual layer was removed. Exposed embryos were fixed in paraformaldehyde (PFA) (Merck) 2% in PBS overnight at 4ºC. After fixation embryos were washed in PBS several times.

3. Mouse embryonic fibroblasts culture

Mouse embryonic fibroblasts (MEFs) were only used as a feeder layer for the stem cells. Fibroblasts have been previously extracted from E10.5 embryos by the Pluripotent Cell Technology Unit staff. Approximately 5 million of cells from one vial were plated on 100-mm 0.1% gelatine-coated plastic plates (Falcon). After 2 days cells were passed to 2 150-mm 0.1% gelatine-coated plastic plates (Falcon) and cultured again for another 2 days. Fibroblasts were then inactivated with mitoMycin-C (Sigma), trypsinized (Trypsin-EDTA 10x, Gibco) and frozen. MEF culture medium contained the following reagents:

- High glucose DMEM, GlutaMAX™ Pyruvate (LifeTech)
- 15% Fetal Bovine Serum (FBS)
- 1% Penicillin/Streptomycin (10,000U/ml; 100x)
- 0,2% 2-beta-mercaptoethanol (50mM)

MEFs freezing medium contained:

- 60% MEF culture medium
- 20% FBS
- 20% DMSO (Sigma)

4. Mouse ESC derivation and establishment

Mouse ESCs were derived from E3.5 embryos. Female sacrifice and uterus extraction was done as described. Embryos extraction was performed by flushing the blastocysts out of the uterus under a dissection scope using a 1-ml syringe with 23-G needle. Blastocysts were collected and transferred individually to wells of a 24-well plate (Falcon) containing fresh mitoMycin-C-inactivated MEF feeder layer. Culture was maintained for 5-8 days in 2i (GSK3β and Mek 1/2 inhibitors) medium. Medium was not changed until the blastocysts attached, then it was changed every day. Those hatching blastocysts whose inner cell mass expanded were properly trypsinized and seeded on a well of 12-well plate (Falcon) and then went through several passages in order to expand the clone.

2i derivation medium contained:

- High glucose DMEM, GlutaMAX™ Pyruvate (LifeTech)
- 15% KO-Serum Replacement (Invitrogen)
- Leukemia Inhibitor Factor (LIF)
- 1% nonessential amino acids (100x)
- 1% Penicillin/Streptomycin (10,000U/ml; 100x)
- 0.3 μM GSK3β inhibitor CHIR99021 (Stemolecule™)
- 0.1 μM Mek 1/2 inhibitor PD0325901 (Stemolecule™)

Cultures were checked for Mycoplasma by the Cell Culture Unit staff and for normal karyotype (protocol explained below) at their establishment.

For time-lapse studies, the ESC lines were stably transfected with a PGK-tdTomato construct that drives expression of a membrane-attached Tomato fluorescent protein.

4.1. Karyotyping

Approximately 1,5x10^6 cells in a p-60mm plate (Falcon) were treated with 0,5μg/ml colcemid (KARYO MAX COLCEMID, Gibco) for 1 hour at 37ºC. Cells were then trypsinized and resuspended in 6 ml of a hypotonic solution (75mM KCl) for 7 minutes at room temperature. 8 drops of a fixative solution (3:1 methanol/glacial acetic acid) were added and then centrifuged for 5 minutes at 900rpm at room temperature. Supernatant was removed and 6ml of the fixative solution were added again, letting 20 minutes in ice. This last step was repeated twice. Finally, a small volume of the solution was dropped on a slice, dried and mounted with DAPI. Karyotype of a cell line was considered suitable when more than 80% of the cells exhibited normal karyotype.

5. Mouse ESC routine culture

ESCs were routinely maintained on mitoMycin-C-inactivated MEF feeder layers. Cells were passed every 2 days and frozen 800,000-900,000 cells per vial. ESC routine culture medium (SR-ES medium) contained the following reagents:

- High glucose DMEM, GlutaMAX™ Pyruvate (LifeTech)
- 15% KO-Serum Replacement (Invitrogen)
- Leukemia Inhibitor Factor (LIF)
- 1% nonessential amino acids (100x)
- 0,1% 2-beta-mercaptoethanol (50mM)

mESCs freezing medium contained:

- 60% ESC culture medium
- 20% FBS
- 20% DMSO (Sigma)

6. *iMOS* induction for functional assays in ESCs

For the $iMOS^{T1\text{-}Myc}$ and $iMOS^{T2\text{-}p35}$ induction, cells were plated without feeder on fibronectin-coated 3.5-mm glass bottom dishes (MatTek) and cultured in 2xLIF SR-ES medium. After 24h $iMOS^{T1\text{-}Myc}$ cells were treated with 10 µM 4-hydroxytamoxifen (4-OHTAM) (Sigma-Aldrich) and $iMOS^{T2\text{-}p35}$ cells with 20 µM for 24 h and cultured for additional 24 h.

7. Immunofluorescence

7.1 Whole mount embryo immunofluorescence

For E5-E6.5 embryos, same procedure was followed for all the stainings. Embryos were permeabilized in 0.5% Triton X-100 (Calbiochem) for 30 minutes. Excess of triton was washed in PBS during 15 minutes. Blocking was performed in

10% goat serum (Gibco-BRL Life-Technologies) 0.1% Triton X-100 for one hour and then incubation with the primary antibodies was performed overnight at 4ºC. Embryos were washed several times and incubated with secondary antibodies and DAPI (1:2000) overnight at 4ºC. Following day and after several washes, embryos were ready to be imaged and store in PBS or Vectashield mounting medium (Vector Laboratories, USA). Primary and the secondary antibodies were diluted in the blocking solution.

7.2. Mouse ESC immunofluorescence

For mouse ESCs the same protocol was followed for all the stainings, excepting for pSTAT3 immunofluorescence. Fixed samples were permeabilized in 0.25% Triton X-100 (Calbiochem) from 10 to 30 minutes depending on the antibody, washed in PBS and blocked with 10% goat serum 0.1% Triton X-100 for one hour. Incubation with the primary antibodies was performed at room temperature for one hour. After several washes, secondary antibodies and DAPI (1:2000) were incubated during 1 hour at room temperature. Cells were then washed and mounted in Vectashield mounting medium.

For pSTAT3 staining, cells were permeabilized in cold 100% methanol for 10 minutes at -20ºC and the blocking solution contains 5% goat serum in 0.25% Triton X-100. Primary and the secondary antibodies were diluted in the blocking buffer.

7.3. Primary antibodies

- anti-Myc polyclonal antibody (06-340, Millipore) 1:300
- anti-Myc T58 (ab85380, abcam)
- phospho-p44/42 MAPK (Erk1/2) (Thr202/Tyr204) (#4370, Cell Signaling) 1:200
- anti-phospho-histone H3 (Ser 10) 'mitosis marker' (06-570, Millipore) 1:300
- Phospho-Histone H3 (Ser10) (6G3) (#9706, Cell Signaling) 1:300
- cleaved-caspase3 (Asp175) Antibody (#9661 Cell Signaling) 1:100

- phospho-Stat3 (Tyr705) D3A7 (#9145, Cell Signaling) 1:100
- anti-GFP (GFP-1010; Aves Lab) 1:500
- phospho-p44/42 MAPK (Erk1/2) (Thr202/Tyr204) (#9106 or #4370, Cell Signaling) 1:200
- Mycn (NCM II 100; sc-56729, Santa Cruz) 1:100
- Anti-mouse Nanog purified (14-5761-80, eBioscience) 1:200

7.4. Secondary antibodies

All of them were used 1:500.

- 488 goat anti-rabbit (Life Tech)
- 488 goat anti-mouse (Life Tech)
- Cy3 goat anti-rabbit (Jackson)
- 568 goat anti-mouse (Life Tech)
- 568 goat anti-chicken (Life Tech)
- 633 goat anti-rabbit (Life Tech)
- 633 goat anti-mouse (Life Tech)
- 647 donkey anti-chicken (Jackson)

8. Confocal microscopy

Immunofluorescence of fixed cells was imaged with either a Leica TCS SP5 inverted conventional confocal microscope fitted with a HCX PL APO CS 40x 1.25 oil objective, an SP8 inverted conventional confocal microscope fitted with HC PL Apo CS2 40x/1.3 oil objective, or a Zeiss LSM 780 upright microscope fitted with W Plan-Apochromat 40x/1,0 DIC M27 objective. Whole mouse embryos were imaged with a Zeiss LSM 780 upright microscope fitted with a W Plan-Apochromat 20x/1,0 DIC M27 75mm WD 1.8mm objective in confocal mode at 405, 488, 568 or 663 nm. Z-stacks were acquired in order to image the whole embryo. Acquisitions were commonly 1024x1024 pixels, A.U. set to 1.5.

9. Time-lapse video microscopy of ESC cultures

200,000 GFP-Myc ESCs were seeded on 3.5-mm 0.1% gelatine-coated plastic plates (Falcon) without feeder and cultured in 2xLIF SR-ES medium. 24 h later cells were transferred to the environmental chamber of a Zeiss LSM 780 upright microscope. In every imaging experiment, the incubation chamber was previously stabilized to 37ºC and 5% CO2 by mixing and humidification. To avoid liquid evaporation, embryo-grade mineral oil was added on top of the medium after objective immersion. Samples were imaged with a W Plan-Apochromat 40x/1,0 DIC M27 objective every 7 minutes for 24 h. Z-stacks with sections spaced at 2 µm are acquired at each timepoint. In addition, a multi-position map was generated, and every ESC colony was manually assigned an x-y-z location. We used confocal lasers with two excitation channels (488 nm excitation for GFP-Myc visualization and 561 nm excitation for the tdTomato membrane marker), and all images were 512x512 pixels (0.415x0.415 µm resolution), taken at speed 7 and with 2 scans/Z-slice. A trade-off between spatial resolution, temporal resolution and total acquisition time was carefully selected to minimize photobleaching while enabling tracking of cell division, apoptosis and cell-cell interactions. For apoptosis detection, we added either Hoechst33258 (B-2883, Sigma) (1:2000) or caspase3-reporter (CaspGLOW™ Red Caspase Staining kit, MBL) (1:1000) to the medium immediately before imaging.

For *iMOS*$^{T1\text{-}Myc}$ induction analysis, we started time-lapse confocal analysis 10 h after the induction. The timings of new EYFP^{+} cells and apoptotic events were scored manually.

In the GFP-Myc and *iMOS*$^{T1\text{-}Myc}$ coculture, both populations were seeded in a proportion 1:1. The timings of new EYFP^{+} cells and apoptotic events were scored manually.

10. Clonal analysis assay

150,000 ESCs were plated without feeder on fibronectin-coated 3.5-mm glass bottom dishes (MatTek) and cultured in 2xLIF SR-ES medium. To generate clones we used the *iMOS*^{WT} cell line (Claveria *et al.*, 2013) and induced EYFP clones at a very

low recombination rate. For this, cells were treated 48h after plating for 1 h with 5 µM 4-hydroxytamoxifen (4-OHTAM) (Sigma-Aldrich) and cultured for an additional 60h. Only 15% of colonies were recombined, so the expected frequency of polyclonal groups was around 2% (0.15^2X100). Cells were fixed and analyzed by confocal immunofluorescence for Myc, and subject to confocal analysis. We then calculated the variation of Myc levels within clonal groups identified by EYFP signal and for a set of equivalent randomly chosen cell groups. We repeated the process at least 100 times per colony to have a sample representative of the whole population and considered the median standard deviation of the 100 subsamples.

11. Flow Citometry

For cell cycle analysis, cells were trypsinized, incubated in culture medium with 5 µg/ml Hoechst33342 (B2261-Sigma) for 45 minutes at 37ºC, washed and resuspended in 2% FBS PBS and analysed by flow cytometry in a BD FACSCanto™ II (laser wavelengths 405, 488, 561, 640). Propidium iodide (P4864-Sigma) was used to identify dead cells.

For the DNA demethylation experiments, 5-Azacytidine was previously dissolved at 20.5 mM in water:acid acetic (1:1) and cells were treated with 0,25 µM 5-Azacytidine (A2385, Sigma). After treatment cells were washed, trypsinized, resuspended in 2% FBS PBS and stained with Hoechst33258 (B-2883, Sigma) for dead cell exclusion. Cell suspensions were analysed in a BD LSRFortessa™ Special Order Research Product (laser wavelengths 405, 488).

For the LIF withdrawal assay, cells were trypsinized, resuspended in 2% FBS PBS and stained with Hoechst33258 (B-2883, Sigma) for dead cell exclusion. Cell suspensions were analysed in a BD LSRFortessa™ Special Order Research Product (laser wavelengths 405, 488, 561).

For the analysis, FACSDiva and FlowJo softwares were used.

12. RNA isolation from cells

In order to perform RNA differential expression analysis, RNA from cells was isolated. For assess the difference in gene expression depending on Myc levels, total RNA was purified from GFP-Myc ES cells sorted in BD FACSAria™ II flow cytometer according to GFP-Myc (three biological replicas). RNA was extracted using RNeasy Mini Kit (Qiagen). Isolated RNA was then handed to Genomic Unit in CNIC to proceed with sequencing.

13. RNASeq. Data analysis

13.1. RNAseq library production

In order to assess the difference in gene expression among the three populations depending on Myc levels, total RNA was purified from ES cells sorted in a cytometer according to GFP-Myc (three biological replicas). A cDNA library was prepared according to Illumina recommendations and sequenced in a GAII analyzer using the paired-end 50bp protocol. Sequencing reads were pre-processed by means of a pipeline that used FastQC to asses read quality, and Cutadapt v1.3 (Martin, 2011) to trim sequencing reads, eliminating Illumina adaptor remains and discarding reads shorter than 30 bp. Reads were mapped against the mouse transcriptome (GRCm38 assembly, Ensembl release 76) and quantified using RSEM v1.2.3 (Li and Dewey, 2011).Raw data have been deposited in the GEO database with reference number GSE89196 .Raw expression counts were then processed with an analysis pipeline that used the Bioconductor package EdgeR (Robinson *et al.*, 2010) for normalization and differential expression testing. Only genes expressed at a minimal level of 1 count per million, in at least 3 samples, were considered for differential expression analysis.

13.2. RNAseq meta-analysis

Gene set enrichment analysis was performed using the online tools in the Broad Institute GSEA web site (http://software.broadinstitute.org/gsea/). Genes with significant variation between Myc-H and Myc-L cells (adj pval <0.001) were

screened against the curated "chemical and genetic perturbations" database. 8 of the top-ten hits corresponding to experiments in embryonic stem cells were gene sets identifying targets of pluripotency factors (p-values between $<3.78^{-25}$ and $<1{,}73^{-62}$).

For Principal Components Analysis, we compared our RNA-seq dataset to Gene Expression Omnibus RNA-Seq datasets GSE67259 and GSE56138. For GSE67259 dataset, expression levels in RPMs were compared with the TPMs calculated from FPKMs of dataset GSE56138 and to the TPMs of our dataset. For each gene symbol, we considered the TPMs of all samples from all datasets. 16,998 genes were expressed in all experiments. Combat (Robinson *et al.*, 2010) without covariate was then used on the log2-TPMs matrix to remove batch differences among the datasets. ggfortify and gplots packages were used for visualization of the Principal Components Analysis and main gene set contributing to the Principal Component 1.

14. Image analysis

14.1. Nuclear and cytoplasmic signal detection

Confocal images were analyzed with ImageJ (http://imagej.nih.gov/ij). To quantify nuclear signal, nuclei were detected by DAPI staining and segmented by using threshold tool to create a mask. Manual correction was applied to ensure the segmented objects belonged to individual cells. Masks were applied to the corresponding channel and a measure tool gave the mean intensity for every single object. For cytoplasm signal quantification masks were obtained by subtracting DAPI mask to the whole cell mask, which was created thanks to Tomato membrane marker. Signal intensity measuring was performed as in the nuclei.

14.2. Video editing

Time-lapse videos were edited using Imaris x64 sotware. Imaris allowed to generate a video file from lsm format files (Zen lite files from Zeiss microscopy). Videos were re-edited with Adobe After Effects software.

14.3. 4D tracking workflow

Image processing and analysis methods were developed using Definiens Developer version XD2.4 (Definiens AG, Germany) and Matlab (R2015a, Bioinformatics, Image Processing, Optimization, Statistics and Machine Learning toolboxes). A manual-editing tool was implemented, allowing the user to visualize and correct errors. Quantitative cellular parameters in the pipeline are automatically extracted from the segmented and tracked nuclei, generating tables ready for data mining. The tables contain information on cell and nuclear position and shape, nuclear GFP intensity, cell neighbourhood, nuclear size, mitosis and apoptosis. The complete set of primary data generated is in Table 1.

During time-lapse analysis, photobleaching of GFP-Myc fluorescence produced a progressive signal reduction throughout the first third of the tracking period (Figure 8). After the initial photobleaching, the GFP-Myc signal was stable during the remainder of the tracking period (Figure 8). To avoid interference from photobleaching during the analysis, we used established methods (Gopinath *et al.*, 2008) to normalize the values, using the endpoint mean and standard deviation as reference values. All quantitative analyses were made using the normalized data. This procedure allowed to perform meaningful *in silico* synchronizations.

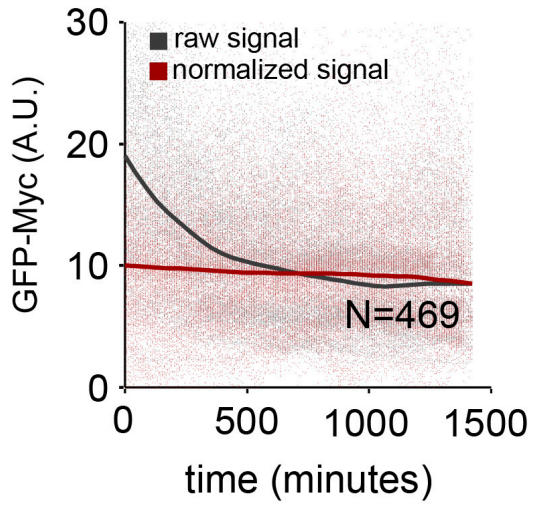

Figure 8. Correction of GFP-Myc signal after photo-bleaching.

Graph displays individual data (dots) and locally weighted scatterplot smooth lines showing raw and corrected GFP-Myc levels of all recorded data synchronized to the start of time-lapse analysis.

15. Statistical analysis

Comparisons and graphs were made with either GraphPad Prism 5.0a or NCSS 11 Statistical Software (2016). Statistical analysis have been included in Figure legends.

RESULTS

1. Myc is the main driver of spontaneous cell competition in ESCs

Myc has been reported to be involved in natural cell competition in the epiblast and ESCs (Claveria *et al.*, 2013). Nevertheless, taking into account the similar regulation and cooperation in development and ESCs between Myc and Mycn (Malynn *et al.*, 2000; Scognamiglio *et al.*, 2016), we also wanted to explore the implication of Mycn in this phenomenon.

It has been shown that Mycn can largely replace most Myc functions necessary for normal murine growth and development (Malynn *et al.*, 2000). We thus explored whether Mycn could be compensating for Myc in ES cells. To address this, we first analysed the correlation between Myc and Mycn endogenous expression levels (Figure 9 A). Interestingly, in similarity to Myc, Mycn expression also showed a heterogeneous pattern in ESC cultures (Figure 9 A). However, quantification of both Myc and Mycn did not show any negative or positive significant correlation between both signals (Figure 9 A, B). This suggests that Mycn does not depend on Myc activity or undergoes compensatory regulation depending on Myc levels in ESCs.

Engulfing of loser cells by neighbouring winner cells has been observed in mESC and epiblast cells (Claveria *et al.*, 2013). It has been reported that in these winner-loser pairs Myc expression levels are much higher in the winner than in the loser cells (Claveria *et al.*, 2013). To directly assess the implication of Mycn in cell competition, we then analysed Mycn expression in pairs of engulfing/engulfed cells (Figure 9 C). Quantification of Mycn levels of engulfing and engulfed cells showed no differences between them in Mycn expression levels (Figure 9 C, D).

Given that not always cell competition involves engulfing events, we also examined caspase3-positive cells for Mycn levels (Figure 10 A). In WT cultures, Myc levels of apoptotic cells were reduced by half in comparison with Myc levels of non-apoptotic cells (Figure 10 B), as already shown in previous works (Claveria *et al.*, 2013). On the contrary, Mycn levels did not show any difference between the apoptotic and non-apoptotic population (Figure 10 C). These data suggest that Mycn is not involved in ESC competitive behaviour.

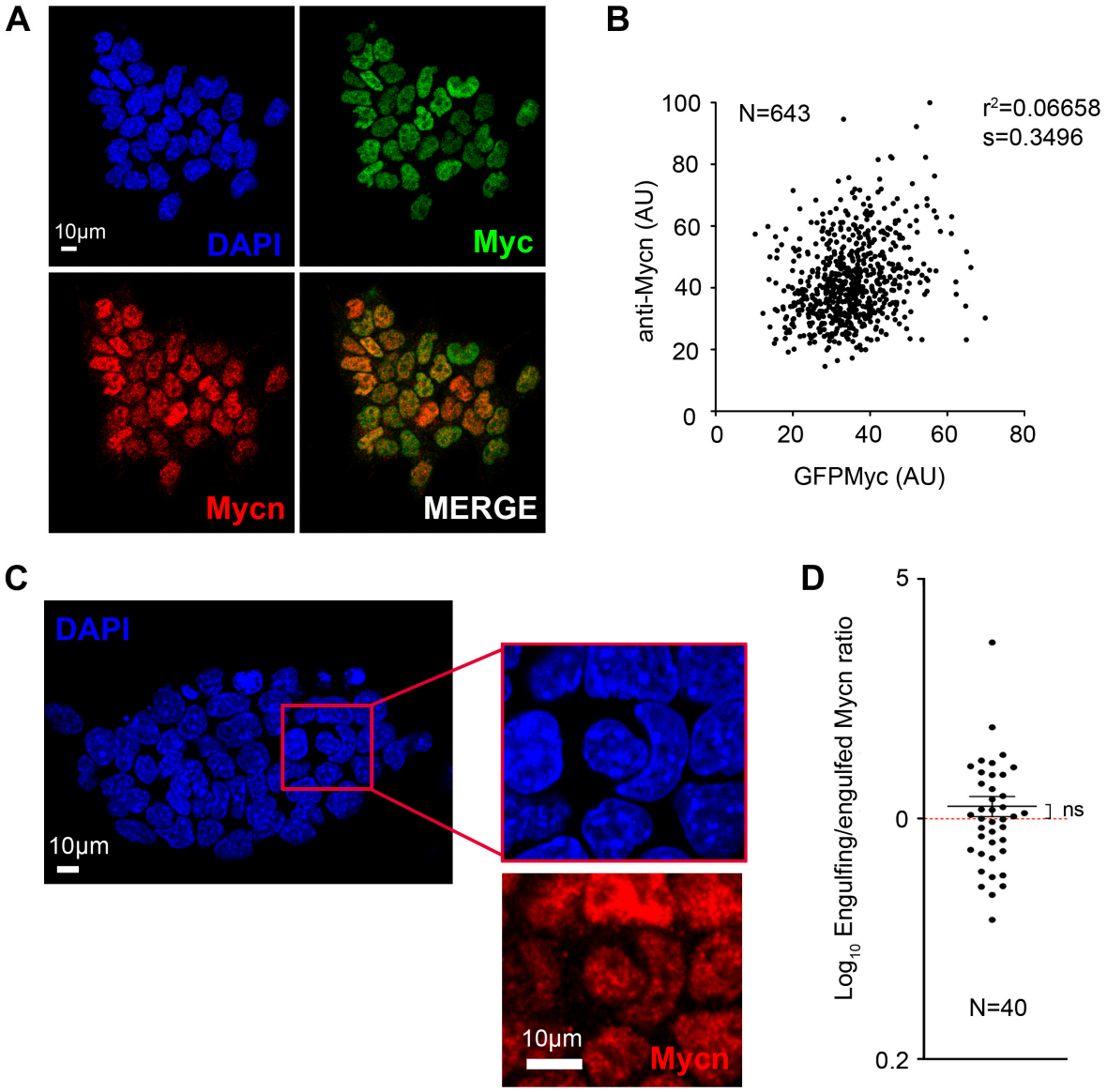

Figure 9. Mycn expression pattern and its implication in cell competition.

A. Co-localization of Myc and Mycn in ESCs. **B**. Quantification of the correlation between Myc and Mycn immunofluorescence in single cells of ESC cultures. **C**. DAPI staining of an ESC colony; The magnified frame shows an engulfing event and Mycn immunofluorescence. **D**. Mycn level paired ratios in engulfing and engulfed ES cells in WT culture. Dotplot in **D** shows mean and standard error of the mean (SEM) and one sample t-test was used for statistical analysis; ns, adjusted p-val>0,05.

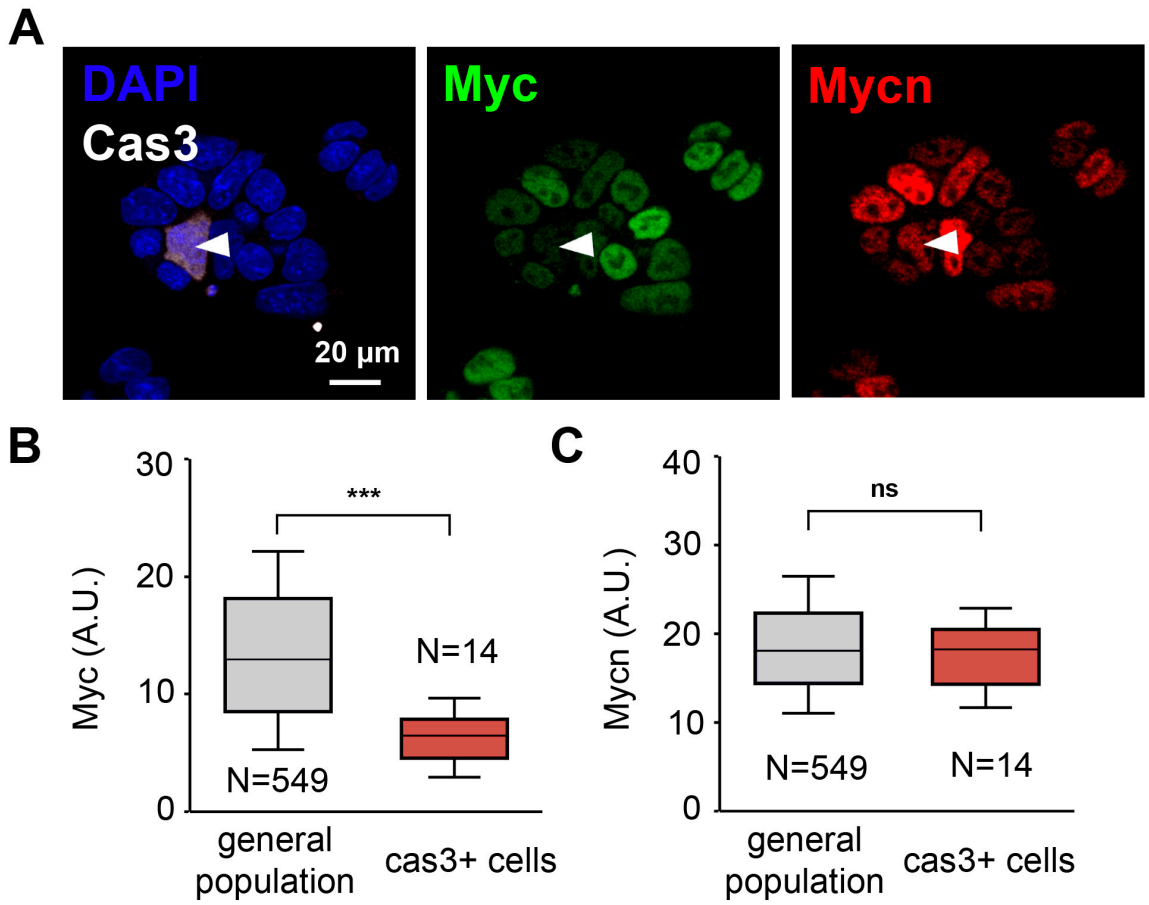

Figure 10. Study of Mycn role in apoptotic-mediated cell competition.

A. Confocal detection of caspase-3, Myc and Mycn immunofluorescence in an ESC colony. **B**. Myc levels in non-apoptotic (general population) and apoptotic (caspase-3 positive) cells. **C**. Mycn levels in non-apoptotic (general population) and apoptotic (caspase-3 positive) cells. Boxplots in **B** and **C** show median, 25 and 75 percentiles (boxes), 10 and 90 percentiles (whiskers). Mann Whitney test was used for statistics. ns, adjusted p-val>0,05; p<0,001***.

These observations suggest that, even though endogenous Mycn is not homogeneously expressed in ESCs, the differences in Mycn levels between cells are not determinant in spontaneous cell competition in ESCs. Myc is thus the only factor of its family in determining the competitive ability of ESCs.

2. Live imaging analysis of Myc levels in mESCs

2.1. The GFP-Myc knock-in line faithfully reports endogenous Myc expression

Although the implication of Myc in cell metabolism and proliferation in ESCs (Hu *et al.*, 2009; Kim *et al.*, 2010; Claveria *et al.*, 2013; Gu *et al.*, 2016; Scognamiglio *et al.*, 2016) and cell reprogramming (Cartwright *et al.*, 2005; Takahashi and Yamanaka, 2006) has been studied, the biological basis and dynamics of Myc-mediated cell competition remains elusive. To address this question, we used live reporting and tracking of endogenous Myc levels in mouse pluripotent cells. As a tool for this we derived a homozygous ESC line from previously described knock-in mice expressing a GFP-Myc fusion protein from the *Myc* locus (Huang *et al.*, 2008) (see Material and Methods).

In the first place, as Myc protein (Cartwright *et al.*, 2005) and mRNA (Dani *et al.*, 1984; Hann and Eisenman, 1984) have very short half-lives, we wanted to determine the reliability of this GFP-Myc knock-in line in reporting endogenous Myc levels. To this end, we studied the mouse embryo epiblast and found that GFP-Myc faithfully reported Myc levels in this tissue, despite the cell-to-cell highly heterogeneous Myc pattern (Claveria *et al.*, 2013) (Figure 11 A, B). In addition, in ESCs we also found a strong and fast variation of Myc during mitosis (Figure 11 C). Both Myc, detected by immunofluorescence, and GFP-Myc levels showed a drastic decreased in the transition from prophase to metaphase and a sharped increase during late telophase, being almost undetectable during metaphase, anaphase and cytokinesis (Figure 11 C, D). Moreover, we observed that this decrease during mitosis matches an increase in T58-phosphorylation (Figure 11 D), which targets Myc for degradation (Welcker *et al.*, 2004). During interphase, T58-phosphorylated Myc was not detected, which indicates that Myc is specifically degraded during mitosis. These results demonstrated that the GFP-Myc knock-in line is a reliable reporter for endogenous Myc expression, even when the protein is rapidly degraded and re-synthesized as occurs during mitotic phases.

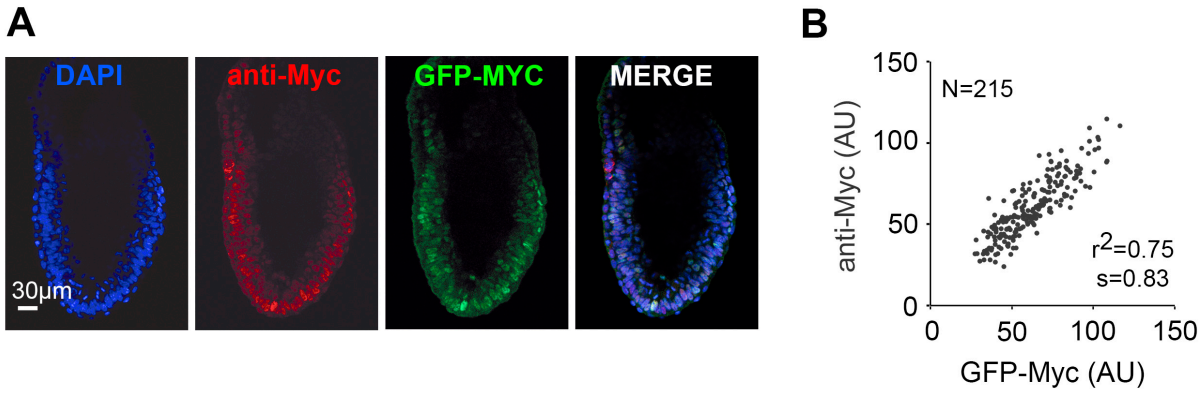
A
DAPI
anti-Myc
GFP-MYC
MERGE
30µm
B
N=215
anti-Myc (AU)
GFP-Myc (AU)
r2=0.75
s=0.83
0
50
100
150

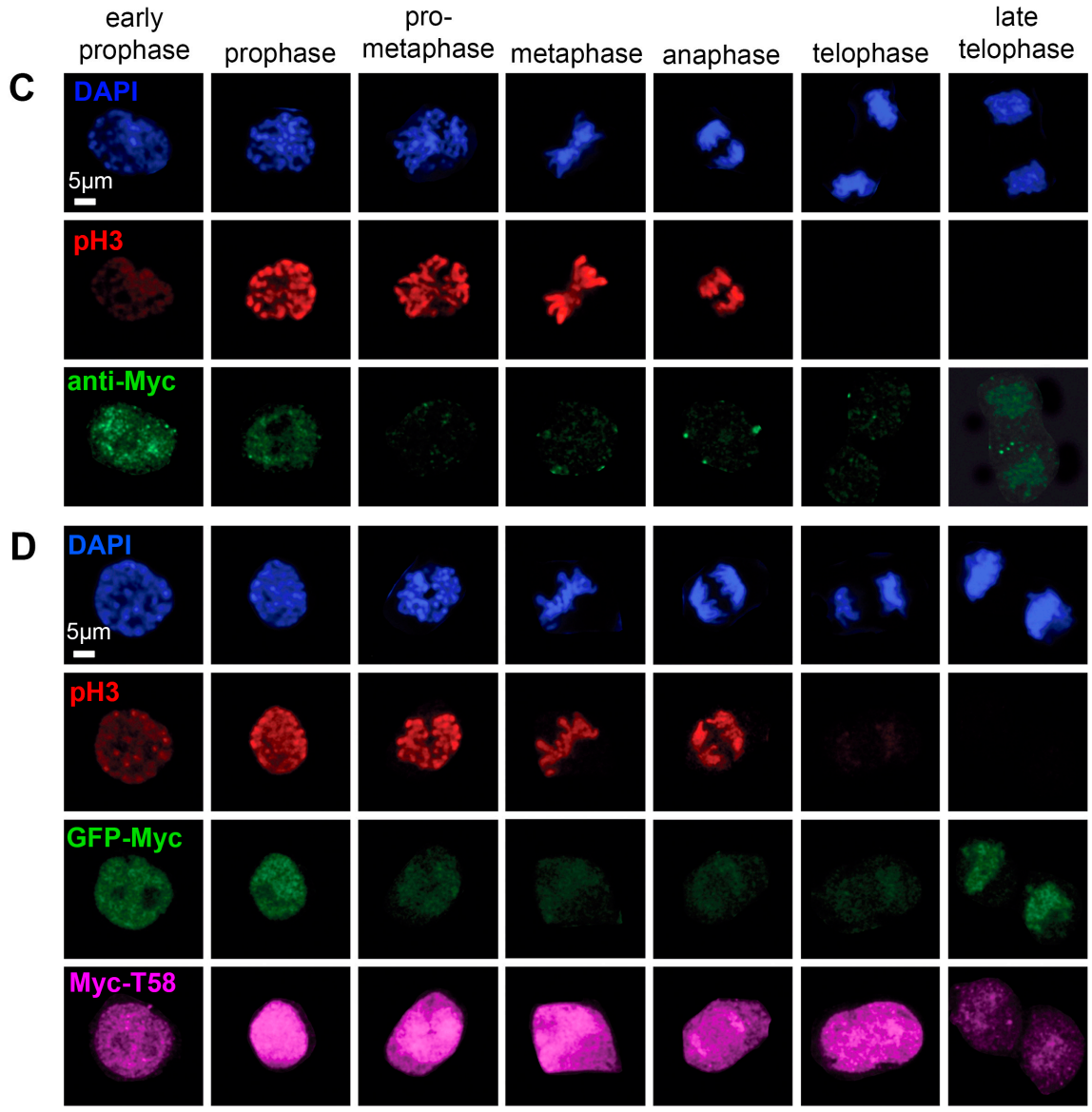
early prophase
prophase
pro-metaphase
metaphase
anaphase
telophase
late telophase
C
DAPI
5µm
pH3
anti-Myc
D
DAPI
5µm
pH3
GFP-Myc
Myc-T58

Figure 11. GFP-Myc line faithfully reports endogenous Myc expression.

A. Confocal detection (optical sections) of Myc immunofluorescence and GFP native fluorescence in an E6.5 mouse embryo carrying the *GFP-Myc* knock-in allele in heterozygosis. **B**. Quantification of the correlation between GFP and Myc immunofluorescence in single cells of the E6.5 epiblast. **C**. Confocal images showing detection of Myc protein and co-localization with Ph3 and DAPI in different phases of mitosis in WT cells. **D**. Similar data are presented for the GFP-Myc reporter with an additional co-localization with Myc-T58 phosphorylation detection.

2.1. Setting up 24h 3D+t time-lapse and computer workflow for analysis

In order to characterize Myc dynamics during endogenous cell competition we performed time-lapse experiments in which homozygous Myc-GFP cells were scanned in 3D during 24 hours. These 24h 3D+t time-lapses were then used to track all cells. As cells moved very actively in ESC colonies (video 1), 3D scans were acquired every 7 minutes in order to allow an accurate tracking (Figure 12 A). Nuclear GFP-Myc signal and tdTomato cell membrane marker were acquired with green (488nm) and red (555nm) channels respectively (Figure 12 B) in a Zeiss LSM 780 upright microscope (see more details in Materials and Methods).

Next, in collaboration with the Cellomics Unit from CNIC, we developed a computer workflow for automatically segmentation and tracking the 3D+t acquisitions (Video 2) (Fernández de Manuel *et al*, 2017). This software also allowed to inspect and correct manually any incorrect outcome from the automatic segmentation and tracking (Figure 12 C) (see more details in Materials and Methods). With this approach, we were able to track cells across cell division, generating lineage trees in which the information on the progenitor cell identity was incorporated to daughter cell identities (Figure 12 D, E; videos 2 and 3). In this way, we obtained not only lineage trees for every cell family in the analysed colonies, but also multiple quantitative parameters, such as nuclear volume, cell trajectories, shapes and their fluctuations, GFP-Myc levels and information on neighbour cells (Figure 12 E; Table 1).

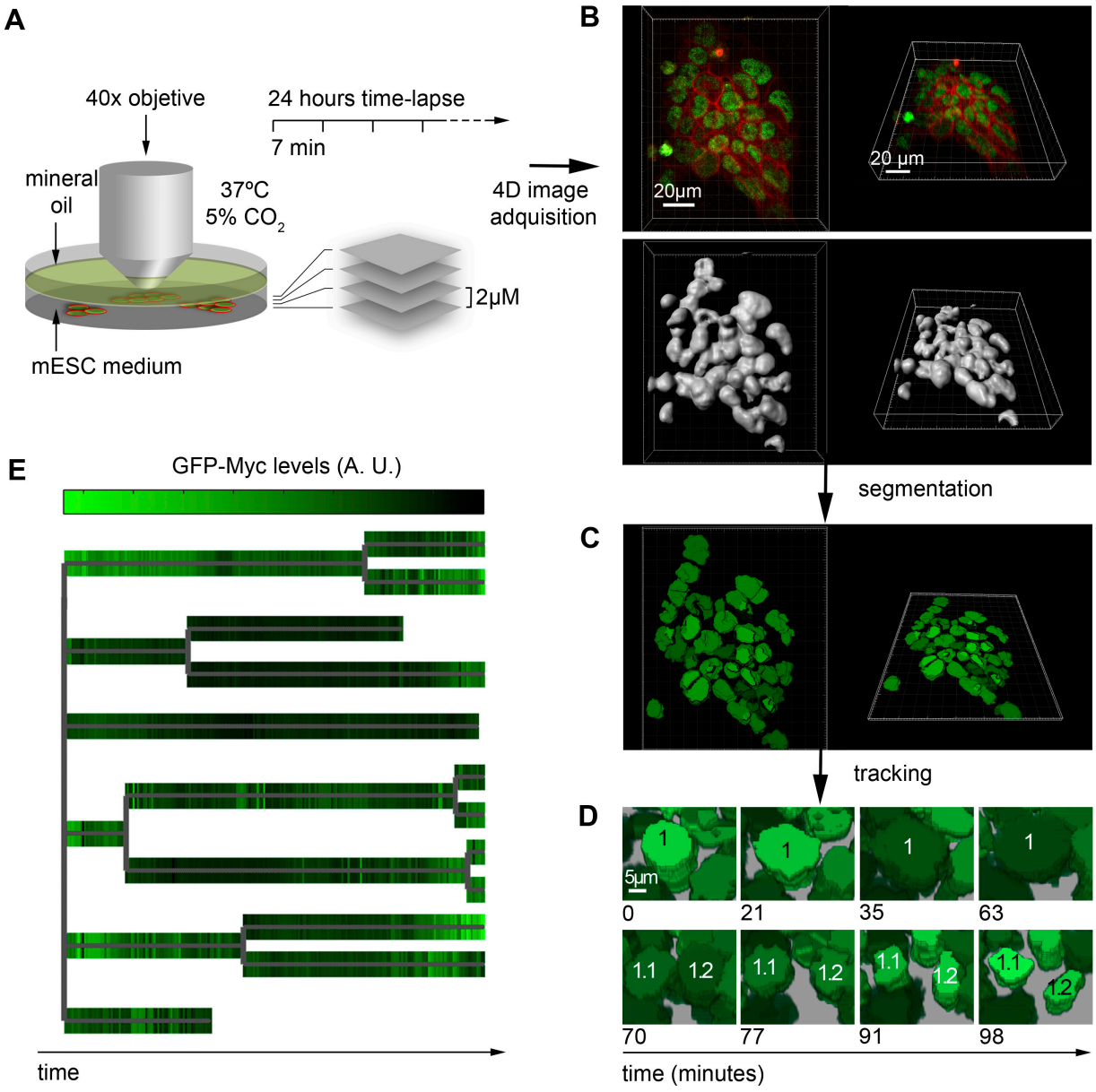

Figure 12. Multiparametric 4-dimensional analysis of embryonic stem cells, including lineage analysis and tracking of endogenous Myc levels.

A. Live confocal microscopy set-up. **B**. Example of 3D raw data acquisition from live GFP-Myc, membrane-Tomato ESCs (top) and whole volumes 3D rendering from these images (bottom). **C**. 3D segmentation of the nuclei of the ESC colony in A, with GFP-Myc levels displayed as green brightness intensity. **D**. Example of the tracking of segmented nuclei during mitosis. **E**. Cell lineage tree deduced from the tracking data, displaying the temporal pattern of GFP-Myc levels.

3. Myc is mostly regulated by cell-intrinsic heritable features

3.1. Study of Myc stability along the tracking

As it has been shown above and described in previous works (Claveria *et al.*, 2013), Myc is heterogeneously expressed both in ESCs and in the embryo. Therefore, we wanted to test what was the nature of this heterogeneity. We previously observed no detection of T58-phosphorylated Myc in ES cultures (excepting mitotic cells) (Figure 11 D), discarding any implication of Myc degradation in driving Myc heterogeneity.

We then determined the stability of Myc levels in the tracked cells. Classification of the whole cell population into three groups according to mean GFP-Myc level (top 30%, Myc-high (H); lower 30%, Myc-low (L); the rest, Myc-medium (M)) showed that Myc-H cells have 2.5X higher GFP-Myc intensity than Myc-L cells (Figure 13 A). Next, we performed *in silico* synchronisation of the cell cycle in order to determine the fluctuations of Myc during cell cycle. The resulting expression profile captured the drastic reduction of GFP-Myc levels during mitosis and the rapid recovery during telophase (Figure 13 B; Figure 11 C, D). In addition, mitosis was preceded by a moderate increase in Myc levels, and typical fluctuations were detected afterwards (Figure 13 B). However, the severe fluctuations during mitosis did not extend enough time to explain the cell-to-cell heterogeneity observed in GFP-Myc levels (Figure 13 A).

Next, we examined the stability of Myc-levels within the three groups previously established. During 24h tracking these groups revealed little variation (Figure 13 C). Interestingly, even after *in silico* synchronization, Myc levels were maintained through cell division, despite rapid Myc degradation and resynthesis (Figure 13 D). The fact that Myc levels are maintained through mitosis suggests that they are to some extent imprinted in ESC lineages.

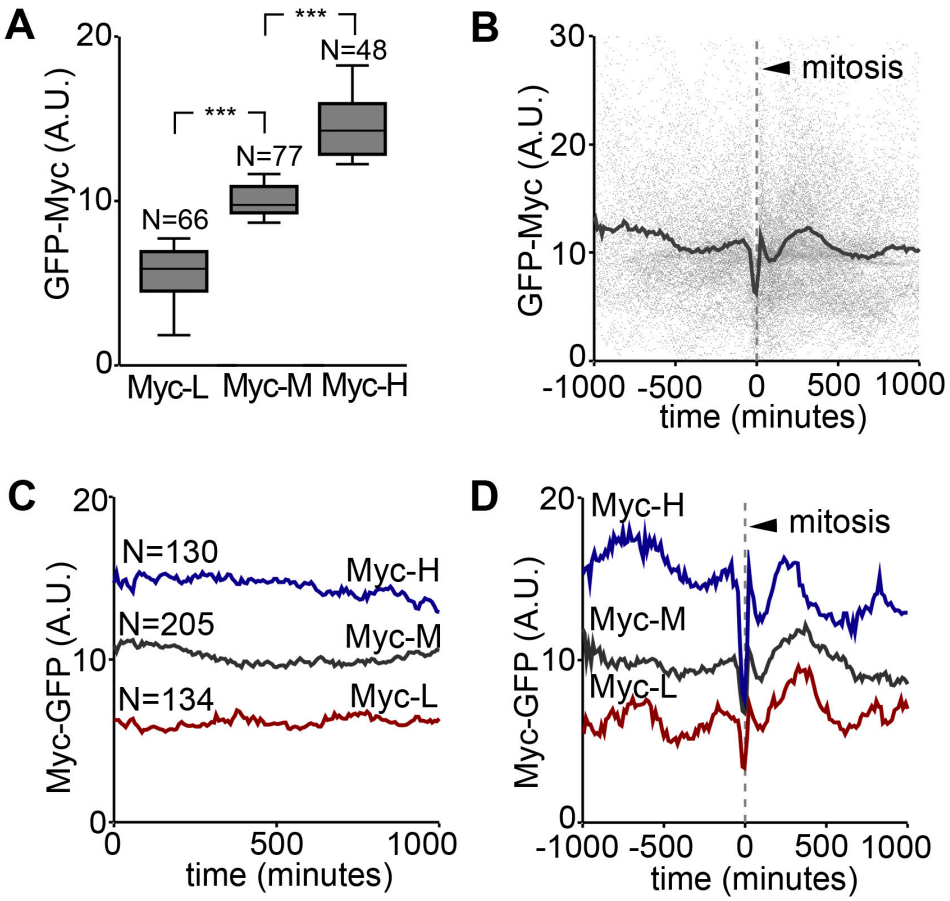

Figure 13. Myc is to some extent imprinted in ESC lineages.

A. Distribution of GFP-Myc levels after *in silico* classification of ESCs into groups according to live-recorded average GFP-Myc levels before cell's first division. **B**. Display of individual (dots) and spline smooth line (SSL) of GFP-Myc levels of all dividing cells *in silico* synchronized to cell division. **C**. Tracking of GFP-Myc levels (SSLs) in Myc-H, Myc-M and Myc-L ESCs during the observation period. **D**. Similar data to C, synchronized to cell division time. Boxplots show median, 25 and 75 percentiles (boxes), 10 and 90 percentiles (whiskers). Mann Whitney test was used for statistical analysis, $p<0.001$***.

3.2. Retrospective clonal analysis of Myc

Since from the time-lapse experiments we only have information of 24-hour periods, we decided to perform retrospective clonal analysis in ESCs. We used the *iMOS*^{WT} cell line (Claveria *et al.*, 2013) to generate EYFP+ clonal cell marks by inducing recombination at very low rate (see Materials and Methods for further

details). Cells were cultured for additional 60 hours after 4-hydroxytamoxifen removal. We then determined the variability of Myc levels between clonal groups of cells and randomly chosen equivalent groups. We found that Myc levels showed much lower variation in clonally related cells than in randomly chosen cells, with an estimated heritability of 0.8 per cell division, indicating that Myc levels display high heritability (Figure 14 A, B). In contrast with the predominant regulation of Myc in somatic cells, in which extracellular signals such as nutrients, mitogens or growth factors are described to be the main regulators (Wierstra and Alves, 2008), the clonal analysis, together with the previous observations in time-lapse and the cell-to-cell heterogeneity in Myc levels, indicates that Myc is mostly regulated by some intrinsic heritable mechanism in ESCs. Thus, sub-families of Myc expression levels seem to coexist in ESC cultures and largely transmit their Myc levels to their progeny.

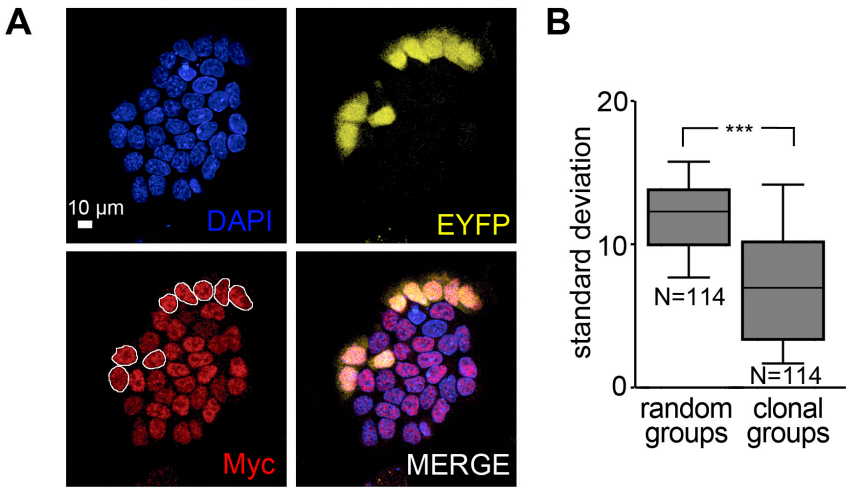

Figure 14. Retrospective clonal analysis of Myc.

A. Example of a clonal mark induced by *iMOS*^{WT} activation in an ESC colony together with immunofluorescence detection of Myc levels. **B**. Variation of Myc levels in clonal groups and equivalent groups of randomly chosen cells. Boxplots show median, 25 and 75 percentiles (boxes), 10 and 90 percentiles (whiskers). Mann Whitney test was used for statistical analysis, $p<0.001$***.

This form of heterogeneity is thus different from that reported for other transcription factors, such as Nanog, which has been shown to be regulated by stochastic transitions from low to high states of Nanog expression (Chambers *et al.*,

2007; Kalmar *et al.*, 2009). Moreover, quantification of both Myc and Nanog expression in ES cells did not show any significant correlation between both transcription factors (Figure 15 A, B).

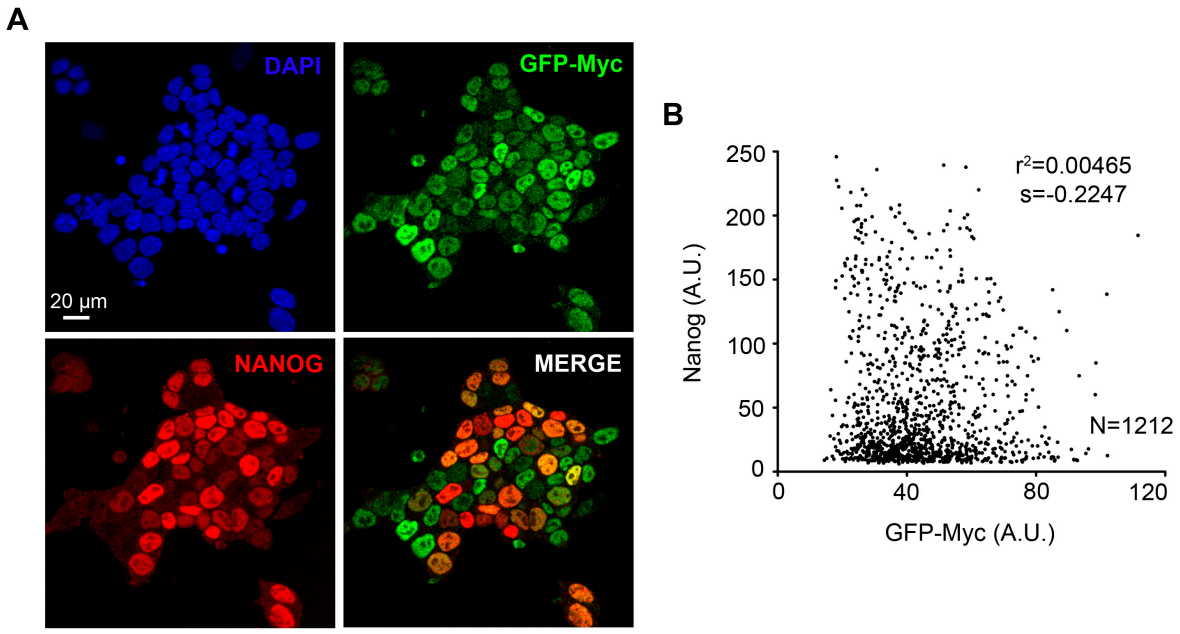

Figure 15. Myc and Nanog expression do not correlate.

A. Confocal detection of Myc and Nanog immunofluorescence in an ESC colony showing colonization of both signals. **B**. Quantification of the correlation between GFP and Myc immunofluorescence in single cells of ESC colonies.

4. Temporal integration in losers of discrepant Myc levels with neighbours leads to cell competition

4.1. Identification and characterization of apoptotic cells

To study how MYC heterogeneity leads to cell competition we performed neighbour analysis by manual inspection using the computer workflow. First, we tracked apoptosis events during the 24-hours time-lapse analysis, identifying 24 apoptotic cells, that we called prospective-dying cells (PDC) (videos 4-6). Three of these apoptotic events were discarded from further analysis as they were considered Myc-independent death events. First, we analysed the average Myc-GFP level of

PDCs during the observation time, finding that, in agreement with previous works of Myc-driven competition (Claveria *et al.*, 2013; Sancho *et al.*, 2013), it was lower than that of the non-dying cells (NDCs) (Figure 16 A) and that it approximately matched the level found in MYC-L cells (Figure 13 A). Moreover, PDCs showed persistently lower GFP-Myc levels than NDCs, as revealed by the temporal profile of GFP-Myc levels synchronized to the time of PDC death (Figure 16 B). These results indicate that pre-existing low Myc levels correlate with the loser fate. Interestingly, this synchronization also revealed that PDCs show a tendency to reduce their Myc-GFP levels starting approximately 500 minutes before death (Figure 16 B). For comparison, we characterized a group of cells that showed similar Myc-GFP levels to those found in PDCs (Figure 16 C) but did not die during the tracking; this group was named Myc-L non-dying cells (ML-NDCs). These cells also showed continuously lower Myc-GFP levels than the general population during the observation time but did not undergo any GFP-Myc level reduction (Figure 16 D).

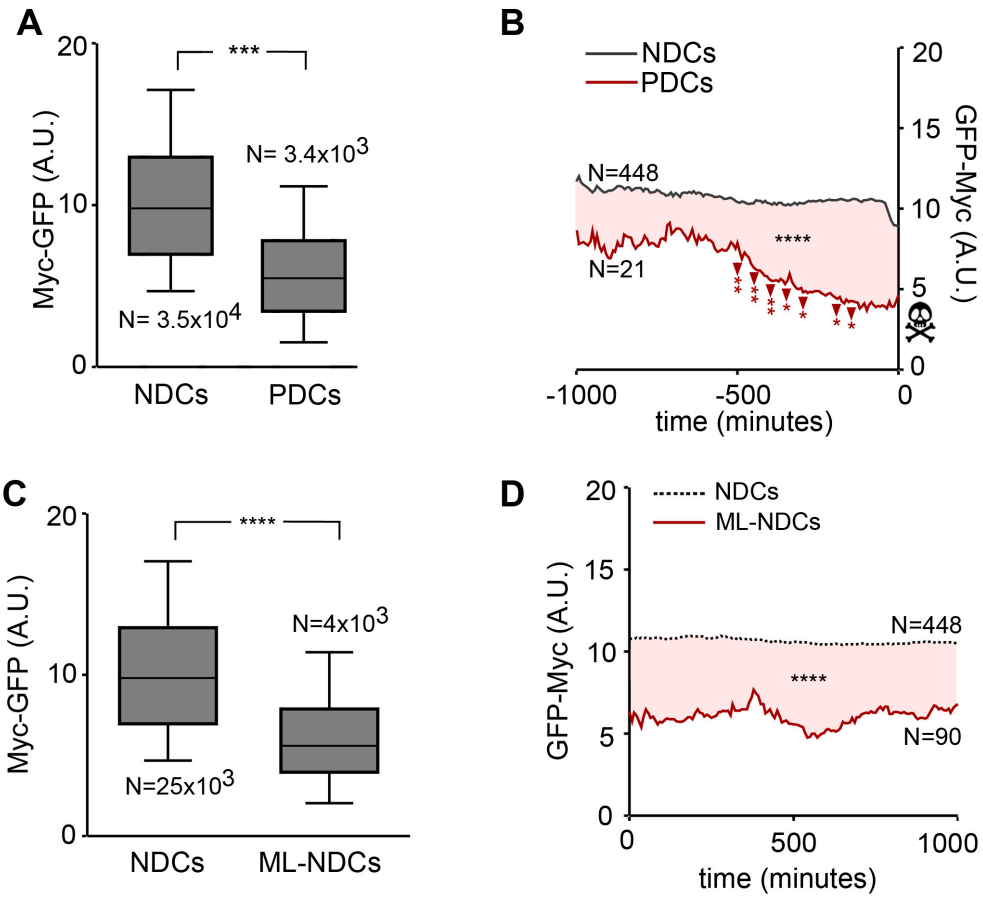

Figure 16. Characterization of apoptotic cells.

A. Distribution of GFP-Myc levels during 24h live analysis of prospective dying cells (PDCs) and non-dying cells (NDCs). **B**. Temporal evolution of GFP-Myc levels (spline smooth line, SSL) in PDCs and NDCs, synchronized to the time of cell disappearance (death for PDCs and division for NDCs). Significant decreases between consecutive 100-minute sections are shown (arrowheads). **C**. Graph showing the distribution of GFP-Myc levels during 24h live analysis of non-dying cells (NDCs) and Myc-low non-dying cells (ML-NDC). **D**. Temporal evolution of GFP-Myc levels (SSLs) in NDCs and ML-NDCs. Boxplots in **A** and **C** show median, 25 and 75 percentiles (boxes), 10 and 90 percentiles (whiskers). Mann Whitney test was used for statistics, p-val<0.001***, <0.0001****. Statistical analysis in **B** and **D** were performed by comparing 100-minute sections between the represented data sets using a Mann Whitney test; pink areas between graph lines indicate p-values <0.0001****. Longitudinal changes of PDCs shown in **A** were studied using Mann Whitney test to determine significant changes between consecutive 100-minute sections centred at 50-minute sliding positions. Transitions between consecutive temporal sections showing significant differences are shown by an arrowhead and indicate the p-value; p-val<0,05*; 0,01**.

4.2. Analysis of PDC neighbourhood

We then performed neighbourhood analysis of the GFP-Myc expression profiles. NDCs showed a GFP-Myc profile similar to that of their neighbours (Figure 17 A). In contrast, in PDC neighbours GFP-Myc levels are initially lower than those of the general population but rise from 800 minutes before loser death up to matching the levels in NDCs and maintain a plateau until the death event (Figure 17 B, E). The increase in PDC neighbours' GFP-Myc levels therefore precedes the decline in PDC GFP-Myc levels (Figure 17 B). The difference in GFP-Myc levels between PDCs and their neighbours was thus exacerbated before the death event (Figure 17 D). Conversely, ML-NDCs neighbours did not show any increase in their GFP-Myc level profile and they stably maintained lower levels than NDCs (Figure 17 C). The contrast in GFP-Myc levels between ML-NDCs and their neighbours is therefore always below that preceding PDCs death (Figure 17 D). Furthermore, by synchronizing ML-NDCs neighbours to the timepoints in which their GFP-Myc levels increase to match those of the plateau preceding PCD death, we observed that ML-NDC neighbours did not experience any increase in their GFP-Myc levels extending longer than 500 minutes (Figure 17 F). These results suggest that Myc-low cells survive in ESC colonies as long as the discrepancy in Myc expression with their neighbours is moderate. However,

sustained high discrepancies for periods above 600-800 minutes lead to their elimination.

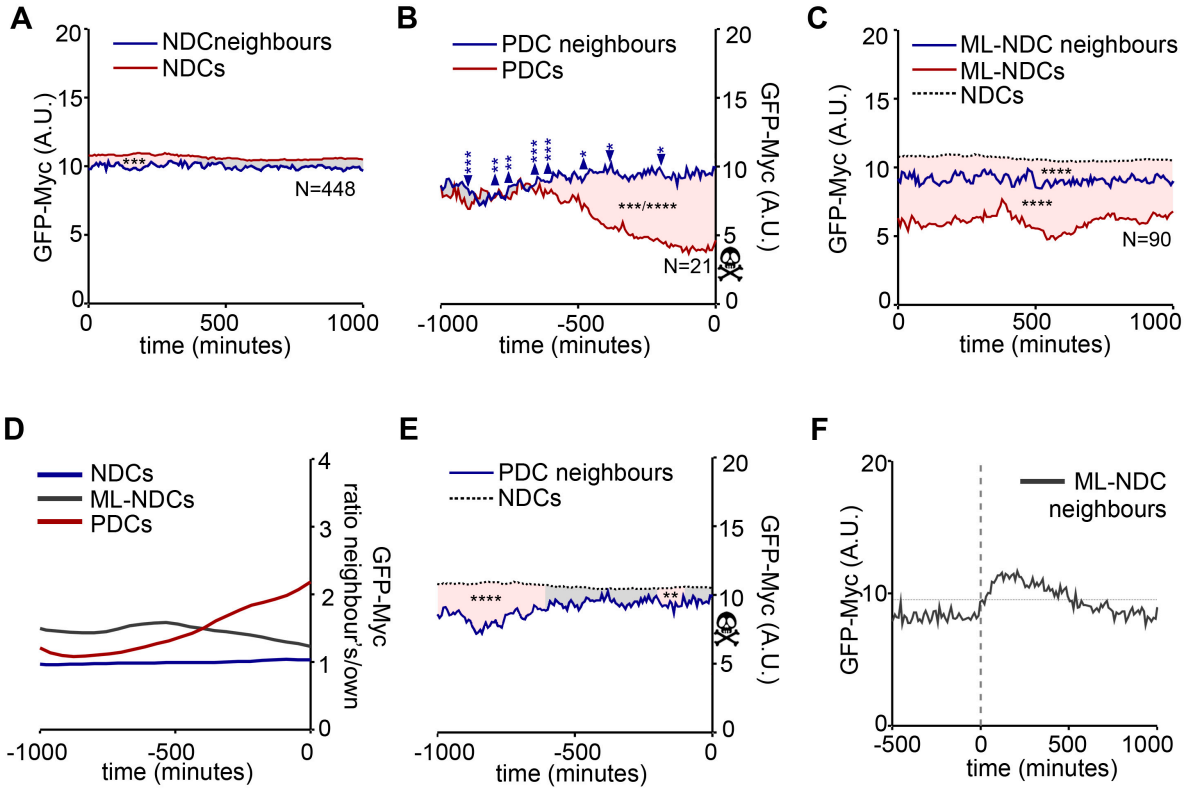

Figure 17. Analysis of Prospective Dying Cells neighbourhood.

A. Temporal evolution of GFP-Myc levels in NDCs and their neighbour (means). **B**. Temporal evolution of GFP-Myc levels in PDCs and PDC-neighbour means synchronized to PDC death. Significant increases between consecutive 100-minute sections are shown (arrowheads). **C**. Temporal evolution of GFP-Myc levels in Myc-Low non-dying cells (ML-NDCs), ML-NDC neighbour means and NDCs. **D**. Temporal evolution (locally weighted scatterplot smooth line) of the ratios between GFP-Myc levels in NDCs, PDCs, ML-NDCs and their respective neighbour means. **E**. Temporal evolution of Myc-GFP levels in NDCs and PDC neighbour means. **F**. GFP-Myc levels of ML-NDC neighbours synchronised to the initiation of periods in which their mean level is equal or higher to that shown by PDC neighbours before PDC death. **A-C**, **E-F** display SSLs. Pink areas between graph lines in **A-C**, **E** indicate p-values <0.01**; 0.001***; 0.0001****. Statistical analysis in **A-C**, **E** were performed by comparing 100-minute sections between the represented data sets, using a Wilcoxon matched-pairs signed rank test for comparing PDCs, NDCs and ML-NDCs with their neighbours and a Mann Whitney test for the rest of comparisons. Longitudinal changes of PDCs neighbours shown in **B** were studied using a Mann Whitney test to determine significant changes between consecutive 100-minute sections centred at 50-minute sliding positions. Transitions between temporal sections showing significant differences are shown by an arrowhead and indicate the p-value; p-val<0,05*; 0,01**, 0,001***.

5. Random contacts between cells with pre-existing discrepancy in Myc levels drive cell competition

Given that the first event anticipating a loser-cell fate is the increase of Myc level in its neighbourhood, we decided to study the nature of this increase. The results observed could correspond to replacement of neighbours by cells with higher Myc levels than their own, or to Myc upregulation in pre-existing neighbours. To analyse these options, we inspected individual GFP-Myc profiles of PDC neighbours and found that the increase in neighbour's aggregate GFP-Myc levels normally correspond to the presence of only one neighbour at a time with very high GFP-Myc levels (Myc-highest neighbours, MHNs) (see examples in Figure 18 A). The total number of contacts contributing to the GFP-Myc plateau and the duration of these contacts were highly variable (Figure 18 A, B), indicating that MHNs do not engage in the interaction with PDCs. When we represented GFP-Myc level temporal profiles considering only MHNs we observed similar profiles to those including all neighbours (Figure 17 A-C), but with a wider discrepancy in GFP-Myc levels (Figure 18 C-E). In addition, we synchronised the complete temporal profile of PDC neighbours to the time of their first contact with PDCs and we found that Myc levels in neighbours are insensitive to these contacts (Figure 18 F, G). We also found no correlation between the frequency of the contacts and the cell cycle phase (Figure 18 B). Moreover, the distribution of the duration of PDC contacts with their MHNs was similar to that observed with their Myc-low neighbours (Figure 18 H), which indicates that there is no specific pattern of direct contacts between prospective winner and loser cells.

These results indicate that it is neighbour exchange and not Myc regulation what produces the increase in GFP-Myc levels that precedes cell death (see example in video 7); therefore, spontaneous cell competition is driven by apparently random contacts between ESCs that autonomously express highly discrepant Myc levels.

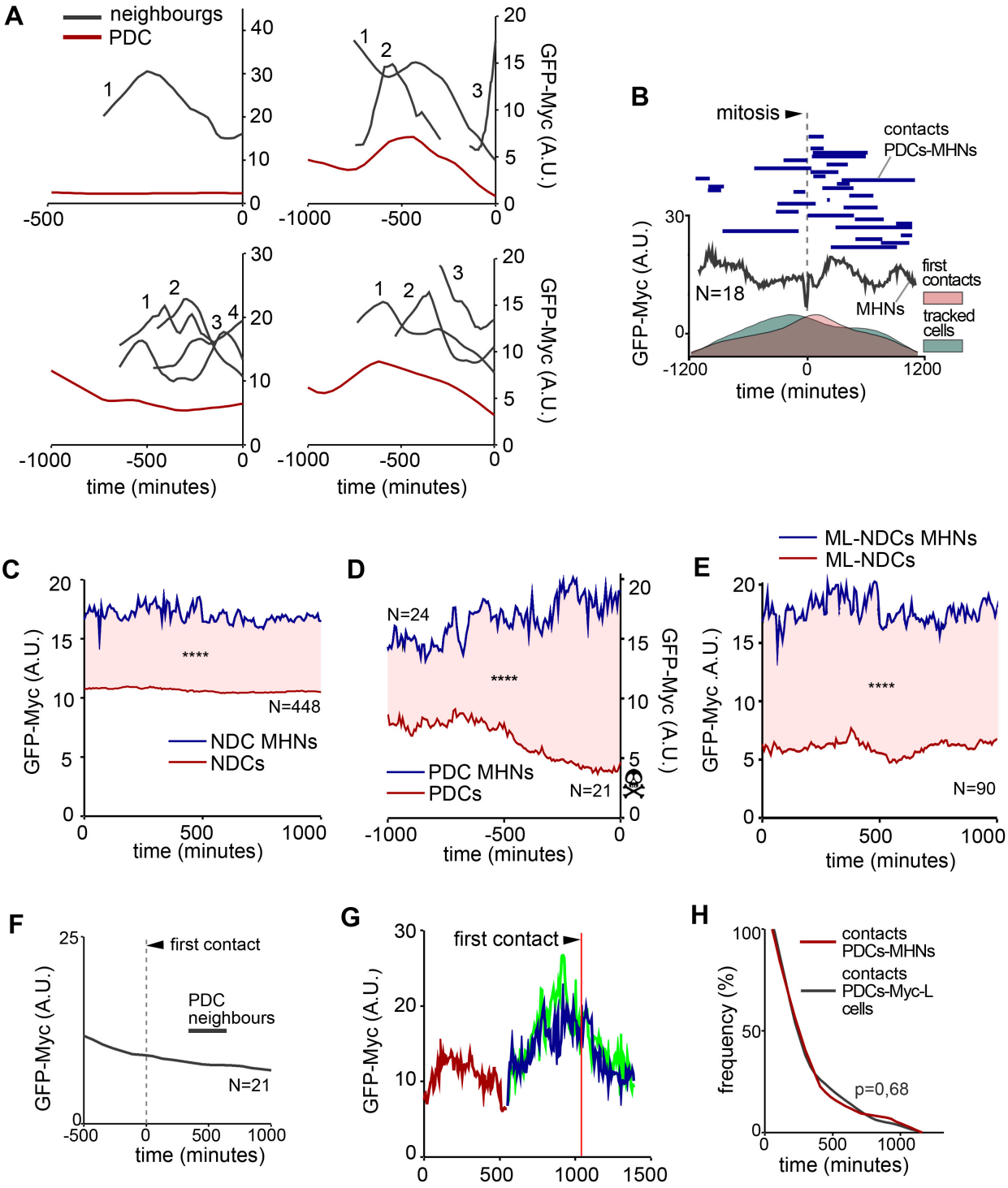
A
neighbourgs
PDC
GFP-Myc (A.U.)
time (minutes)
B
mitosis
contacts
PDCs-MHNs
GFP-Myc (A.U.)
N=18
first
contacts
MHNs
tracked
cells
time (minutes)
C
GFP-Myc (A.U.)
****
N=448
NDC MHNs
NDCs
time (minutes)
D
N=24
****
PDC MHNs
PDCs
N=21
GFP-Myc (A.U.)
time (minutes)
E
ML-NDCs MHNs
ML-NDCs
GFP-Myc .A.U.)
****
N=90
time (minutes)
F
first contact
PDC
neighbours
GFP-Myc (A.U.)
N=21
time (minutes)
G
first contact
GFP-Myc (A.U.)
H
contacts
PDCs-MHNs
contacts
PDCs-Myc-L
cells
frequency (%)
p=0,68
time (minutes)

Figure 18. Dynamics of Myc level regulation and winner-loser interactions.

A. Individual examples of competition, showing the GFP-Myc temporal profile in PDCs (red) and PDC-Myc Highest Neighbours (MHNs) (black). Examples show the contribution from one to various PDC-MHNs to the increase in GFP-Myc levels in PDC neighbours. **B**. GFP-Myc levels of PDC-MHNs synchronized to cell division (line), together with contact periods of PDC-MHN with PDCs (bars, top), and temporal profiles of number first contacts and number of tracked cells. **C**. Temporal evolution of GFP-Myc levels in NDCs and their Myc Highest Neighbours (NDC-MHNs). **D**. Temporal evolution of GFP-Myc levels in PDCs and their Myc Highest Neighbours (PDC-MHNs). **E**. Temporal evolution of GFP-Myc levels in ML-NDCs, their Myc Highest Neighbours (ML-NDC-MHNs). **F**. Temporal evolution of mean GFP-Myc levels in PDC neighbours synchronized to the time of first contact with a PDC. **G**. Example of the temporal evolution of an individual PDC-MHN in green, sister cell - never in contact with the PDC – in blue, mother in red. This example supports the idea that MHNs autonomously express Myc and that random contact with PDC trigger the elimination of the latest. **H**. Frequency profile of duration of the periods of contact between PDCs and their MHNs and their Myc-L neighbours. **A**, **F**, **H** display locally weighted scatterplot smooth lines. **B**, **C**-**E**, **G** display SSLs. Pink areas between graph lines in **C**-**E** indicate p-value < 0.0001****. Statistical analysis in **C**-**E** were performed by comparing 100-minute sections between the represented data sets using Wilcoxon matched-pairs signed rank test.

6. iMOS-mediated induction of cell competition confirms the conclusions from the live analysis of spontaneous cell competition

Our results suggest that Myc-low cell elimination takes place when accumulated contacts lead to sustained discrepancies for longer than 600-800 minutes and is preceded by a progressive decrease of Myc levels in the loser cell.

To test this model, we used the *iMOS* system (Claveria *et al.*, 2013) to experimentally induce cell competition by overexpressing Myc in a mosaic manner (see Material and Methods). We performed a time-lapse experiment in which we studied the temporal profile of EYFP-Myc cell induction and neighbour death events (Figure 19 A-C; video 8, 9; see Material and Methods). In accordance with the observations from the live-analysis of spontaneous cell competition, we found an increase over 3-fold of the cell death rate at 600 minutes from the onset of EYFP-Myc induction (Figure 19 D). Furthermore, when we quantified the death events that were not in contact with EYFP-Myc cells, the temporal profile did not exhibit any increase

in the death rate, which remained linear during the observation time (Figure 19 D). In addition, this observation is in accordance with previous works reporting that cell competition is cell-to-cell contact dependent (Simpson and Morata, 1981; Moreno *et al.*, 2002; Moreno and Basler, 2004; Li and Baker, 2007; Claveria *et al.*, 2013).

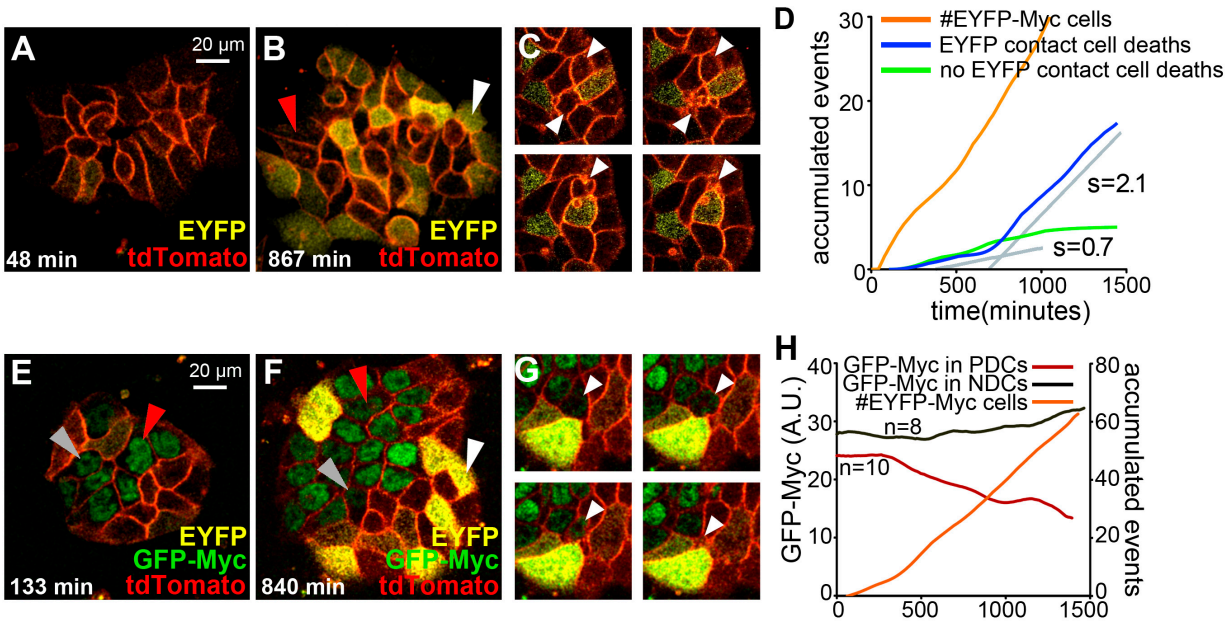

Figure 19. *iMOS*-mediated induction of cell competition.

A, **B**. Confocal images showing the EYFP pattern in *iMOS*$^{T1\text{-}Myc}$ ESCs at two time-points during the time-lapse after conditional activation. EYFP reveals cells overexpressing Myc. Red arrowhead indicates negative cells and white arrowhead indicates EYFP-Myc cells. **C.** Selected frames from live analysis of *iMOS*-induced cell competition showing apoptosis of non-activated cells neighbouring activated *iMOS*$^{T1\text{-}Myc}$ cells. **D**. Cumulative temporal representation of EYFP activation events and cell death events in non-EYFP cells - in contact or not with *iMOS*$^{T1\text{-}Myc}$ cells - after *iMOS*$^{T1\text{-}Myc}$ activation. s, slope (events/hour). **E**, **F**. confocal images showing the EYFP and GFP-Myc patterns in *iMOS*$^{T1\text{-}Myc}$ / GFP-Myc mixed ESC colonies at two time-points during time-lapse analysis after conditional activation. Widespread EYFP reveals cells overexpressing Myc and nuclear GFP reveals GFP-Myc cells. White arrowhead indicates EYFP-Myc cells, grey arrowheads indicate a PDC and red arrowheads indicate a NDC, both neighbours of EYFP-Myc cells. **G**. Cumulative temporal representation of EYFP activation events and GFP-MYC levels in PDC and NDC neighbours of EYFP-Myc cells in *iMOS*$^{T1\text{-}Myc}$ / GFP-Myc mixed ESC cultures following *iMOS* induction. **D**, **H** display locally weighted scatterplot smooth lines.

Next, in order to study the evolution of GFP-Myc levels in EYFP-Myc cell neighbours, we repeated the experiment but co-culturing the *iMOS*$^{T1\text{-}Myc}$ cell line with the GFP-Myc knock-in line (Figure 19 E-G; video 10). We then identified and traced the Myc levels of GFP-Myc cells that were neighbours of EYFP-Myc cells and died during the observation period. We found that they showed a sustained decreased in their GFP-Myc levels starting shortly after EYFP-Myc induction (Figure 19 H). On the contrary, GFP-Myc levels of EYFP-Myc neighbour cells that did not die during the tracking were stable during the total period of observation (Figure 19 H). These results confirm the conclusions from the live-analysis of spontaneous cell competition.

7. The competitive ability of ESCs correlates with Myc levels but not with proliferation

We next questioned what was the biological basis of different Myc levels in ESC sub-lineages. It has been previously shown that deletion of both Myc and Mycn or pharmacological inhibition of Myc activity leads to proliferation arrest by decreasing transcription, splicing and protein synthesis (Scognamiglio *et al.*, 2016). We then studied the correlation between Myc levels and proliferation and its implication in cell competition. The live-imaging analysis allowed us to measure the proliferative activity of each cell sub-lineage. We observed that the Myc-Low population exhibited a much lower fraction of the population in S-phase than Myc-High cells (Figure 20 A) and a higher fraction of cells not dividing during tracking (Figure 20 B). This means that Myc-L cells proliferate less that the rest of the population. In contrast, we found no difference in the proliferative activity between Myc-M and Myc-L cell populations (Figure 20 B). Moreover, in cells that divided during the period of observation, GFP-Myc levels did no correlate with the frequency of mitosis (Figure 20 C). In addition, we were able to track cell cycle progression by synchronizing nuclear sizes to the moment of mitosis. This analysis showed that nuclear volume increased linearly during interphase and halved across mitosis (Figure 20 D), showing that the increase in nuclear size reports the S-phase of the cell cycle. These observations agree with the extremely short G1 and G2 phases in the ESC cycle (Savatier *et al.*, 1994; Boheler, 2009). Study of the temporal profile of nuclear size increase indicated similar cycling speeds for Myc-H, Myc-M and Myc-L

cell populations (Figure 20 E). These results suggest that Myc levels over a certain threshold are required for ESCs to enter the proliferative status, but once in proliferation, Myc levels do not determine the cell cycle speed.

Interestingly, both dividing and non-dividing Myc-L cells showed substantially increased apoptosis rates (Figure 20 F) meaning that the proliferative status of Myc-L cells did not affect their chance to undergo apoptosis. This indicates that ES cells compete according to their Myc levels irrespective of their cycling activity.

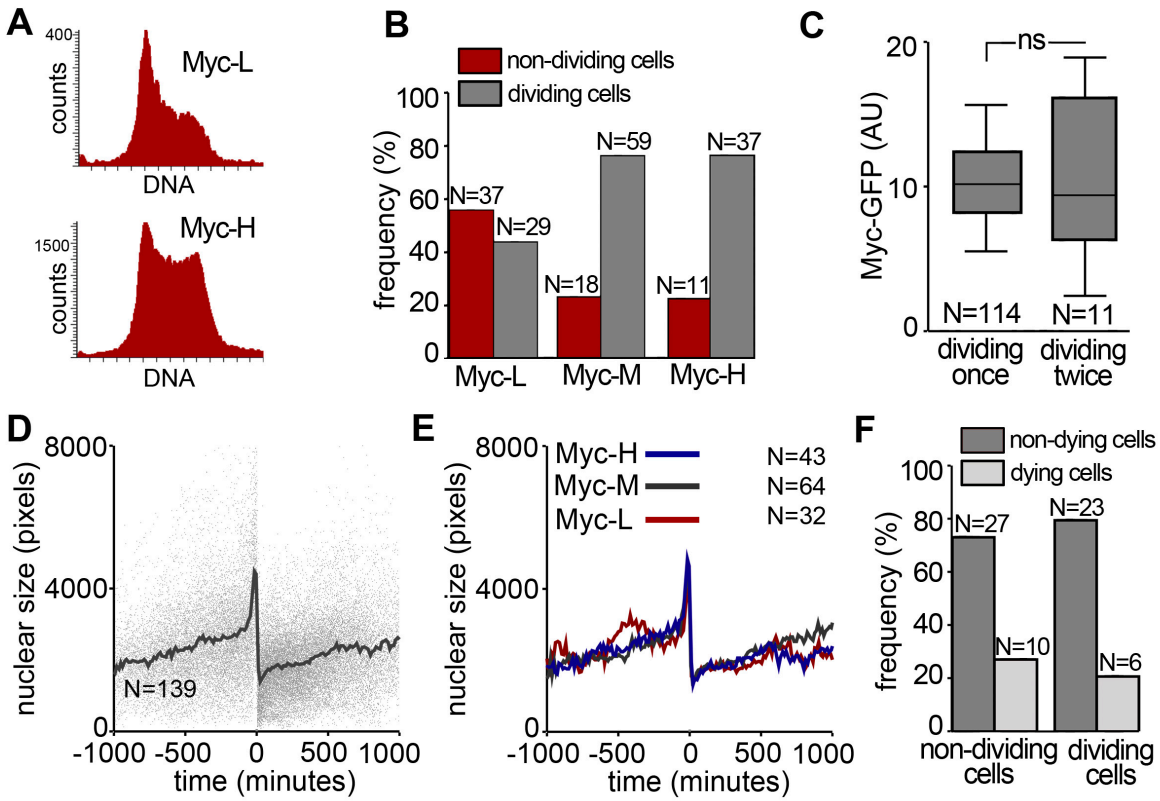

Figure 20. Myc levels and proliferation in ESCs.

A. DNA content cytometry profiles. **B**. Percentage of dividing and non-dividing cells during time-lapse analysis in ESCs classified according to Myc levels. **C**. Average GFP-Myc levels in ESCs dividing once or twice during tracking. **D**. Display of individual (dots) and SSL of nuclear size tracking in dividing cells synchronized to cell division time (time 0). **E**. Similar data as in **D**, in ESCs classified by Myc levels. **F**. Frequency of apoptosis in Myc-L ESCs according to their proliferative behaviour during tracking. Boxplots in **C** show median, 25 and 75 percentiles (boxes), 10 and 90 percentiles (whiskers). Mann Whitney test was used for statistical analysis. ns, p>0,05.

8. Study of cellular dynamics and Myc levels in ESC colonies

We also used the tracking data to examine several parameters related with cell motility and its correlation with GFP-Myc levels. We compared those parameters between the Myc-H and Myc-L cell populations. We found no difference between both populations in cellular speed, total distance travelled and net displacement (Figure 21 A-C). These results indicate that differences in cell motility are not involved in the competitive behaviour, supporting the idea of random and passive contacts between winners and PDCs.

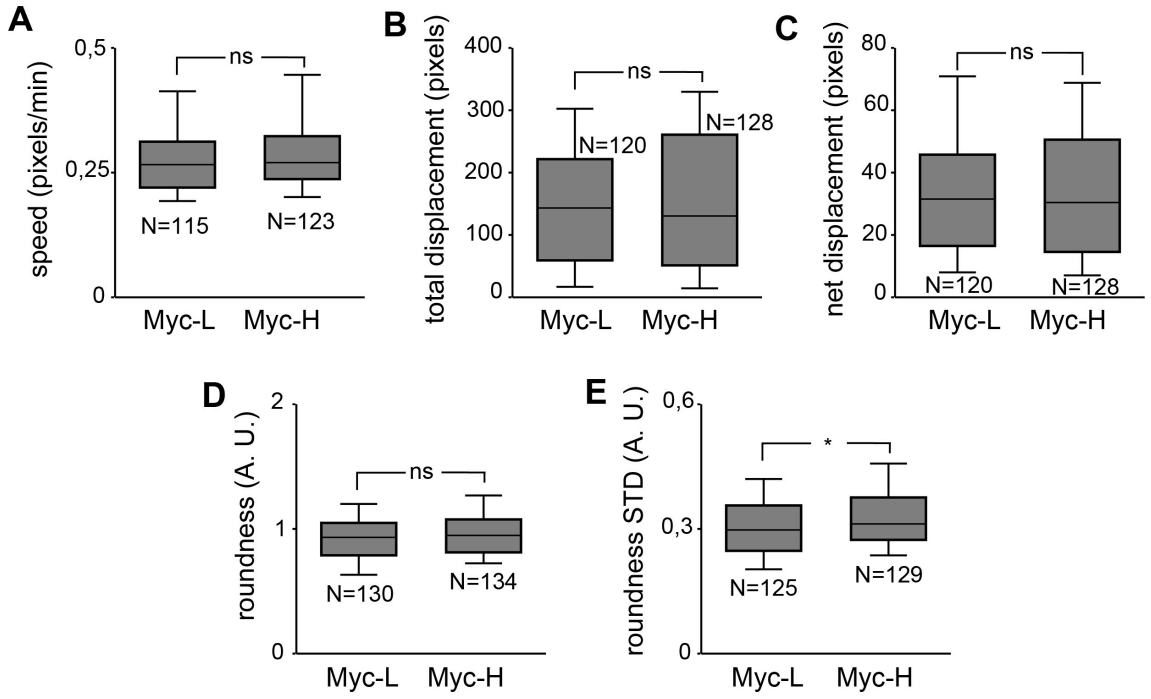

Figure 21. Myc levels and cellular dynamics in ESCs.

A. Measurement of cell speed between Myc-L and Myc-H populations. **B**. Measurement of total displacement between Myc-L and Myc-H populations. **C**. Measurement of net displacement between Myc-L and Myc-H populations. **D**. Measurement of cell roundness between Myc-L and Myc-H populations. **E**. Measurement of cell roundness variation (deformability) between Myc-L and Myc-H populations. Boxplots show median, 25 and 75 percentiles (boxes), 10 and 90 percentiles (whiskers). Mann Whitney test was used for statistics. ns, p-value>0.05; p<0.05*.

We also measured cell roundness and we observed no difference in this parameter between Myc-H and Myc-L cells (Figure 21 D). Remarkably, Myc-H cells did show higher variance of roundness over time than Myc-L cells (Figure 21 E), which indicates higher cell deformability associated with higher Myc levels.

9. Myc expression levels correlate with the pluripotency status

Since we wanted to study the biological origin of Myc-driven endogenous cell competition, we next performed a transcriptome analysis of mouse ESCs. We sorted three sub-populations of cells according to their Myc levels (Myc-Low, Myc-Medium and Myc-High) (Figure 22 A), we extracted RNA of the three sub-populations and performed RNAseq. These groups were comparable to those artificially generated in the computer workflow for the previous studies (Figure 13 A). After examination of the transcriptome, we found that the most significant difference between the populations was the regulation of the pluripotency network (Figure 22 B). We then decided to compare our transcriptome of ESCs classified by Myc levels with those of the naive and primed pluripotent states. We used RNAseq analysis from previous works that described these pluripotent states in naive ESCs and epiblast-like cells (EpiLCs) (Buecker *et al.*, 2014; Sasaki *et al.*, 2015). EpiLCs are cells in transition between naive and primed states that are accomplished *in vitro* (Hayashi *et al.*, 2011). Analysing principal components, we observed that Myc-L cells were closer to differentiation-primed EpiLCs, whereas the Myc-H population was more similar to naive ESCs and Myc-M cells were located at an intermediate position between both states (Figure 22 C). This observation was also supported by the examination of the main regulators of pluripotency (Martello and Smith, 2014) (Figure 22 D-E). The fact that the expression profile of the Myc-M population showed an intermediate position suggests that Myc levels correlate with changes in the transcriptome that occur in the transition from the naive to the primed primed pluripotent state.

Next, we examined whether Myc levels correlated with the activation of the two main signalling pathways that characterize the naive and primed pluripotency status. We found that in ESCs GFP-Myc levels negatively correlate with pERK expression (Figure 23 A, B), whose activation conveys acquisition and maintenance of the primed state (Kunath *et al.*, 2007). Contrary, GFP-Myc levels correlate positively

with pSTAT3 activation (Figure 23 C, D), which characterizes and promotes naive pluripotency state (Niwa *et al.*, 1998; van Oosten *et al.*, 2012). These observations further support that the differentiation status correlates with endogenous Myc levels in ESC culture and suggest that differentiation-primed lineages might be outcompeted by their naive neighbours.

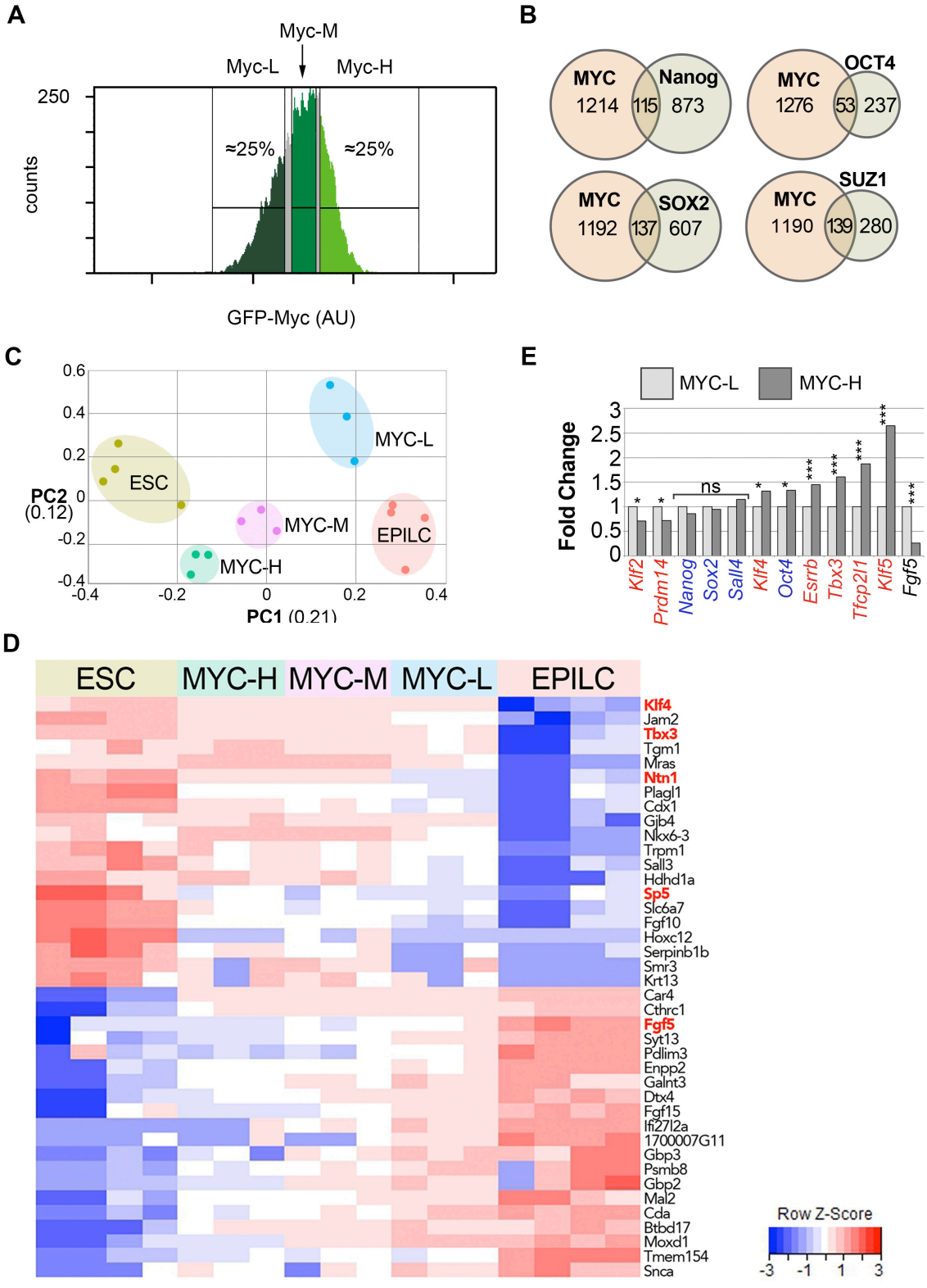

Figure 22. Transcriptome analysis of GFP-Myc ESCs.

A. Flow cytometry profile of GFP-Myc ESC line showing how populations - Myc-L, Myc-M and Myc-H - were established depending on GFP levels. **B**. Top overlaps between gene sets in the GSEA database and the group of genes that change expression between Myc-H and Myc-L cells in RNAseq analysis. **C**. Principal components analysis between Myc-H, Myc-M and Myc-L cells, and published expression data reports (Buecker *et al.*, 2014; Sasaki *et al.*, 2015) for naive ESCs and epiblast-like stem cells (EpiLC). **D**. Analysis of the genes contributing most to PC1; genes functionally involved in pluripotency status regulation or reporting (Guo *et al.*, 2009; Niwa *et al.*, 2009; Marks *et al.*, 2012; Ozmadenci *et al.*, 2015; Khoa le *et al.*, 2016; Ye *et al.*, 2016) are shown in red. **E**. Variations between Myc-H and Myc-L ESCs in the amounts of mRNAs encoding major regulator of pluripotency status. In blue, the core-pluripotency transcription factors; in red, the naive-pluripotency transcription factors; in black, Fgf5, a marker of primed pluripotency. In **E**, ns, adjusted p-val>0,05; p<0,05*, p<0,001***.

Furthermore, these data agree with our experimental ESC culture conditions, (serum replacement and Leukemia inhibitory factor (LIF) without feeder fibroblasts), which allow heterogeneity in the pluripotency status.

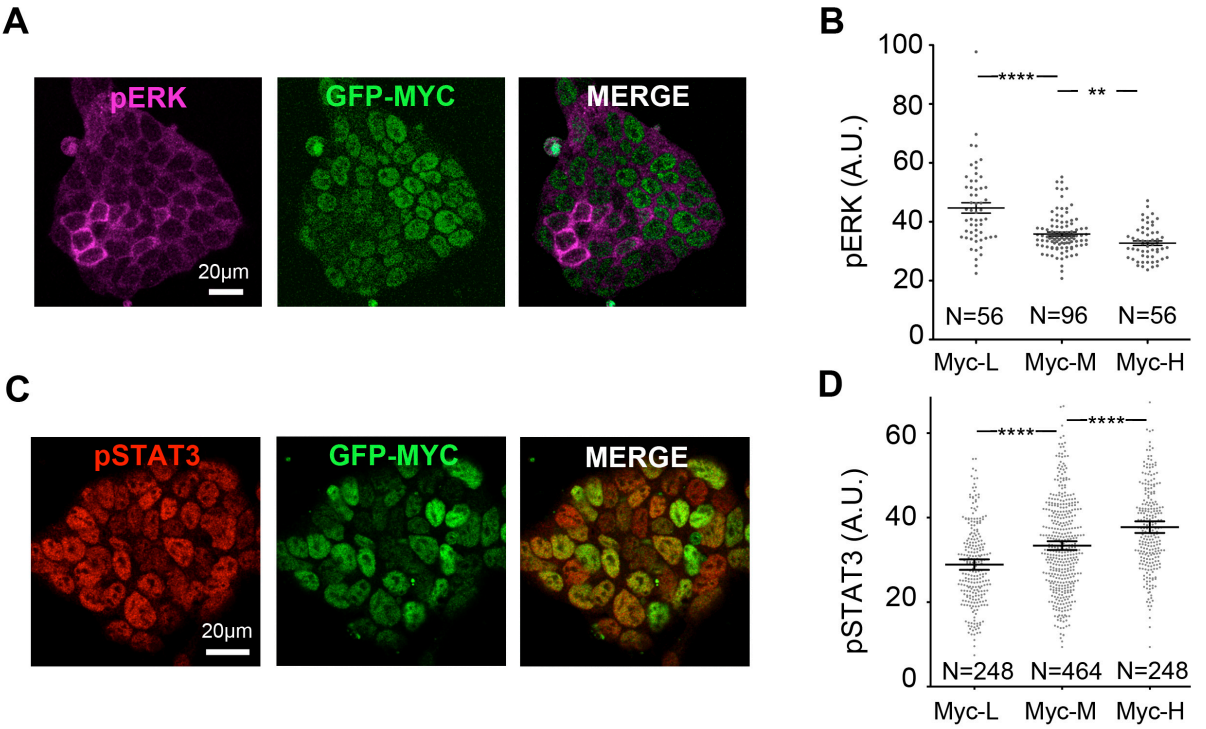

Figure 23. Analysis of the main signalling pathways that characterize the naive and primed pluripotency status.

A. Co-localization of pERK and GFP-Myc in ESCs. **B**. pERK immunofluorescence signal in ESCs classified by GFP-Myc levels. **C**. Co-localization of pSTAT3 and GFP-Myc in ESCs. **D**. pSTAT3 immunofluorescence signal in ESCs classified by GFP-Myc levels. Dotplots show mean ± 95% confidence interval. Mann Whitney test was used for statistics. p-value<0,01**; p<0,0001****.

10. Myc levels are regulated by the DNA methylation status

DNA methylation (5mC) at CpG dinucleotides is an inhibitory epigenetic modification often associated with transcriptional silencing. Other roles of this modification in transposable element regulation, splicing and genome integrity have also been identified (Smith and Meissner, 2013; Hackett and Surani, 2014). DNA methylation mostly faithfully kept through cell divisions, stabilizing restriction of cellular identity, except during early development where 5mC is dynamically remodeled (Smallwood *et al.*, 2011; Smith *et al.*, 2012; Hackett and Surani, 2014). Naive pluripotent cells of the early epiblast show very low levels of methylation because of the activity of de-methylating enzymes (TET proteins) and global eradication of DNA methylation is needed to eliminate epigenetic barriers against the acquisition of naive pluripotency (Hackett *et al.*, 2013). Previous works have reported that naive ESCs show globally hypomethylated DNA when derived in 2i/LIF. However, ESCs cultivated in serum exhibit increased levels of DNA methylation typically associated with the primed status and further differentiation into specific lineages typical of the late epiblast (Hackett and Surani, 2014). In fact, ESCs exhibit 3-fold higher 5mC in serum in comparison with 2i/LIF culture medium (Ficz *et al.*, 2013; Habibi *et al.*, 2013; Leitch *et al.*, 2013). Therefore, ES cells maintained in 2i/LIF conditions show similar levels and distribution of 5mC to the naive epiblast cells, whereas cultures grown in serum contains not only naive cells but also cells that are closer to primed epiblast cells and show significant DNA methylation.

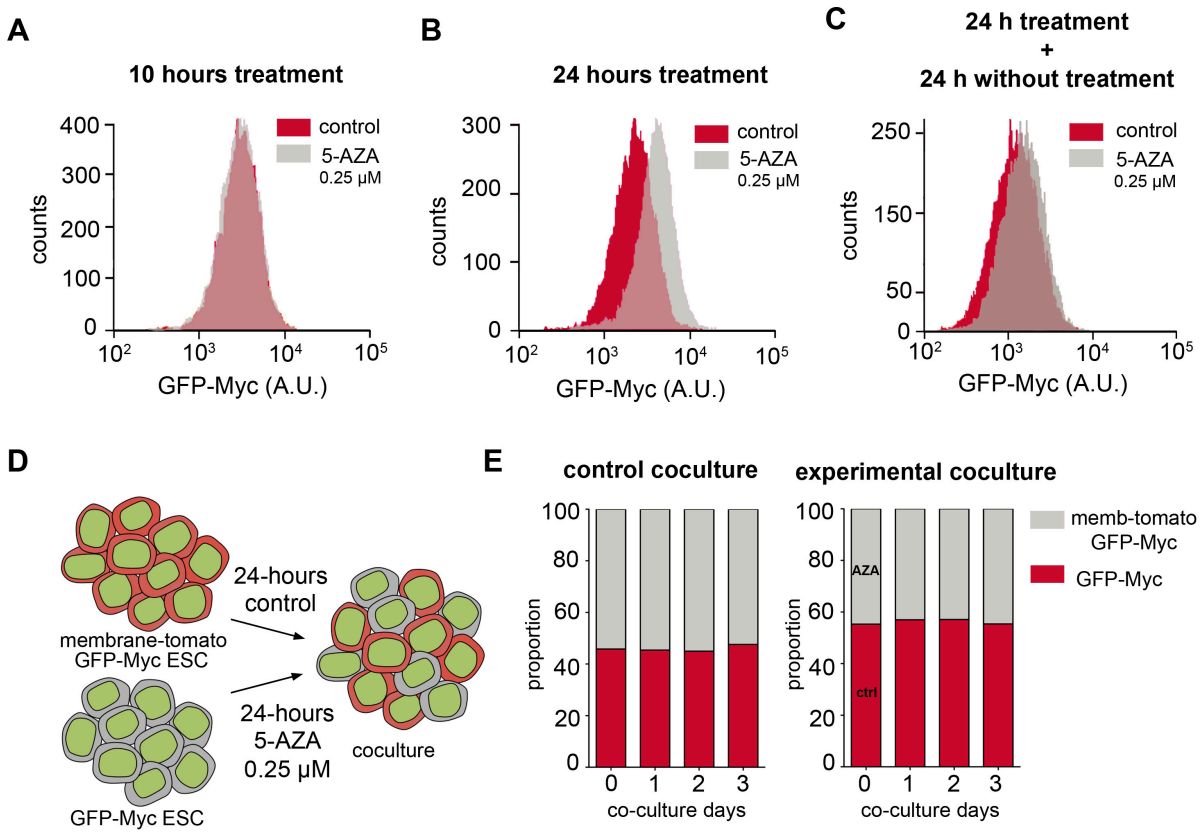

Figure 24. Analysis of DNA methylation and Myc expression in ESCs.

A. Flow cytometry profile of GFP-Myc ES cells with or without 10 hours of 5-Azacitidine treatment. **B**. Flow cytometry profile of GFP-Myc ES cells with or without 24 hours of 5-Azacitidine treatment, showing the displacement of the curve in the experimental condition. **C**. Flow cytometry profile of GFP-Myc ES cells with or without 24 hours of 5-Azacitidine treatment plus other additionally 24 hours in normal medium, showing the partial recovery of the initial GFP-Myc levels in the experimental condition. **D**. Procedure for confronting control cells (Tomato$^+$) – grown in normal medium – and 24-hours treated cells (Tomato$^-$). **E**. Frequency of Tomato$^+$ and Tomato$^-$ cell populations after different periods of co-culture. On the left, none of the populations was treated; on the right, Tomato$^-$ population was treated with 0.25 μM 5-Azacytidine.

As reflected in our RNAseq analysis, our ESC culture conditions allow pluripotency heterogeneity, with some cells closer to naive status and others closer to differentiation-primed status, which associates with Myc expression levels. We thus tested whether experimental epigenetic modification of the methylation status would affect Myc levels. To address this question, we used the drug 5-Azacitidine, which

inhibits DNA methyltransferases, causing DNA hypomethylation. We observed that Myc levels of GFP-Myc ESCs did not show any variation after 10 hours of treatment (Figure 24 A). Notably, ESCs treated with Azacitidine for 24 hours did show an increase in their Myc-GFP levels (Figure 24 B; video 11). In addition, we measured Myc-GFP levels at 24 hours after treatment removal and observed a partial recovery of Myc expression levels in the absence of any treatment (Figure 24 C). These data suggest that Myc levels are controlled to a certain extent by DNA methylation and, together with the correlation between Myc and the pluripotency status, suggests that differentiation-associated methylation is one of the factors that determines the heritable modification of Myc levels in ES cell sub-lineages.

Next, we examined whether the increase in Myc levels mediated by 5-Azacitydine could trigger cell competition. To this end, we cultured GFP-Myc ESCs with 0.25 μM 5-Azacitydine for 24 hours and confronted them with membrane-tomato GFP-Myc ESCs kept in control medium for several days (Figure 24 D). We then analysed the proportions of both populations in coculture and found that the proportion of the treated cell population –exhibiting higher Myc levels- did no increase when confronted with a control cell population (Figure 24 E). This observation shows that increasing Myc level by exposure to the demethylating agent 5-Azacytidine is not sufficient to induce cell competition, suggesting that pleiotropic effects of the drug abrogate ESC competitive ability.

11. 2i culture conditions reduce Myc heterogeneity and blocks endogenous cell competition

As previously shown, our experimental ESC culture conditions allow heterogeneity in pluripotency status. In addition, since LIF limits the transition from naive to primed pluripotent states and the primed state is not reversible by changes in the signalling environment (Guo *et al.*, 2009), our observations are also in accordance with the heritability of Myc levels.

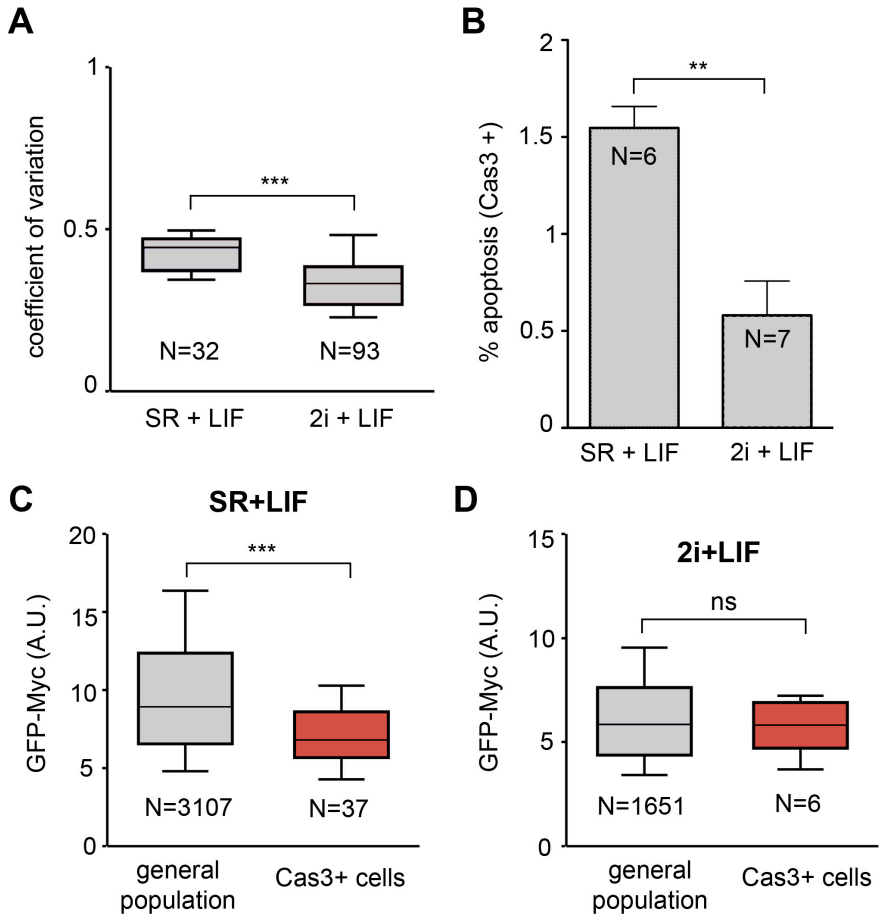

Figure 25. Study of 2i culture condition effects on Myc expression and cell competition in ESCs.

A. Coefficient of variation (heterogeneity) of GFP-Myc levels in SR+LIF medium and in 2i+LIF medium. **B**. Relative frequency of caspase-3 positive cells in SR+LIF and in 2i+LIF. **C**. GFP-Myc levels in non-apoptotic (general population) and apoptotic (caspase-3 positive) cells in SR+LIF. **D**. GFP-Myc levels in non-apoptotic (general population) and apoptotic (caspase-3 positive) cells in 2i+LIF. Boxplot in **A**, **C** and **D** show median, 25 and 75 percentiles (boxes), 10 and 90 percentiles (whiskers). Column bar graph in **B** show mean and standard error of the mean (SEM). Mann Whitney test was used for statistics. ns, adjusted p-val>0,05; p<0,01**, p<0,001***.

Previous work reported that ESCs cultured with MAPK and GSK inhibitors (2i) maintain the naive state, giving rise to cultures expressing pluripotency markers in a more homogeneous manner (Ying *et al.*, 2008). As we showed that cell competition takes place when cells with discrepant Myc levels are confronted and these levels correlate with the pluripotency status, we examined the effect of 2i culture conditions on Myc expression and the competitive behaviour of ESCs. To address this question,

we cultured GFP-Myc ES cells with or without 2i for three days. We found that Myc level heterogeneity was reduced in 2i conditions (Figure 25 A). Next, we studied whether the decrease in Myc heterogeneity led to a change in the competitive ability by measuring the frequency of apoptotic events and Myc levels of those apoptotic cells. Interestingly, the death frequency was 3-fold less in the 2i conditions with respect to serum+LIF culture conditions (Figure 25 B). We then measured Myc levels in non-apoptotic cells and in dying cells in the first phases of apoptosis, when they present active caspase-3 staining but still intact nuclei. As expected (Claveria *et al.*, 2013), in serum replacement+LIF culture conditions Myc levels were higher in non-apoptotic cells than in early apoptotic cells (Figure 25 C). However, in 2i culture conditions there was no significant difference in Myc levels between apoptotic and non-apoptotic cells (Figure 25 D). These results show that, in similarity to the core pluripotency factors, Myc expression heterogeneity is reduced in ESCs cultured in 2i conditions, which further supports the idea of the correlation between Myc and the pluripotency status. Moreover, Myc-mediated spontaneous cell competition does not take place in naive ESC cultures where discrepancies in Myc levels between cells are reduced.

12. Cell competition can be experimentally induced by confronting cells with different pluripotency status

We showed in previous experiments that differentiation-primed cells might be eliminated by their naive neighbours. To directly test this hypothesis, we induced ES cells to differentiate by LIF withdrawal and confronted them with naive ES cells kept in LIF, plus 2i (Figure 26 A). We analysed the proportions of both populations over time and found that the differentiating ESC population was outcompeted by naive ES cells (Figure 26 B). These differentiating ES cells were otherwise viable when cultured alone, but the frequency of apoptosis increased almost 3-fold when co-cultured with naive cells (Figure 26 C), indicating that the elimination of the differentiating population occurs through cell competition. Moreover, in agreement with previous studies (Sumi *et al.*, 2007) and our RNAseq analysis, the differentiating population exhibited lower GFP-Myc levels than the naive population in co-culture (Figure 26 D, E), which confirmed the expected correlation between Myc levels and competitive ability. These observations support that Myc levels associate with different states of

pluripotency in ESCs and that the confrontation of Myc-high naive cells with My-low differentiation-primed cells gives rise to the elimination of the latter through cell competition.

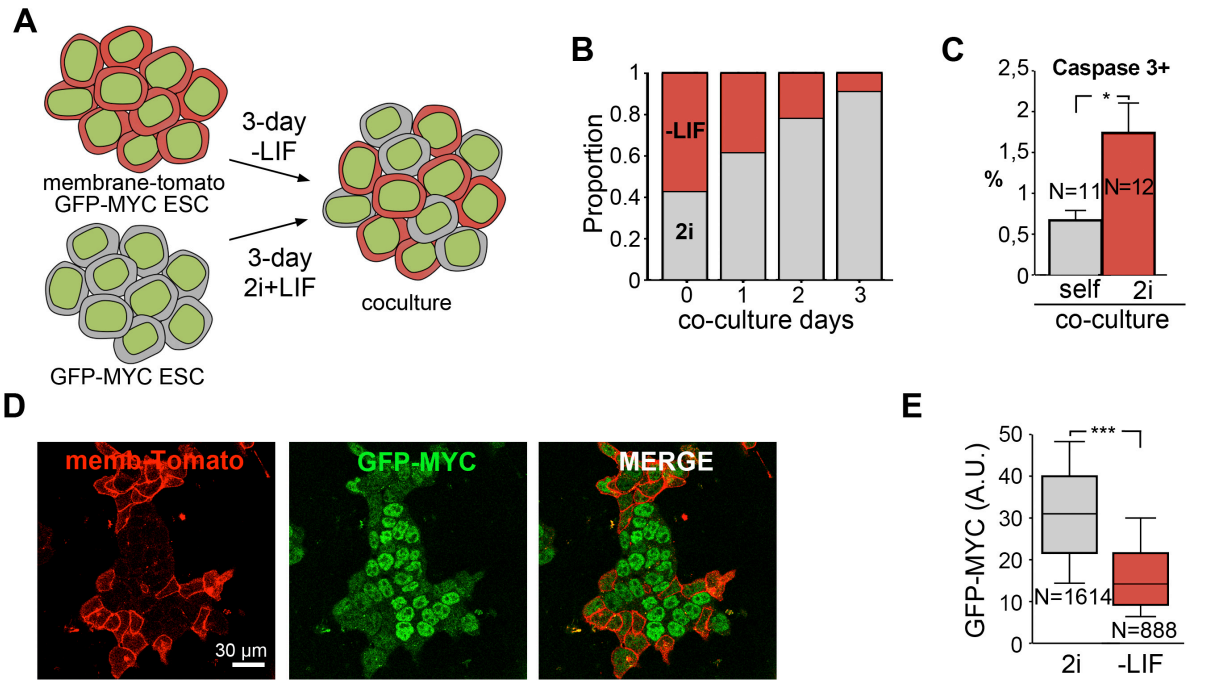

Figure 26. Cell competition induced by confronting population with different pluripotency status.

A. Procedure for confronting differentiating ESCs (Tomato$^+$) and naive ESCs (Tomato$^-$). **B**. Frequency of Tomato$^+$ and Tomato$^-$ cell populations after different periods of co-culture. **C**. Frequency of caspase3-positive cells in the differentiating Tomato$^+$ cell population alone or in co-culture with naive ESCs. Data were collected by microscopic fields (N). **D**. Immunofluorescence study of Myc levels after 2-day co-culture of Tomato$^-$ ESCs pre-cultured for 3 days with LIF+2i and Tomato$^+$ ESCs pre-cultured for 3 days without LIF. **E**. GFP-Myc levels in Tomato$^+$ and Tomato$^-$ cell populations in co-culture. Column bar graph in **C** show mean and standard error of the mean (SEM). Boxplot in **E** show median, 25 and 75 percentiles (boxes), 10 and 90 percentiles (whiskers). Mann Whitney test was used for statistical analysis. p-value<0,05*; p<0,001***.

13. Blocking cell competition results in the accumulation of differentiation-primed cells

We next explored whether cell competition could be acting as a mechanism to prevent the accumulation of cells that are prone to differentiate in ESC cultures. To address this question we used the *iMOS*$^{T1\text{-}p35}$ ESC line (Claveria *et al.*, 2013), in which following tamoxifen addition, a mosaic of EYFP- and ECFP-expressing cells is induced and apoptosis is inhibited in the ECFP population because of the expression of the caspase inhibitor p35, whereas the EYFP population remains WT and is allowed to undergo apoptosis (Figure 27 A). ECFP protein was not well detected in the microscope, therefore we recognize ECFP positive cells by doing immunostaining with anti-GFP antibodies, which recognize both ECFP and EYFP, so that cells positive for anti-GFP staining and negative for EYFP were identify as ECFP p35-expressing cells (Figure 27 B).

We then compared the death-blocked population 48 hours after the induction (see Material and Methods) with the wild type neighbours and found that the rescued cells showed a higher proportion of active-pERK levels than the control population (Figure 27 B, C). This result suggests that cell competition might be acting in maintaining ESC cultures in a naive pluripotent state by restricting the differentiating population.

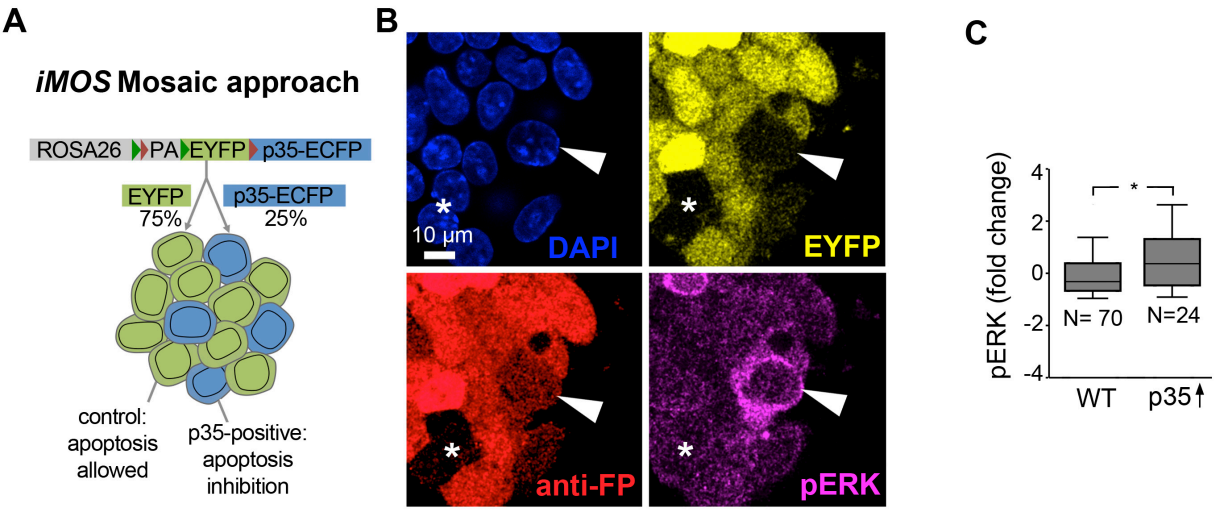

Figure 27. Cell competition and pluripotency status studied by cell death inhibition using the *iMOS*$^{T2\text{-}p35}$ mosaic approach in ESCs.

A. Scheme showing the *iMOS* strategy for inhibiting cell competition in ESCs. **B**. Co-localization of direct detection of EYFP with immunofluorescent detection of total fluorescent protein (FP) and active pERK. Arrowhead indicates an ECFP-p35^{+} cell, identified by absence of EYFP and presence of FP immunodetection. Asterisk indicates FP-negative cells. **C**. Active-pERK levels fold change in ECFP-p35^{+} cells vs neighbouring wild type cells. Boxplot show median, 25 and 75 percentiles (boxes), 10 and 90 percentiles (whiskers). Mann Whitney test was used for statistical analysis. p-value<0,05*.

14. Differentiating-primed cells are eliminated from pre-gastrulation embryos through cell competition

14.1. Myc/pERK regulation in the epiblast

We then studied whether this observed mechanism applies to epiblast cells in the early mouse embryo. To this end, we first examined the pattern of pERK activation in early postimplantation embryos. We found that at E5.0 the epiblast did not contain any pERK positive cell (Figure 28 A). In contrast, E6.0 embryos showed around 1-4% of isolated cells positive for pERK in an apparently random pattern (Figure 28 B-D). This pERK positive cell population exhibited lower Myc levels than the pERK negative cells (Figure 28 C, D), suggesting a similar relationship *in vivo* as that found in ESCs.

Next, we studied the pattern of pERK expression in early gastrulating embryos. The embryo gastrulates by the recruitment of epiblast cells to the primitive streak. During this process, a coordinated loss of pluripotency occurs in the vicinity of the primitive streak for mesoderm formation. At this embryonic stage, we found a regional expression of pERK and downregulation of Myc close to the primitive streak region (Figure 28 E). These results suggest that Myc/pERK regulation in the epiblast correlates with the patterns found in ESC cultures.

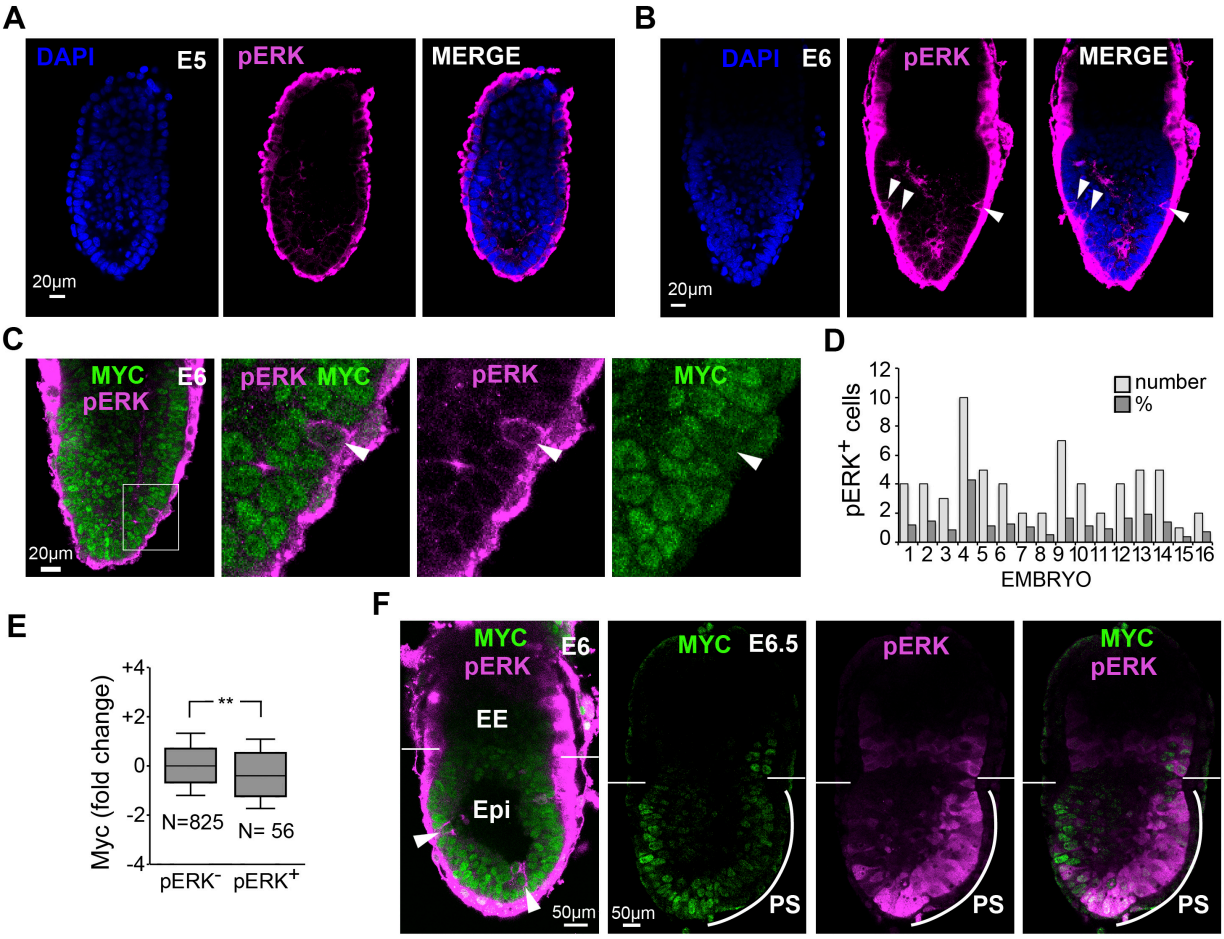

Figure 28. Analysis of pERK activation in the epiblast and correlation with Myc levels.

A. Confocal detection (optical sections) of pERK immunofluorescence in an E5.0 mouse embryo showing no pERK$^+$ cells in the epiblast. **B**. Confocal detection (optical sections) of pERK immunofluorescence in an E6.0 mouse embryo. White arrowheads show pERK$^+$ cells. **C**. Co-localization by immunofluorescence of Myc and active pERK in the epiblast of E6.0 mouse embryos. White arrowhead shows a pERK$^+$ cell exhibiting low GFP-Myc levels. **D**. Scoring of detected active pERK$^+$ cells in the E6 mouse epiblast. **E**. Normalized Myc level distributions in active pERK$^+$ and pERK$^-$ cells of the mouse E6 epiblast. **F**. Co-localization by immunofluorescence of Myc and active pERK in the epiblast of E6 and E6.5 mouse embryos. EE, extraembryonic; Epi, Epiblast; PS, primitive streak. Boxplot in **E** shows median, 25 and 75 percentiles (boxes), 10 and 90 percentiles (whiskers). Mann Whitney test was used; p-value<0,01**.

14.2. pERK positive cells are accumulated when blocking apoptosis in early embryos

We next studied whether the population of isolated pERK+ cells is restricted by cell competition in the pre-gastrulation embryo, as it does in ESC cultures. To address this question, we used the *iMOS* system to induce mosaics of p35-expressing cells and WT cells in embryos. We analyzed embryos at E5.5-6 where pERK-activated cells were scarcely present in the wild type population (Figure 29 A). Interestingly, we observed that pERK positive cells specifically accumulated in the death-blocked p35-expressing population (Figure 29 B, C). This observation suggests that differentiation-primed cells are eliminated through apoptosis from the pre-gastrulation epiblast.

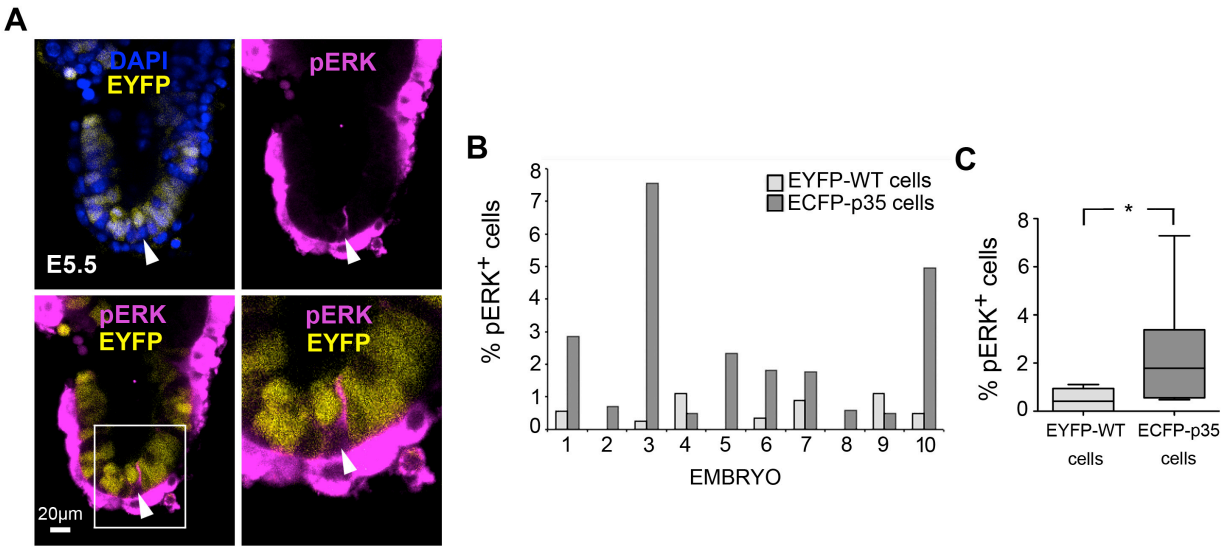

Figure 29. Cell competition inhibition and pluripotency status analysed using the *iMOS*$^{T2\text{-}p35}$ mosaic approach in the epiblast.

A. Co-localization of EYFP and active pERK^{+} cells in the epiblast of E5.5 *iMOS*^{T2p35} mouse embryos recombined with *Sox2Cre*. **B**. Scoring of detected pERK^{+} cells in the epiblast of E5.5 *iMOS*$^{T2\text{-}p35}$ embryos recombined with *Sox2Cre*. **C**. Frequency of EYFP-WT and ECFP-WT cells in the 10 embryos. Boxplot in **C** show median, 25 and 75 percentiles (boxes), 10 and 90 percentiles (whiskers). Mann Whitney test was used for statistical analysis; p-value<0,05*.

15. Myc directly defines the ESC competitive ability irrespective of the pluripotency status

We next studied the functional relationship between Myc and the pluripotency status. To this end we used the *iMOS*$^{T1\text{-}Myc}$ cell line, in which we induced Myc overexpression in a random subset of cells cells (Figure 30 A). This *iMOS* mediated Myc overexpression is enough to induce cell competition as it has been described (Claveria *et al.*, 2013) and we showed above (Figure 19). We found that after Myc-overexpressing cells in mosaic cultures did not decrease pERK levels in comparison to their WT neighbors; in fact, they underwent a slight increase (Figure 30 A, B).

In addition, a compared transcriptome analysis by RNAseq between EYFP-Myc and control populations from mosaic cultures (C. Clavería, unpublished) not only did not show promotion of the naive pluripotency signature but rather a mild inhibition of this (Figure 30 C). Conversely, ESC differentiation by LIF withdrawal leads to GFP-Myc downregulation (Figure 26 D, E), in agreement with previous studies (Sumi *et al.*, 2007).

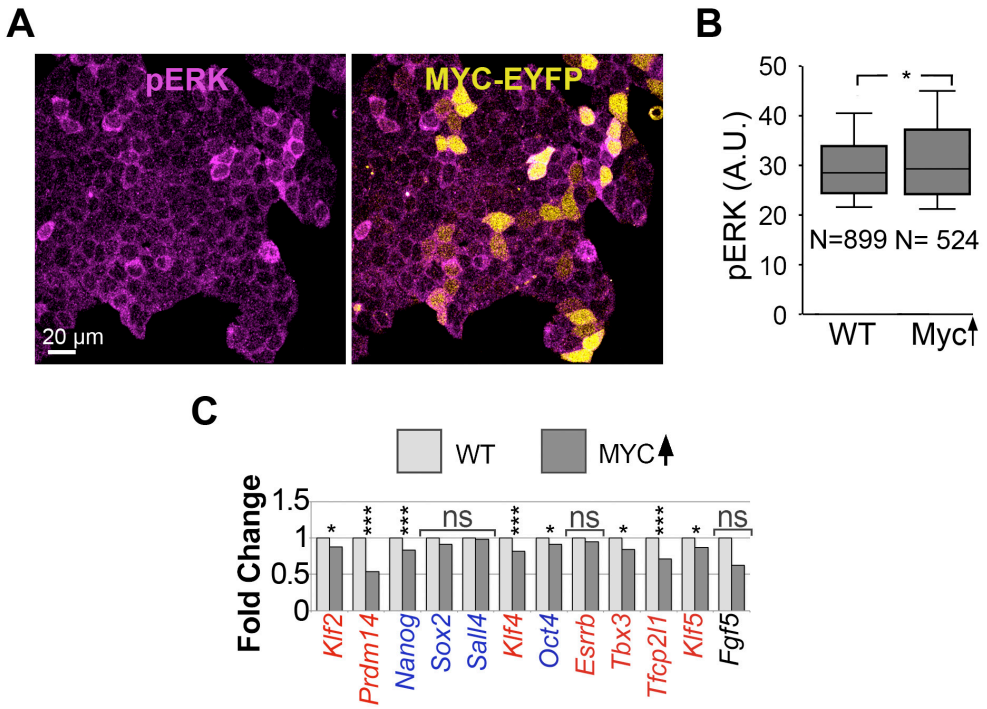

Figure 30. Study of the functional relationship between Myc and the pluripotency status.

A. Co-localization of active pERK and Myc in ESCs with mosaic overexpression of EYFP-Myc from the *iMOS^{T1}-Myc* allele. **B**. Distributions of active-pERK levels in WT ESCs and ESCs overexpressing EYFP-Myc from the *iMOS^{T1-Myc}* allele. **C**. Variations between WT and EYFP-Myc overexpressing cells in the amounts of mRNAs encoding major regulators of pluripotency status. In blue, the core-pluripotency transcription factors; in red, the naive-pluripotency transcription factors; in black, Fgf5, a marker of primed pluripotency. Boxplot in **B** show median, 25 and 75 percentiles (boxes), 10 and 90 percentiles (whiskers). For statistics Mann Whitney test was used. ns, adjusted p-val>0,05; p<0,05*, p<0,001***.

These results, together with the induction of the winner phenotype by the *Myc* induction (Claveria et al., 2013), suggest a linear pathway in which Myc lies downstream the differentiation status and Myc directly determines the competitive ability of ESCs without modifying the pluripotency status.

DISCUSSION

In this doctoral thesis we have studied how Myc is regulated and how its heterogeneous expression and dynamics leads to spontaneous cell competition in ESCs. Additionally, we have explored the biological relevance of Myc-dependent endogenous cell competition both in ESCs and in early mouse development.

Despite the key role reported for both Myc and Mycn during embryogenesis (Charron *et al.*, 1992; Trumpp *et al.*, 2001; Dubois *et al.*, 2008) and their redundant and cooperative function in maintaining the ESC proliferative program (Malynn *et al.*, 2000; Scognamiglio *et al.*, 2016), we showed that Mycn expression does not correlate with Myc expression in ESCs and, contrary to observations with Myc (Claveria *et al.*, 2013), that endogenous Mycn levels do not correlate with the winner/loser ESC status. These observations, together with the absence of Mycl in ESCs, indicate that Myc regulation is the main driver of spontaneous cell competition in ESCs, with no contribution from other members of the proto-oncogene Myc family.

Given the major role of Myc in cell competition in ESCs, in this thesis we have developed new time-lapse microscopy and image analysis tools to track Myc levels during cell competition. To this end, we used an ESC line expressing a GFP-Myc fusion protein that faithfully reports endogenous Myc levels. To our knowledge, this new developed technique for tracking ESC lineages and endogenous Myc levels in 3D+t is the first described in the field of study. In a recently published work ESCs are tracked in 2D in conditions in which cell-to-cell interactions are inhibited and therefore it is not suitable for cell-interactive studies (Filipczyk *et al.*, 2015). Our methodology allowed us to track ESC lineages through cell division and under entirely interactive conditions.

Furthermore, cell competition in ESCs and in the mouse epiblast is regulated by Myc expression heterogeneity among cells, however due to the lack of a strategy for isolating and tracking live cells according to Myc levels, the biological basis of Myc-low cells outcompetition from ESC cultures and early embryos was unknown. In this thesis, these limitations have been overcome by implementing this new microscopy and image analysis tool. Moreover, we also tracked the temporal evolution of Myc levels during cell proliferation, which has never been reported in any cell type. This approach allowed us to generate cell lineage trees that contain

information on the history of Myc levels for each cell, together with 3D information that allows to determine neighbourhood relationships between cells.

Using this tool we studied the stability of Myc levels in different subpopulations defined by Myc levels, both during the observation period and through cell divisions. We showed that Myc expression levels in ESCs are imprinted to a large extent, such they are conserved trough mitosis. Additionally, retrospective clonal analysis experiments suggest that Myc levels display high heritability (0.8 per cell division). These data allow the emergence of a new concept that we called heritable fitness and consists on the heritable competitive ability of cells based on the transmission of Myc levels in ESCs sublineages coexisting in culture. The concept of Myc heritability is different from previous knowledge on the main factors contributing to Myc regulation. While Myc is generally found to be regulated by extracellular signals in somatic cells (Wierstra and Alves, 2008), both the cell-to-cell heterogeneous pattern and the heritability of MYC expression levels in ESCs indicate an important contribution of cell-intrinsic heritable features, in Myc regulation in ES cells.

The computer workflow established also allowed us to track Myc expression levels in individual cells and its neighbours, which allows the study of the dynamics of endogenous cell competition in a quantitative manner. Using this methodology, we have demonstrated that cell competition is driven by random contacts between cells with high discrepancies in Myc levels. Low-Myc cells are thus able to survive in ESC colonies as long as the differences in Myc expression levels between them and their neighbours are moderate or transient, however sustained discrepancies for longer than 600-800 leads to the elimination of the loser cells. We observed that the Myc expression profile during the 600-800 minutes preceding death of the loser shows a plateau shape. This observation indicates that loser cells measure time in exposure to neighbours with a discrepancy in Myc levels above a certain threshold, rather than accumulated Myc discrepancy. In case loser cells were measuring accumulated Myc discrepancies, then shorter exposures to higher Myc levels would also lead to cell competition and the shape of the Myc expression profile in neighbour of loser cells would show a continuous positive slope instead of a plateau.

Nevertheless, as the computer workflow only tracks and measures Myc levels of neighbour cells whose membranes are in direct contact with those of the loser cells, we only explored cell-to-cell contact dependent cell competition. Our initial hypothesis agrees with previous work reporting that direct contact is needed for competitive interactions (Simpson and Morata, 1981; Moreno *et al.*, 2002; Moreno and Basler, 2004; Li and Baker, 2007; Claveria *et al.*, 2013). Furthermore, since in our induced cell competition time-lapse experiments cell death rate is only increased in the population in direct contact with EYFP-Myc overexpressing cells, we obtained here further evidence of the need for cell-to-cell contact to induce apoptosis of loser cells.

We also observed, both in endogenous and in induced cell competition, a tendency in PDCs to reduce their Myc levels approximately 500 minutes before death and just after the increase in their neighbours' Myc expression levels. The nature of this decrease is not known yet; however, in our time-lapse analyses using a caspase-3 reporter, we observed that caspase-3 is activated only few minutes before the cell death suggesting that Myc reduction in PDCs is not due to the activation of caspase-apoptotic pathway. Thus, competitive interactions might be operating on pathways triggering Myc downregulation for extended periods in loser cells.

Our analysis shows that in ESC cultures Myc-low cells are continuously eliminated and replaced by Myc-high cells. If this process were continuous, after cultures would continuously evolve towards higher and more homogeneous Myc levels; nevertheless, ESCs cultures always exhibit heterogeneous levels of Myc. Thus, we hypothesize that continuous and spontaneous generation of low-Myc cells and their elimination by fitter cells should maintain the equilibrium between ESC populations with different Myc levels in ESC colonies.

We also explored the different roles and dynamics of loser and winner cells during cell competition. On one hand, previous works have shown the involvement of increased cell mixing activity of winner cells in Myc-induced cell competition in *Drosophila* imaginal discs (Levayer *et al.*, 2015), which contrast with our observations of any obvious active role of either winner or loser cells. In our model, interactions between loser and winner cells result from apparently random passive

contacts. Nevertheless, *Drosophila* imaginal discs cells are organized in a columnar epithelium where different sublineages mix poorly, whereas in ESC cultures there is a constitutive intense mixing, suggesting that the different environments may explain the differences observed between these two models.

On the other hand, we observed that Myc-high cells show higher variance of roundness over time that Myc-low cells. This result agrees with previous works in mammalian cells in which the winner phenotype presents higher deformability mediated by RhoA and actomyosin (Sun *et al.*, 2014b). In addition, engulfment of losers by winner cells, which may involve differences in cytoskeleton dynamics, was also observed in mouse ESC and epiblast cells (Claveria *et al.*, 2013) . Engulfment was also reported to be the main system to eliminate loser cells in the *Drosophila* (Li and Baker, 2007); nonetheless, this observation contrasts with other recent works also performed in this model (Levayer *et al.*, 2015).

Transcriptome analysis and the subsequent study of the main pathways characterizing naive and primed states allowed us to correlate Myc expression levels with the pluripotency status. A pool of pluripotent cells is maintained in early mammalian embryos for several days, however pluripotency is a highly unstable state, suggesting that specific mechanisms should be in place for pluripotency maintenance during this period. In this thesis we described a mechanism in which differentiation-primed cells are eliminated due to discrepancies in Myc levels with surrounding naive pluripotent cells. The fact that differences in pluripotency status may drive cell competition agrees with previous works reporting outcompetition of BMP-receptor-defective cells from ESC cultures and mouse epiblast (Sancho *et al.*, 2013). BMP signalling collaborates with STAT3 in maintaining the naive pluripotency status, and therefore BMP receptor mutants may not be able to maintain the naive pluripotent status, leading to Myc downregulation and cell competition.

However, since not all Myc-low cells show differentiation-primed signatures, the difference in the pluripotent status may only explain part of the Myc-low population. Therefore, it would be important to identify additional cellular features characteristic of the Myc-low population to achieve a fully characterization of endogenous cell competition in the epiblast. Moreover, we only explored the

phenomenon of cell competition during one phase of the development and this mechanism could be also playing a role in other stages of the early mouse embryo. In fact, previous works already reported apoptosis in the inner cell mass of the blastocyst (Plusa *et al.*, 2008), much before the stage in which this thesis is focused. At that stage the primitive endoderm differentiates and segregates from the inner cell mas of the blastocysts, which is the second event of differentiation after trophectoderm differentiation (Stephenson *et al.*, 2012). In a first step, primitive endoderm cell specification takes place in a spatially disorganized manner within the inner cell mass, so that cells of the PE lineage and those of the epiblast are intermingled. In a second step, cells specified as primitive endoderm segregate towards the blastocoel lumen. Interestingly, cells specified as primitive endoderm that fail to segregate from the pool of pluripotent cells of the inner cells enter in apoptosis (Plusa *et al.*, 2008; Stephenson *et al.*, 2012). Moreover, Myc levels are heterogeneously expressed also in the inner cell mass of blastocyst (Claveria *et al.*, 2013) and is downregulated when cells differentiate to primitive endoderm (Smith *et al.*, 2010). All these observations suggest that Myc-driven cell competition triggered by discrepant differentiation status may not only occur in the context described here, but may function as a more general mechanism affecting other developmental stages.

Additionally, recent work reports an apoptosis-dependent selection process during the colonization of the blastocyst inner cell mass by injected ESCs. In this model, naive ESCs preferentially colonize the inner cell mass, while primed ESCs are preferentially eliminated from the embryo by apoptosis (Alexandrova et al., 2016). This observation agrees with the model described here, however, in this work, ESC elimination does not correlate with Myc levels in the inner cell mass cells, which contrasts with the direct role of Myc in cell competition in the early epiblast and ESCs.

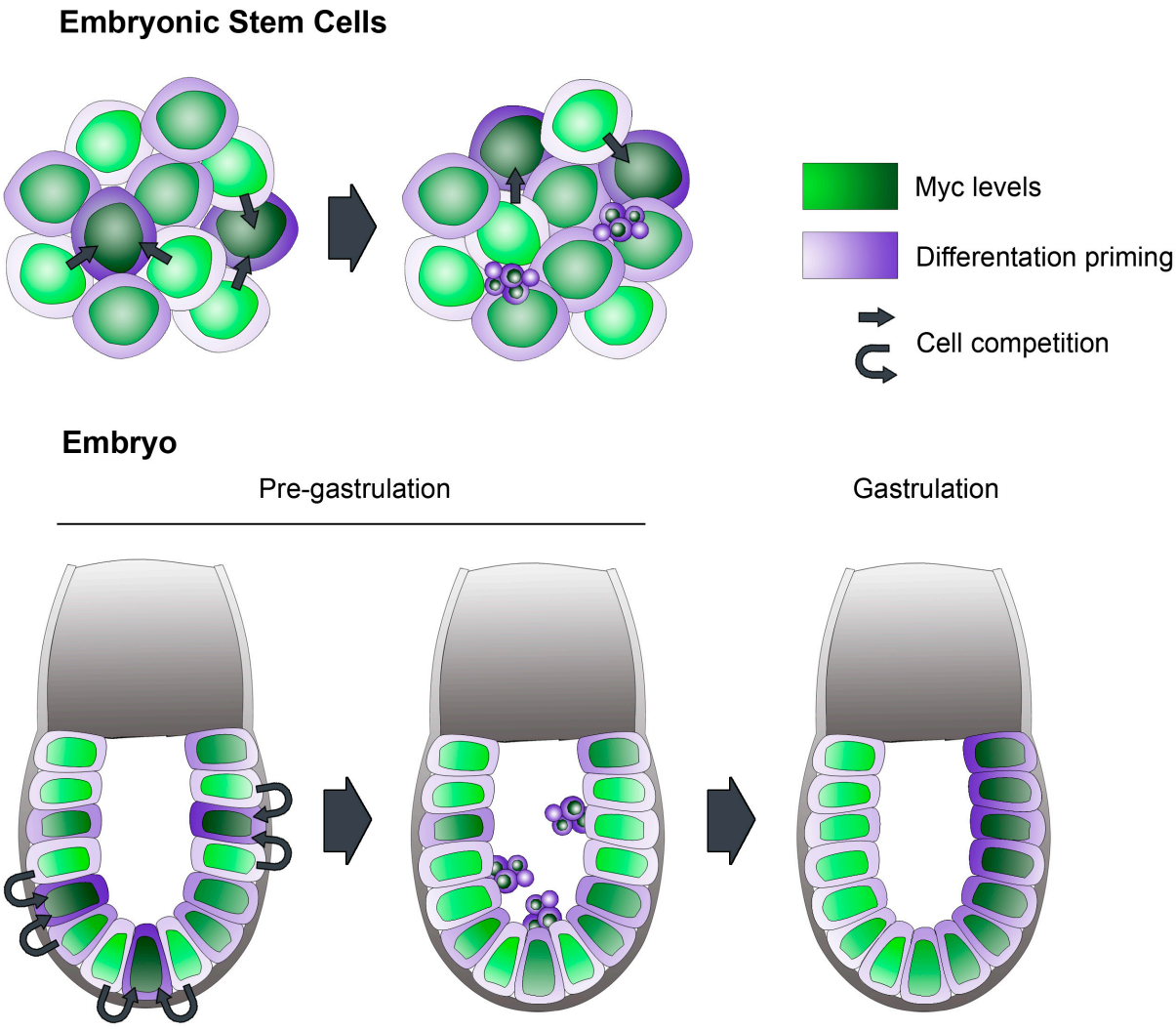

Figure 31. Proposed model of Myc-driven cell competition protecting pluripotent cells against differentiation in ESCs and epiblast.

In ESCs differentiation-primed Myc-low cells are continuously outcompeted and replaced by naive Myc-high cells. However, there is a spontaneous generation of these primed low-Myc cells that maintains equilibrium in ESC colonies.
In the embryo cell competition is preserving the naive pluripotent status of the epiblast by eliminating cells in transit to differentiation before the time is right for differentiation. In contrast, when epiblast gastrulates a coordinated differentiation occurs in the posterior part of the epiblast and Myc is simultaneously downregulated, which allow controlled differentiation with no competitive interactions.

Myc has a role during induced pluripotent stem cell generation in promoting cell reprogramming of somatic cells in cooperation with transcription factors of the core pluripotency network (Takahashi and Yamanaka, 2006); in this thesis we described a mechanism that could help to better understand Myc implication in this process. First, we show that enhanced Myc activity does not promote the naive pluripotency signature, which fits results from other studies (Kim *et al.*, 2010; Gu *et al.*, 2016; Scognamiglio *et al.*, 2016). Second, we observe that pluripotent cell proliferation can be efficiently driven by low Myc activity suggesting that Myc expression levels would be hardly relevant for stimulating proliferation during reprogramming. Indeed it has been reported that reprogramming of somatic cells can take place at lower efficiency in the absence of Myc overexpression (Nakagawa *et al.*, 2008), which is compatible with our findings suggesting Myc's role in reprogramming relates to promotion of pluripotent cell selection rather than to direct stimulation of pluripotency or proliferation.

Taken altogether, we propose a model in which cell competition maintains the naive pluripotency status in mouse pluripotent stem cell populations by eliminating cells in transit to differentiation (Figure 31). We provide evidence of a linear pathway in which Myc levels are determined by the pluripotency status and set ESC competitive ability without affecting the pluripotency status. This mechanism provides protection of naive pluripotent cell pools from premature differentiation by eliminating differentiation-prone cells; therefore cell competition operates as a surveillance mechanism of the stem cell pools in the mouse epiblast and ESC groups. When isolated cells spontaneously start to differentiate in a context of predominant naive cells, the contrast in Myc levels between the differentiating cell and its neighbours induces their elimination. In the early epiblast, this mechanism controls the naive status of the epiblast cell pool before the time is right for differentiation. In contrast, when the embryo starts to gastrulate, coordinated differentiation occurs and Myc levels and differentiation priming are homogeneously regulated in the posterior area of the epiblast. We therefore hypothesize that at this stage, the homogenous decrease in Myc levels avoids differences between cells and programed differentiation can take place without induction of cell competition (Figure 31).

CONCLUSIONS

1. Myc regulation is the main driver of spontaneous cell competition in ESCs, with no involvement of other members of the *Myc* family.

2. The GFP-Myc knock-in line faithfully reports endogenous Myc levels and the imaging tool established provides a complete and reliable set of biological data during Myc-dependent cell competition in ESCs.

3. Myc expression levels are depleted by specific degradation of the Myc protein during ESC mitosis.

4. Myc levels are largely imprinted in ESCs, being mostly regulated by cell-intrinsic heritable factors.

5. Passive contacts between cells with high discrepancies in Myc levels that extend longer than ~10 h trigger cell competition in ESCs.

6. The proliferative state of ESCs requires Myc levels over a certain threshold, however, Myc levels do not modulate the speed of proliferation in cycling ESCs. The competitive ability of ESCs is dictated by Myc levels irrespective of the proliferation rate.

7. Myc levels correlate with the differentiation status and are controlled by epigenetic control in ESCs.

8. Endogenous cell competition maintains the naive pluripotent status of ESC cultures by eliminating differentiating cells.

9. Myc lies downstream the differentiation status and directly determines the ESC competitive ability.

10. Myc-driven cell competition triggered by discrepant pluripotency status also occurs *in vivo*, where differentiation-primed cells are eliminated from the pre-gastrulation epiblast.

1. La regulación de Myc es el principal factor desencadenante de la competición celular espontánea en CMEs, sin implicación de otros miembros de la familia de genes *Myc*.

2. La línea de ratón *knock-in* GFP-Myc reporta fehacientemente los niveles de expresión endógenos de Myc y la herramienta de imagen desarrollada proporciona un completo y fiable conjunto de datos biológicos durante la competición celular dependiente de Myc en CMEs.

3. Los niveles de expresión de Myc disminuyen por degradación específica de la proteína Myc durante la mitosis en CMEs.

4. Los niveles de Myc son en gran parte "grabados" en CMEs, siendo en general regulados por factores heredables intrínsecos.

5. En CMEs la competición celular se desencadena por contactos pasivos entre células con grandes discrepancias en sus niveles d Myc que se extienden más de ~ 10 horas.

6. El estado proliferativo de las CMEs requiere unos niveles de Myc por encima de un cierto umbral, sin embargo, éstos no modulan la velocidad de proliferación de células en mitosis. La capacidad competitiva de las CMEs está determinada por los niveles de Myc independientemente de la tasa de proliferación.

7. Los niveles de Myc correlacionan con el estado de diferenciación y son controlados mediante regulación epigenética en CMEs.

8. La competición celular endógena mantiene el estado de indiferenciación de los cultivos de CMEs mediante la eliminación de células en proceso de diferenciación.

9. Myc se encuentra por debajo del estado de diferenciación y determina directamente la capacidad competitiva de las CMEs.

10. La competición celular dependiente de Myc y desencadenada por diferencias en el estado de pluripotencia también tiene lugar *in vivo*, donde las células en proceso de diferenciación son eliminadas del epiblasto en estadio de pre-gastrulación.

BIBLIOGRAPHY

Abrams, J.M., 2002. Competition and compensation: coupled to death in development and cancer. Cell 110, 403-406.

Adachi-Yamada, T., Fujimura-Kamada, K., Nishida, Y., Matsumoto, K., 1999. Distortion of proximodistal information causes JNK-dependent apoptosis in Drosophila wing. Nature 400, 166-169.

Adachi-Yamada, T., O'Connor, M.B., 2002. Morphogenetic apoptosis: a mechanism for correcting discontinuities in morphogen gradients. Dev Biol 251, 74-90.

Alcolea, M.P., Greulich, P., Wabik, A., Frede, J., Simons, B.D., Jones, P.H., 2014. Differentiation imbalance in single oesophageal progenitor cells causes clonal immortalization and field change. Nat Cell Biol 16, 615-622.

Alexandrova, S., Kalkan, T., Humphreys, P., Riddell, A., Scognamiglio, R., Trumpp, A., Nichols, J., 2016. Selection and dynamics of embryonic stem cell integration into early mouse embryos. Development 143, 24-34.

Avilion, A.A., Nicolis, S.K., Pevny, L.H., Perez, L., Vivian, N., Lovell-Badge, R., 2003. Multipotent cell lineages in early mouse development depend on SOX2 function. Genes & development 17, 126-140.

Ballesteros-Arias, L., Saavedra, V., Morata, G., Cell competition may function either as tumour-suppressing or as tumour-stimulating factor in Drosophila. Oncogene.

Beddington, R.S., Robertson, E.J., 1999. Axis development and early asymmetry in mammals. Cell 96, 195-209.

Bedzhov, I., Graham, S.J., Leung, C.Y., Zernicka-Goetz, M., 2014. Developmental plasticity, cell fate specification and morphogenesis in the early mouse embryo. Philos Trans R Soc Lond B Biol Sci 369.

Boheler, K.R., 2009. Stem cell pluripotency: a cellular trait that depends on transcription factors, chromatin state and a checkpoint deficient cell cycle. J Cell Physiol 221, 10-17.

Bondar, T., Medzhitov, R., 2010. p53-mediated hematopoietic stem and progenitor cell competition. Cell stem cell 6, 309-322.

Boroviak, T., Loos, R., Bertone, P., Smith, A., Nichols, J., 2014. The ability of inner-cell-mass cells to self-renew as embryonic stem cells is acquired following epiblast specification. Nat Cell Biol 16, 516-528.

Brons, I.G., Smithers, L.E., Trotter, M.W., Rugg-Gunn, P., Sun, B., Chuva de Sousa Lopes, S.M., Howlett, S.K., Clarkson, A., Ahrlund-Richter, L., Pedersen, R.A., Vallier, L., 2007. Derivation of pluripotent epiblast stem cells from mammalian embryos. Nature 448, 191-195.

Brumby, A.M., Richardson, H.E., 2003. scribble mutants cooperate with oncogenic Ras or Notch to cause neoplastic overgrowth in Drosophila. The EMBO journal 22, 5769-5779.

Buecker, C., Srinivasan, R., Wu, Z., Calo, E., Acampora, D., Faial, T., Simeone, A., Tan, M., Swigut, T., Wysocka, J., 2014. Reorganization of enhancer patterns in transition from naive to primed pluripotency. Cell stem cell 14, 838-853.

Burke, R., Basler, K., 1996. Dpp receptors are autonomously required for cell proliferation in the entire developing Drosophila wing. Development 122, 2261-2269.

Cartwright, P., McLean, C., Sheppard, A., Rivett, D., Jones, K., Dalton, S., 2005. LIF/STAT3 controls ES cell self-renewal and pluripotency by a Myc-dependent mechanism. Development 132, 885-896.

Casas-Tinto, S., Lolo, F.N., Moreno, E., 2015. Active JNK-dependent secretion of Drosophila Tyrosyl-tRNA synthetase by loser cells recruits haemocytes during cell competition. Nat Commun 6, 10022.

Chambers, I., Colby, D., Robertson, M., Nichols, J., Lee, S., Tweedie, S., Smith, A., 2003. Functional expression cloning of Nanog, a pluripotency sustaining factor in embryonic stem cells. Cell 113, 643-655.

Chambers, I., Silva, J., Colby, D., Nichols, J., Nijmeijer, B., Robertson, M., Vrana, J., Jones, K., Grotewold, L., Smith, A., 2007. Nanog safeguards pluripotency and mediates germline development. Nature 450, 1230-1234.

Charron, J., Malynn, B.A., Fisher, P., Stewart, V., Jeannotte, L., Goff, S.P., Robertson, E.J., Alt, F.W., 1992. Embryonic lethality in mice homozygous for a targeted disruption of the N-myc gene. Genes & development 6, 2248-2257.

Chazaud, C., Yamanaka, Y., Pawson, T., Rossant, J., 2006. Early lineage segregation between epiblast and primitive endoderm in mouse blastocysts through the Grb2-MAPK pathway. Developmental cell 10, 615-624.

Chen, C.L., Schroeder, M.C., Kango-Singh, M., Tao, C., Halder, G., 2012. Tumor suppression by cell competition through regulation of the Hippo pathway. Proceedings of the National Academy of Sciences of the United States of America 109, 484-489.

Chen, X., Xu, H., Yuan, P., Fang, F., Huss, M., Vega, V.B., Wong, E., Orlov, Y.L., Zhang, W., Jiang, J., Loh, Y.H., Yeo, H.C., Yeo, Z.X., Narang, V., Govindarajan, K.R., Leong, B., Shahab, A., Ruan, Y., Bourque, G., Sung, W.K., Clarke, N.D., Wei, C.L., Ng, H.H., 2008. Integration of external signaling pathways with the core transcriptional network in embryonic stem cells. Cell 133, 1106-1117.

Claveria, C., Giovinazzo, G., Sierra, R., Torres, M., 2013. Myc-driven endogenous cell competition in the early mammalian embryo. Nature 500, 39-44.

Claveria, C., Torres, M., 2016. Cell Competition: Mechanisms and Physiological Roles. Annu Rev Cell Dev Biol 32, 411-439.

Cowan, C.A., Atienza, J., Melton, D.A., Eggan, K., 2005. Nuclear reprogramming of somatic cells after fusion with human embryonic stem cells. Science 309, 1369-1373.

Dani, C., Blanchard, J.M., Piechaczyk, M., El Sabouty, S., Marty, L., Jeanteur, P., 1984. Extreme instability of myc mRNA in normal and transformed human cells. Proceedings of the National Academy of Sciences of the United States of America 81, 7046-7050.

de la Cova, C., Abril, M., Bellosta, P., Gallant, P., Johnston, L.A., 2004. Drosophila myc regulates organ size by inducing cell competition. Cell 117, 107-116.

de la Cova, C., Johnston, L.A., 2006. Myc in model organisms: a view from the flyroom. Seminars in cancer biology 16, 303-312.

Deppmann, C.D., Mihalas, S., Sharma, N., Lonze, B.E., Niebur, E., Ginty, D.D., 2008. A model for neuronal competition during development. Science 320, 369-373.

Doumpas, N., Ruiz-Romero, M., Blanco, E., Edgar, B., Corominas, M., Teleman, A.A., 2013. Brk regulates wing disc growth in part via repression of Myc expression. EMBO reports 14, 261-268.

Dubois, N.C., Adolphe, C., Ehninger, A., Wang, R.A., Robertson, E.J., Trumpp, A., 2008. Placental rescue reveals a sole requirement for c-Myc in embryonic erythroblast survival and hematopoietic stem cell function. Development 135, 2455-2465.

Eichenlaub, T., Cohen, S.M., Herranz, H., 2016. Cell Competition Drives the Formation of Metastatic Tumors in a Drosophila Model of Epithelial Tumor Formation. Current biology : CB 26, 419-427.

Eisenhoffer, G.T., Loftus, P.D., Yoshigi, M., Otsuna, H., Chien, C.B., Morcos, P.A., Rosenblatt, J., 2012. Crowding induces live cell extrusion to maintain homeostatic cell numbers in epithelia. Nature 484, 546-549.

Evans, M.J., Kaufman, M.H., 1981. Establishment in culture of pluripotential cells from mouse embryos. Nature 292, 154-156.

Fagnocchi, L., Cherubini, A., Hatsuda, H., Fasciani, A., Mazzoleni, S., Poli, V., Berno, V., Rossi, R.L., Reinbold, R., Endele, M., Schroeder, T., Rocchigiani, M., Szkarlat, Z., Oliviero, S., Dalton, S., Zippo, A., 2016. A Myc-driven self-reinforcing regulatory network maintains mouse embryonic stem cell identity. Nat Commun 7, 11903.

Fernández de Manuel, Díaz-Díaz, C., Jiménez-Carretero, D., Torres, M., Montoya, M. C., 2017. ESC-Track: a computer workflow for 4D segmentation, tracking, lineage tracing and dynamic context analysis of ESCs. BioTechniques (in press).

Ficz, G., Hore, T.A., Santos, F., Lee, H.J., Dean, W., Arand, J., Krueger, F., Oxley, D., Paul, Y.L., Walter, J., Cook, S.J., Andrews, S., Branco, M.R., Reik, W., 2013. FGF signaling inhibition in ESCs drives rapid genome-wide demethylation to the epigenetic ground state of pluripotency. Cell stem cell 13, 351-359.

Filipczyk, A., Marr, C., Hastreiter, S., Feigelman, J., Schwarzfischer, M., Hoppe, P.S., Loeffler, D., Kokkaliaris, K.D., Endele, M., Schauberger, B., Hilsenbeck, O., Skylaki, S., Hasenauer, J., Anastassiadis, K., Theis, F.J., Schroeder, T., 2015. Network plasticity of pluripotency transcription factors in embryonic stem cells. Nat Cell Biol 17, 1235-1246.

Gardner, R.L., 1998. Contributions of blastocyst micromanipulation to the study of mammalian development. BioEssays : news and reviews in molecular, cellular and developmental biology 20, 168-180.

Gardner, R.L., Beddington, R.S., 1988. Multi-lineage 'stem' cells in the mammalian embryo. J Cell Sci Suppl 10, 11-27.

Gibson, M.C., Perrimon, N., 2005. Extrusion and death of DPP/BMP-compromised epithelial cells in the developing Drosophila wing. Science 307, 1785-1789.

Gopinath, S., Wen, Q., Thakoor, N., Luby-Phelps, K., Gao, J.X., 2008. A statistical approach for intensity loss compensation of confocal microscopy images. J Microsc 230, 143-159.

Grzeschik, N.A., Parsons, L.M., Richardson, H.E., 2010. Lgl, the SWH pathway and tumorigenesis: It's a matter of context & competition! Cell cycle 9, 3202-3212.

Gu, W., Gaeta, X., Sahakyan, A., Chan, A.B., Hong, C.S., Kim, R., Braas, D., Plath, K., Lowry, W.E., Christofk, H.R., 2016. Glycolytic Metabolism Plays a Functional Role in Regulating Human Pluripotent Stem Cell State. Cell stem cell 19, 476-490.

Gu, Y., Forostyan, T., Sabbadini, R., Rosenblatt, J., 2011. Epithelial cell extrusion requires the sphingosine-1-phosphate receptor 2 pathway. The Journal of cell biology 193, 667-676.

Gu, Y., Rosenblatt, J., 2012. New emerging roles for epithelial cell extrusion. Curr Opin Cell Biol 24, 865-870.

Guo, G., Yang, J., Nichols, J., Hall, J.S., Eyres, I., Mansfield, W., Smith, A., 2009. Klf4 reverts developmentally programmed restriction of ground state pluripotency. Development 136, 1063-1069.

Habibi, E., Brinkman, A.B., Arand, J., Kroeze, L.I., Kerstens, H.H., Matarese, F., Lepikhov, K., Gut, M., Brun-Heath, I., Hubner, N.C., Benedetti, R., Altucci, L., Jansen, J.H., Walter, J., Gut, I.G., Marks, H., Stunnenberg, H.G., 2013. Whole-genome bisulfite sequencing of two distinct interconvertible DNA methylomes of mouse embryonic stem cells. Cell stem cell 13, 360-369.

Hackett, J.A., Dietmann, S., Murakami, K., Down, T.A., Leitch, H.G., Surani, M.A., 2013. Synergistic mechanisms of DNA demethylation during transition to ground-state pluripotency. Stem Cell Reports 1, 518-531.

Hackett, J.A., Surani, M.A., 2014. Regulatory principles of pluripotency: from the ground state up. Cell stem cell 15, 416-430.

Hafezi, Y., Bosch, J.A., Hariharan, I.K., 2012. Differences in levels of the transmembrane protein Crumbs can influence cell survival at clonal boundaries. Dev Biol 368, 358-369.

Hann, S.R., Eisenman, R.N., 1984. Proteins encoded by the human c-myc oncogene: differential expression in neoplastic cells. Molecular and cellular biology 4, 2486-2497.

Hanna, J., Markoulaki, S., Mitalipova, M., Cheng, A.W., Cassady, J.P., Staerk, J., Carey, B.W., Lengner, C.J., Foreman, R., Love, J., Gao, Q., Kim, J., Jaenisch, R., 2009. Metastable pluripotent states in NOD-mouse-derived ESCs. Cell stem cell 4, 513-524.

Hanna, J.H., Saha, K., Jaenisch, R., 2010. Pluripotency and cellular reprogramming: facts, hypotheses, unresolved issues. Cell 143, 508-525.

Hatton, K.S., Mahon, K., Chin, L., Chiu, F.C., Lee, H.W., Peng, D., Morgenbesser, S.D., Horner, J., DePinho, R.A., 1996. Expression and activity of L-Myc in normal mouse development. Molecular and cellular biology 16, 1794-1804.

Hayashi, K., Ohta, H., Kurimoto, K., Aramaki, S., Saitou, M., 2011. Reconstitution of the mouse germ cell specification pathway in culture by pluripotent stem cells. Cell 146, 519-532.

Hayashi, S., Lewis, P., Pevny, L., McMahon, A.P., 2002. Efficient gene modulation in mouse epiblast using a Sox2Cre transgenic mouse strain. Mech Dev 119 Suppl 1, S97-S101.

Herz, H.M., Chen, Z., Scherr, H., Lackey, M., Bolduc, C., Bergmann, A., 2006. vps25 mosaics display non-autonomous cell survival and overgrowth, and autonomous apoptosis. Development 133, 1871-1880.

Heyer, B.S., MacAuley, A., Behrendtsen, O., Werb, Z., 2000. Hypersensitivity to DNA damage leads to increased apoptosis during early mouse development. Genes & development 14, 2072-2084.

Hillman, N., Sherman, M.I., Graham, C., 1972. The effect of spatial arrangement on cell determination during mouse development. Journal of embryology and experimental morphology 28, 263-278.

Hogan, C., Dupre-Crochet, S., Norman, M., Kajita, M., Zimmermann, C., Pelling, A.E., Piddini, E., Baena-Lopez, L.A., Vincent, J.P., Itoh, Y., Hosoya, H., Pichaud, F., Fujita, Y., 2009. Characterization of the interface between normal and transformed epithelial cells. Nat Cell Biol 11, 460-467.

Hu, G., Kim, J., Xu, Q., Leng, Y., Orkin, S.H., Elledge, S.J., 2009. A genome-wide RNAi screen identifies a new transcriptional module required for self-renewal. Genes & development 23, 837-848.

Huang, C.Y., Bredemeyer, A.L., Walker, L.M., Bassing, C.H., Sleckman, B.P., 2008. Dynamic regulation of c-Myc proto-oncogene expression during lymphocyte development revealed by a GFP-c-Myc knock-in mouse. European journal of immunology 38, 342-349.

Ivanova, N., Dobrin, R., Lu, R., Kotenko, I., Levorse, J., DeCoste, C., Schafer, X., Lun, Y., Lemischka, I.R., 2006. Dissecting self-renewal in stem cells with RNA interference. Nature 442, 533-538.

Jin, Z., Kirilly, D., Weng, C., Kawase, E., Song, X., Smith, S., Schwartz, J., Xie, T., 2008. Differentiation-defective stem cells outcompete normal stem cells for niche occupancy in the Drosophila ovary. Cell stem cell 2, 39-49.

Johnston, L.A., Prober, D.A., Edgar, B.A., Eisenman, R.N., Gallant, P., 1999. Drosophila myc regulates cellular growth during development. Cell 98, 779-790.

Kaji, K., Nichols, J., Hendrich, B., 2007. Mbd3, a component of the NuRD co-repressor complex, is required for development of pluripotent cells. Development 134, 1123-1132.

Kajita, M., Fujita, Y., 2015. EDAC: Epithelial defence against cancer-cell competition between normal and transformed epithelial cells in mammals. Journal of biochemistry 158, 15-23.

Kajita, M., Hogan, C., Harris, A.R., Dupre-Crochet, S., Itasaki, N., Kawakami, K., Charras, G., Tada, M., Fujita, Y., 2010. Interaction with surrounding normal epithelial cells influences signalling pathways and behaviour of Src-transformed cells. Journal of cell science 123, 171-180.

Kalkan, T., Olova, N., Roode, M., Mulas, C., Lee, H.J., Nett, I., Marks, H., Walker, R., Stunnenberg, H.G., Lilley, K.S., Nichols, J., Reik, W., Bertone, P., Smith, A., 2017. Tracking the embryonic stem cell transition from ground state pluripotency. Development.

Kalmar, T., Lim, C., Hayward, P., Munoz-Descalzo, S., Nichols, J., Garcia-Ojalvo, J., Martinez Arias, A., 2009. Regulated fluctuations in nanog expression mediate cell fate decisions in embryonic stem cells. PLoS biology 7, e1000149.

Khoa le, T.P., Azami, T., Tsukiyama, T., Matsushita, J., Tsukiyama-Fujii, S., Takahashi, S., Ema, M., 2016. Visualization of the Epiblast and Visceral Endodermal Cells Using Fgf5-P2A-Venus BAC Transgenic Mice and Epiblast Stem Cells. PloS one 11, e0159246.

Kim, J., Woo, A.J., Chu, J., Snow, J.W., Fujiwara, Y., Kim, C.G., Cantor, A.B., Orkin, S.H., 2010. A Myc network accounts for similarities between embryonic stem and cancer cell transcription programs. Cell 143, 313-324.

Kunath, T., Saba-El-Leil, M.K., Almousailleakh, M., Wray, J., Meloche, S., Smith, A., 2007. FGF stimulation of the Erk1/2 signalling cascade triggers transition of pluripotent embryonic stem cells from self-renewal to lineage commitment. Development 134, 2895-2902.

Kurimoto, K., Yabuta, Y., Ohinata, Y., Ono, Y., Uno, K.D., Yamada, R.G., Ueda, H.R., Saitou, M., 2006. An improved single-cell cDNA amplification method for efficient high-density oligonucleotide microarray analysis. Nucleic acids research 34, e42.

Laurenti, E., Wilson, A., Trumpp, A., 2009. Myc's other life: stem cells and beyond. Curr Opin Cell Biol 21, 844-854.

Leitch, H.G., McEwen, K.R., Turp, A., Encheva, V., Carroll, T., Grabole, N., Mansfield, W., Nashun, B., Knezovich, J.G., Smith, A., Surani, M.A., Hajkova, P., 2013. Naive pluripotency is associated with global DNA hypomethylation. Nat Struct Mol Biol 20, 311-316.

Levayer, R., Hauert, B., Moreno, E., 2015. Cell mixing induced by myc is required for competitive tissue invasion and destruction. Nature 524, 476-480.

Li, B., Dewey, C.N., 2011. RSEM: accurate transcript quantification from RNA-Seq data with or without a reference genome. BMC Bioinformatics 12, 323.

Li, W., Baker, N.E., 2007. Engulfment is required for cell competition. Cell 129, 1215-1225.

Lolo, F.N., Casas Tinto, S., Moreno, E., 2013. How winner cells cause the demise of loser cells: cell competition causes apoptosis of suboptimal cells: their dregs are

removed by hemocytes, thus preserving tissue homeostasis. BioEssays : news and reviews in molecular, cellular and developmental biology 35, 348-353.

Lolo, F.N., Casas-Tinto, S., Moreno, E., 2012. Cell competition time line: winners kill losers, which are extruded and engulfed by hemocytes. Cell reports 2, 526-539.

Lu, H., Bilder, D., 2005. Endocytic control of epithelial polarity and proliferation in Drosophila. Nat Cell Biol 7, 1232-1239.

Malynn, B.A., de Alboran, I.M., O'Hagan, R.C., Bronson, R., Davidson, L., DePinho, R.A., Alt, F.W., 2000. N-myc can functionally replace c-myc in murine development, cellular growth, and differentiation. Genes & development 14, 1390-1399.

Mamada, H., Sato, T., Ota, M., Sasaki, H., 2015. Cell competition in mouse NIH3T3 embryonic fibroblasts is controlled by the activity of Tead family proteins and Myc. Journal of cell science 128, 790-803.

Marinari, E., Mehonic, A., Curran, S., Gale, J., Duke, T., Baum, B., 2012. Live-cell delamination counterbalances epithelial growth to limit tissue overcrowding. Nature 484, 542-545.

Marks, H., Kalkan, T., Menafra, R., Denissov, S., Jones, K., Hofemeister, H., Nichols, J., Kranz, A., Stewart, A.F., Smith, A., Stunnenberg, H.G., 2012. The transcriptional and epigenomic foundations of ground state pluripotency. Cell 149, 590-604.

Martello, G., Smith, A., 2014. The nature of embryonic stem cells. Annu Rev Cell Dev Biol 30, 647-675.

Martin, F.A., Herrera, S.C., Morata, G., 2009. Cell competition, growth and size control in the Drosophila wing imaginal disc. Development 136, 3747-3756.

Martin, G.R., 1981. Isolation of a pluripotent cell line from early mouse embryos cultured in medium conditioned by teratocarcinoma stem cells. Proceedings of the National Academy of Sciences of the United States of America 78, 7634-7638.

Martin, G.R., Evans, M.J., 1975. Differentiation of clonal lines of teratocarcinoma cells: formation of embryoid bodies in vitro. Proceedings of the National Academy of Sciences of the United States of America 72, 1441-1445.

Martin, M., 2011. Cutadapt removes adapter sequences from high-throughput sequencing reads. EMBnetjournal, North America 17, 10-12.

Martins, V.C., Busch, K., Juraeva, D., Blum, C., Ludwig, C., Rasche, V., Lasitschka, F., Mastitsky, S.E., Brors, B., Hielscher, T., Fehling, H.J., Rodewald, H.R., 2014. Cell competition is a tumour suppressor mechanism in the thymus. Nature 509, 465-470.

Marusyk, A., Porter, C.C., Zaberezhnyy, V., DeGregori, J., 2010. Irradiation selects for p53-deficient hematopoietic progenitors. PLoS biology 8, e1000324.

Menendez, J., Perez-Garijo, A., Calleja, M., Morata, G., 2010. A tumor-suppressing mechanism in Drosophila involving cell competition and the Hippo pathway. Proceedings of the National Academy of Sciences of the United States of America 107, 14651-14656.

Merino, M.M., Rhiner, C., Lopez-Gay, J.M., Buechel, D., Hauert, B., Moreno, E., 2015. Elimination of unfit cells maintains tissue health and prolongs lifespan. Cell 160, 461-476.

Meyer, N., Penn, L.Z., 2008. Reflecting on 25 years with MYC. Nature reviews. Cancer 8, 976-990.

Meyer, S.N., Amoyel, M., Bergantinos, C., de la Cova, C., Schertel, C., Basler, K., Johnston, L.A., 2014. An ancient defense system eliminates unfit cells from developing tissues during cell competition. Science 346, 1258236.

Milan, M., Perez, L., Cohen, S.M., 2002. Short-range cell interactions and cell survival in the Drosophila wing. Developmental cell 2, 797-805.

Mitsui, K., Tokuzawa, Y., Itoh, H., Segawa, K., Murakami, M., Takahashi, K., Maruyama, M., Maeda, M., Yamanaka, S., 2003. The homeoprotein Nanog is required for maintenance of pluripotency in mouse epiblast and ES cells. Cell 113, 631-642.

Morata, G., Ripoll, P., 1975. Minutes: mutants of drosophila autonomously affecting cell division rate. Dev Biol 42, 211-221.

Moreno, E., Basler, K., 2004. dMyc transforms cells into super-competitors. Cell 117, 117-129.

Moreno, E., Basler, K., Morata, G., 2002. Cells compete for decapentaplegic survival factor to prevent apoptosis in Drosophila wing development. Nature 416, 755-759.

Moreno, E., Fernandez-Marrero, Y., Meyer, P., Rhiner, C., 2015. Brain regeneration in Drosophila involves comparison of neuronal fitness. Current biology : CB 25, 955-963.

Nakagawa, M., Koyanagi, M., Tanabe, K., Takahashi, K., Ichisaka, T., Aoi, T., Okita, K., Mochiduki, Y., Takizawa, N., Yamanaka, S., 2008. Generation of induced pluripotent stem cells without Myc from mouse and human fibroblasts. Nat Biotechnol 26, 101-106.

Neto-Silva, R.M., de Beco, S., Johnston, L.A., 2010. Evidence for a growth-stabilizing regulatory feedback mechanism between Myc and Yorkie, the Drosophila homolog of Yap. Developmental cell 19, 507-520.

Nichols, J., Smith, A., 2009. Naive and primed pluripotent states. Cell stem cell 4, 487-492.

Nichols, J., Zevnik, B., Anastassiadis, K., Niwa, H., Klewe-Nebenius, D., Chambers, I., Scholer, H., Smith, A., 1998. Formation of pluripotent stem cells in the mammalian embryo depends on the POU transcription factor Oct4. Cell 95, 379-391.

Niwa, H., Burdon, T., Chambers, I., Smith, A., 1998. Self-renewal of pluripotent embryonic stem cells is mediated via activation of STAT3. Genes & development 12, 2048-2060.

Niwa, H., Ogawa, K., Shimosato, D., Adachi, K., 2009. A parallel circuit of LIF signalling pathways maintains pluripotency of mouse ES cells. Nature 460, 118-122.

Norman, M., Wisniewska, K.A., Lawrenson, K., Garcia-Miranda, P., Tada, M., Kajita, M., Mano, H., Ishikawa, S., Ikegawa, M., Shimada, T., Fujita, Y., 2012. Loss of Scribble causes cell competition in mammalian cells. Journal of cell science 125, 59-66.

Oertel, M., Menthena, A., Dabeva, M.D., Shafritz, D.A., 2006. Cell competition leads to a high level of normal liver reconstitution by transplanted fetal liver stem/progenitor cells. Gastroenterology 130, 507-520; quiz 590.

Ogawa, K., Nishinakamura, R., Iwamatsu, Y., Shimosato, D., Niwa, H., 2006. Synergistic action of Wnt and LIF in maintaining pluripotency of mouse ES cells. Biochemical and biophysical research communications 343, 159-166.

Ohsawa, S., Sugimura, K., Takino, K., Xu, T., Miyawaki, A., Igaki, T., 2011. Elimination of oncogenic neighbors by JNK-mediated engulfment in Drosophila. Developmental cell 20, 315-328.

Oliver, E.R., Saunders, T.L., Tarle, S.A., Glaser, T., 2004. Ribosomal protein L24 defect in belly spot and tail (Bst), a mouse Minute. Development 131, 3907-3920.

Orkin, S.H., 2005. Chipping away at the embryonic stem cell network. Cell 122, 828-830.

Overholtzer, M., Mailleux, A.A., Mouneimne, G., Normand, G., Schnitt, S.J., King, R.W., Cibas, E.S., Brugge, J.S., 2007. A nonapoptotic cell death process, entosis, that occurs by cell-in-cell invasion. Cell 131, 966-979.

Ozmadenci, D., Feraud, O., Markossian, S., Kress, E., Ducarouge, B., Gibert, B., Ge, J., Durand, I., Gadot, N., Plateroti, M., Bennaceur-Griscelli, A., Scoazec, J.Y., Gil, J., Deng, H., Bernet, A., Mehlen, P., Lavial, F., 2015. Netrin-1 regulates somatic cell reprogramming and pluripotency maintenance. Nat Commun 6, 7398.

Paoli, P., Giannoni, E., Chiarugi, P., 2013. Anoikis molecular pathways and its role in cancer progression. Biochimica et biophysica acta 1833, 3481-3498.

Penzo-Mendez, A.I., Chen, Y.J., Li, J., Witze, E.S., Stanger, B.Z., 2015. Spontaneous Cell Competition in Immortalized Mammalian Cell Lines. PloS one 10, e0132437.

Petrova, E., Lopez-Gay, J.M., Rhiner, C., Moreno, E., 2012. Flower-deficient mice have reduced susceptibility to skin papilloma formation. Dis Model Mech 5, 553-561.

Petrova, E., Soldini, D., Moreno, E., 2011. The expression of SPARC in human tumors is consistent with its role during cell competition. Communicative & integrative biology 4, 171-174.

Plusa, B., Piliszek, A., Frankenberg, S., Artus, J., Hadjantonakis, A.K., 2008. Distinct sequential cell behaviours direct primitive endoderm formation in the mouse blastocyst. Development 135, 3081-3091.

Poelmann, R.E., 1980. Differential mitosis and degeneration patterns in relation to the alterations in the shape of the embryonic ectoderm of early post-implantation mouse embryos. Journal of embryology and experimental morphology 55, 33-51.

Portela, M., Casas-Tinto, S., Rhiner, C., Lopez-Gay, J.M., Dominguez, O., Soldini, D., Moreno, E., 2010. Drosophila SPARC is a self-protective signal expressed by loser cells during cell competition. Developmental cell 19, 562-573.

Prober, D.A., Edgar, B.A., 2000. Ras1 promotes cellular growth in the Drosophila wing. Cell 100, 435-446.

Rhiner, C., Diaz, B., Portela, M., Poyatos, J.F., Fernandez-Ruiz, I., Lopez-Gay, J.M., Gerlitz, O., Moreno, E., 2009. Persistent competition among stem cells and their daughters in the Drosophila ovary germline niche. Development 136, 995-1006.

Rhiner, C., Lopez-Gay, J.M., Soldini, D., Casas-Tinto, S., Martin, F.A., Lombardia, L., Moreno, E., 2010. Flower forms an extracellular code that reveals the fitness of a cell to its neighbors in Drosophila. Developmental cell 18, 985-998.

Rhiner, C., Moreno, E., 2009. Super competition as a possible mechanism to pioneer precancerous fields. Carcinogenesis 30, 723-728.

Robinson, M.D., McCarthy, D.J., Smyth, G.K., 2010. edgeR: a Bioconductor package for differential expression analysis of digital gene expression data. Bioinformatics 26, 139-140.

Rodrigues, A.B., Zoranovic, T., Ayala-Camargo, A., Grewal, S., Reyes-Robles, T., Krasny, M., Wu, D.C., Johnston, L.A., Bach, E.A., 2012. Activated STAT regulates growth and induces competitive interactions independently of Myc, Yorkie, Wingless and ribosome biogenesis. Development 139, 4051-4061.

Sancho, M., Di-Gregorio, A., George, N., Pozzi, S., Sanchez, J.M., Pernaute, B., Rodriguez, T.A., 2013. Competitive interactions eliminate unfit embryonic stem cells at the onset of differentiation. Developmental cell 26, 19-30.

Sasaki, K., Yokobayashi, S., Nakamura, T., Okamoto, I., Yabuta, Y., Kurimoto, K., Ohta, H., Moritoki, Y., Iwatani, C., Tsuchiya, H., Nakamura, S., Sekiguchi, K., Sakuma, T., Yamamoto, T., Mori, T., Woltjen, K., Nakagawa, M., Yamamoto, T., Takahashi, K., Yamanaka, S., Saitou, M., 2015. Robust In Vitro Induction of Human Germ Cell Fate from Pluripotent Stem Cells. Cell stem cell 17, 178-194.

Sato, N., Meijer, L., Skaltsounis, L., Greengard, P., Brivanlou, A.H., 2004. Maintenance of pluripotency in human and mouse embryonic stem cells through activation of Wnt signaling by a pharmacological GSK-3-specific inhibitor. Nat Med 10, 55-63.

Savatier, P., Huang, S., Szekely, L., Wiman, K.G., Samarut, J., 1994. Contrasting patterns of retinoblastoma protein expression in mouse embryonic stem cells and embryonic fibroblasts. Oncogene 9, 809-818.

Scognamiglio, R., Cabezas-Wallscheid, N., Thier, M.C., Altamura, S., Reyes, A., Prendergast, A.M., Baumgartner, D., Carnevalli, L.S., Atzberger, A., Haas, S., von Paleske, L., Boroviak, T., Worsdorfer, P., Essers, M.A., Kloz, U., Eisenman, R.N., Edenhofer, F., Bertone, P., Huber, W., van der Hoeven, F., Smith, A., Trumpp, A., 2016. Myc Depletion Induces a Pluripotent Dormant State Mimicking Diapause. Cell 164, 668-680.

Selwood, L., Johnson, M.H., 2006. Trophoblast and hypoblast in the monotreme, marsupial and eutherian mammal: evolution and origins. BioEssays : news and reviews in molecular, cellular and developmental biology 28, 128-145.

Senoo-Matsuda, N., Johnston, L.A., 2007. Soluble factors mediate competitive and cooperative interactions between cells expressing different levels of Drosophila Myc. Proceedings of the National Academy of Sciences of the United States of America 104, 18543-18548.

Shen, J., Dahmann, C., 2005. Extrusion of cells with inappropriate Dpp signaling from Drosophila wing disc epithelia. Science 307, 1789-1790.

Shraiman, B.I., 2005. Mechanical feedback as a possible regulator of tissue growth. Proceedings of the National Academy of Sciences of the United States of America 102, 3318-3323.

Simpson, P., 1979. Parameters of cell competition in the compartments of the wing disc of Drosophila. Dev Biol 69, 182-193.

Simpson, P., Morata, G., 1981. Differential mitotic rates and patterns of growth in compartments in the Drosophila wing. Dev Biol 85, 299-308.

Smallwood, S.A., Tomizawa, S., Krueger, F., Ruf, N., Carli, N., Segonds-Pichon, A., Sato, S., Hata, K., Andrews, S.R., Kelsey, G., 2011. Dynamic CpG island methylation landscape in oocytes and preimplantation embryos. Nat Genet 43, 811-814.

Smith, A.G., Heath, J.K., Donaldson, D.D., Wong, G.G., Moreau, J., Stahl, M., Rogers, D., 1988. Inhibition of pluripotential embryonic stem cell differentiation by purified polypeptides. Nature 336, 688-690.

Smith, K.N., Singh, A.M., Dalton, S., 2010. Myc represses primitive endoderm differentiation in pluripotent stem cells. Cell stem cell 7, 343-354.

Smith, Z.D., Chan, M.M., Mikkelsen, T.S., Gu, H., Gnirke, A., Regev, A., Meissner, A., 2012. A unique regulatory phase of DNA methylation in the early mammalian embryo. Nature 484, 339-344.

Smith, Z.D., Meissner, A., 2013. DNA methylation: roles in mammalian development. Nat Rev Genet 14, 204-220.

Snippert, H.J., Schepers, A.G., van Es, J.H., Simons, B.D., Clevers, H., 2014. Biased competition between Lgr5 intestinal stem cells driven by oncogenic mutation induces clonal expansion. EMBO reports 15, 62-69.

Stephenson, R.O., Rossant, J., Tam, P.P., 2012. Intercellular interactions, position, and polarity in establishing blastocyst cell lineages and embryonic axes. Cold Spring Harb Perspect Biol 4.

Suijkerbuijk, S.J., Kolahgar, G., Kucinski, I., Piddini, E., 2016. Cell Competition Drives the Growth of Intestinal Adenomas in Drosophila. Current biology : CB 26, 428-438.

Sumi, T., Tsuneyoshi, N., Nakatsuji, N., Suemori, H., 2007. Apoptosis and differentiation of human embryonic stem cells induced by sustained activation of c-Myc. Oncogene 26, 5564-5576.

Sun, Q., Cibas, E.S., Huang, H., Hodgson, L., Overholtzer, M., 2014a. Induction of entosis by epithelial cadherin expression. Cell research 24, 1288-1298.

Sun, Q., Luo, T., Ren, Y., Florey, O., Shirasawa, S., Sasazuki, T., Robinson, D.N., Overholtzer, M., 2014b. Competition between human cells by entosis. Cell research 24, 1299-1310.

Tada, M., Takahama, Y., Abe, K., Nakatsuji, N., Tada, T., 2001. Nuclear reprogramming of somatic cells by in vitro hybridization with ES cells. Current biology : CB 11, 1553-1558.

Takahashi, K., Yamanaka, S., 2006. Induction of pluripotent stem cells from mouse embryonic and adult fibroblast cultures by defined factors. Cell 126, 663-676.

Tamori, Y., Bialucha, C.U., Tian, A.G., Kajita, M., Huang, Y.C., Norman, M., Harrison, N., Poulton, J., Ivanovitch, K., Disch, L., Liu, T., Deng, W.M., Fujita, Y., 2010. Involvement of Lgl and Mahjong/VprBP in cell competition. PLoS biology 8, e1000422.

Tamori, Y., Deng, W.M., 2013. Tissue repair through cell competition and compensatory cellular hypertrophy in postmitotic epithelia. Developmental cell 25, 350-363.

Tesar, P.J., Chenoweth, J.G., Brook, F.A., Davies, T.J., Evans, E.P., Mack, D.L., Gardner, R.L., McKay, R.D., 2007. New cell lines from mouse epiblast share defining features with human embryonic stem cells. Nature 448, 196-199.

Trumpp, A., Refaeli, Y., Oskarsson, T., Gasser, S., Murphy, M., Martin, G.R., Bishop, J.M., 2001. c-Myc regulates mammalian body size by controlling cell number but not cell size. Nature 414, 768-773.

Tyler, D.M., Li, W., Zhuo, N., Pellock, B., Baker, N.E., 2007. Genes affecting cell competition in Drosophila. Genetics 175, 643-657.

van Oosten, A.L., Costa, Y., Smith, A., Silva, J.C., 2012. JAK/STAT3 signalling is sufficient and dominant over antagonistic cues for the establishment of naive pluripotency. Nat Commun 3, 817.

Villa del Campo, C., Claveria, C., Sierra, R., Torres, M., 2014. Cell competition promotes phenotypically silent cardiomyocyte replacement in the mammalian heart. Cell reports 8, 1741-1751.

Vincent, J.P., Kolahgar, G., Gagliardi, M., Piddini, E., 2011. Steep differences in wingless signaling trigger Myc-independent competitive cell interactions. Developmental cell 21, 366-374.

Wang, J., Rao, S., Chu, J., Shen, X., Levasseur, D.N., Theunissen, T.W., Orkin, S.H., 2006. A protein interaction network for pluripotency of embryonic stem cells. Nature 444, 364-368.

Welcker, M., Orian, A., Jin, J., Grim, J.E., Harper, J.W., Eisenman, R.N., Clurman, B.E., 2004. The Fbw7 tumor suppressor regulates glycogen synthase kinase 3 phosphorylation-dependent c-Myc protein degradation. Proceedings of the National Academy of Sciences of the United States of America 101, 9085-9090.

Wierstra, I., Alves, J., 2008. The c-myc promoter: still MysterY and challenge. Adv Cancer Res 99, 113-333.

Williams, R.L., Hilton, D.J., Pease, S., Willson, T.A., Stewart, C.L., Gearing, D.P., Wagner, E.F., Metcalf, D., Nicola, N.A., Gough, N.M., 1988. Myeloid leukaemia inhibitory factor maintains the developmental potential of embryonic stem cells. Nature 336, 684-687.

Wilmut, I., Schnieke, A.E., McWhir, J., Kind, A.J., Campbell, K.H., 1997. Viable offspring derived from fetal and adult mammalian cells. Nature 385, 810-813.

Wilson, A., Murphy, M.J., Oskarsson, T., Kaloulis, K., Bettess, M.D., Oser, G.M., Pasche, A.C., Knabenhans, C., Macdonald, H.R., Trumpp, A., 2004. c-Myc controls the balance between hematopoietic stem cell self-renewal and differentiation. Genes & development 18, 2747-2763.

Woods, D.F., Bryant, P.J., 1991. The discs-large tumor suppressor gene of Drosophila encodes a guanylate kinase homolog localized at septate junctions. Cell 66, 451-464.

Yamada, T., Ohno, S., Kitamura, N., Sasabe, E., Yamamoto, T., 2015. SPARC is associated with carcinogenesis of oral squamous epithelium and consistent with cell competition. Med Mol Morphol 48, 129-137.

Yamanaka, S., Blau, H.M., 2010. Nuclear reprogramming to a pluripotent state by three approaches. Nature 465, 704-712.

Ye, S., Zhang, D., Cheng, F., Wilson, D., Mackay, J., He, K., Ban, Q., Lv, F., Huang, S., Liu, D., Ying, Q.L., 2016. Wnt/beta-catenin and LIF-Stat3 signaling pathways converge on Sp5 to promote mouse embryonic stem cell self-renewal. Journal of cell science 129, 269-276.

Ying, Q.L., Nichols, J., Chambers, I., Smith, A., 2003. BMP induction of Id proteins suppresses differentiation and sustains embryonic stem cell self-renewal in collaboration with STAT3. Cell 115, 281-292.

Ying, Q.L., Wray, J., Nichols, J., Batlle-Morera, L., Doble, B., Woodgett, J., Cohen, P., Smith, A., 2008. The ground state of embryonic stem cell self-renewal. Nature 453, 519-523.

Zhou, Q., Chipperfield, H., Melton, D.A., Wong, W.H., 2007. A gene regulatory network in mouse embryonic stem cells. Proceedings of the National Academy of Sciences of the United States of America 104, 16438-16443.

Ziosi, M., Baena-Lopez, L.A., Grifoni, D., Froldi, F., Pession, A., Garoia, F., Trotta, V., Bellosta, P., Cavicchi, S., Pession, A., 2010. dMyc functions downstream of Yorkie to promote the supercompetitive behavior of hippo pathway mutant cells. PLoS genetics 6, e1001140.

ACKNOWLEDGMENTS

La parte más importante.

Gracias a todas esas personas que en mayor o menor medida han ayudado a que esta tesis fuera posible.

Ante todo, dar las gracias a Miguel, no solo por ofrecerme la oportunidad de trabajar en su grupo, sino también por la confianza y el apoyo profesional y personal que he sentido durante todos estos años. Por enseñarme tu ciencia, por motivarme y transmitirme tu pasión por la investigación.

Por supuesto agradecer a todos mis compañeros del grupo MT por hacer más fácil mi día a día. A Cristina, mi mentora, porque su gran trabajo ha sido el origen de esta tesis. A Rocío (mi mano derecha) y Susana que vivieron esto de principio a fin. A Kenzo, Ghislaine, Noelia, Sandra, José, mi compi Isaac (por sufrir mis invasiones), Ester y Lin. A Vane, gran consejera y amiga. Gracias también a los antiguos miembros con los que he compartido momentos: Laura P., Félix, Alber, Ricardo, Dani, Mónica, Daniel A. y especialmente a Laura C. (un gran ejemplo a seguir). Y por supuesto a mis dos soles; a Irene, la positividad, la sonrisa y el mejor apoyo que he podido tener tanto dentro como fuera del laboratorio, y a Cris, la pasión, la energía, pura ciencia, por estar aquí cuando yo llegué, porque, y suscribo tus palabras, *she will never really understand how responsible she is for this thesis*; a vosotras, nunca dejaré de agradeceros.

A esas personas que llegaron y se quedaron. A Bea E., porque desde que te conozco nunca has dejado de sonreír. A Bea P. porque su humor alegra el peor de los momentos. A Sofía, por endulzarme los días. A mi coterráneo Iván, por ser como eres, una mente brillante y el alma de la fiesta. A Tania, la mujer que todo lo puede, realmente envidiable.

Gracias a todo el Área de Biología Celular y Desarrollo, especialmente a los grupos de la 3 Norte, gente del grupo de José Luis, Nadia, Nacho, Rui y Silvia.

A Laura, Vir, Gonzalín y resto del personal de animalario. A las unidades de Transgénesis, Genómica y Bioinformática. A la Unidad de Microscopía, donde he

pasado muchas horas de mi tesis, gracias a Elvira, Vero y Antonio por sufrir conmigo la puesta a punto del *time-lapse*. Agradecer especialmente a la Unidad de Celómica, María, Laura y Daniel, porque detrás de esta tesis está vuestro enorme trabajo.

Y una mención especial a la Unidad de Tecnología de Células Pluripotentes, donde he crecido. A Nines y Paco, compañeros de cultivos, maestros y confidentes. Y por supuesto a Giovanna, por enseñarme todo lo que sé, por acogerme desde el principio, por tu confianza y cariño. Esta tesis también es vuestra.

Gracias a todo el equipo de gestión y administración, a Beatriz y Marta. A Teresa, por tu divertida presencia. A Cristina Giménez por facilitar todos los trámites imposibles. Y a toda la gente del CNIC que se haya quedado sin nombrar pero que estuvieron ahí en algún momento.

Gracias a François Spitz por darme la oportunidad de hacer la estancia en su laboratorio, y a su equipo por haber conseguido que nunca dejara de echar de menos esos meses.

Gracias a esas personas eventuales y permanentes. A Silvia, David. A Blanch, por estar conmigo desde mi primer contacto con Madrid, por las meriendas y charlas semanales, por ser un apoyo incesante.

A mis fantásticas, Clau, Leti y Ángela, porque con vosotras empezó todo, y todo sigue sucediendo a vuestro lado. A mi doble titulado Sergius, un gran amigo, por los abrazos refuerza-amistad, por hacerme reír siempre. A Lau y al resto de biólogos, por esas cenas universitarias inspiradoras.

A mis tres pilares. Marti, mi constante inconstante. Edu, mi amor loco, *mon amour fou*. Teri, mi otro yo. Por escucharme siempre aún sin saber de lo que hablo. Sin ellos, éste ni ningún otro momento de mi vida habrían sido lo mismo. Gracias, por ser vosotros.

Gracias a la familia, pequeña pero ruidosa. A los primos, a Julio, a Marina por acompañarme en los inicios en la capital. A Víctor, por estar siempre y desde siempre.

Mis hermanos, a Tomás, porque su humildad me inspira, y a Luis, que después de todo aún no sabe cuánto vale. A Elvira, por haber aparecido. A Lucas, el amor de mi vida, porque desde que estás aquí todo se hace más fácil. Y por supuesto a mis padres. A mi madre, por su admirable e incansable lucha. A mi padre, ojalá llegar a vivir esta profesión como tú vives la tuya. Gracias a los dos, mis referentes, porque ahora estoy aquí.

Y a Juan, mi todo. Mi compañero de viaje. Por sufrir conmigo todos y cada uno de los días. Por impulsar mis inquietudes. Por celebrar mis alegrías. Por entender lo incomprensible. *I love you more than words can say*.

Cover page. Confocal image of an ESC culture showing GFP-Myc levels (green) and tdTomato reporting the cell membrane (red).

Back page. Confocal image of an E6.0 mouse embryo showing tdTomato reporting the cell membrane (red), DAPI staining the nuclei (blue) and pERK immunofluorescence (green).